



UNIVERSIDADE ESTADUAL DE CAMPINAS  
Instituto de Geociências

GUILHERME FURLAN CHINELATTO

ANÁLISE PETROFÍSICA EM COQUINAS ABORDANDO O CONCEITO DE  
TAFOFÁCIES

PETROPHYSICAL ANALYSIS IN COQUINAS ADDRESSING THE CONCEPT OF  
TAPHOFACIES

CAMPINAS  
2020

GUILHERME FURLAN CHINELATTO

ANÁLISE PETROFÍSICA EM COQUINAS ABORDANDO O CONCEITO DE  
TAFOFÁCIES

TESE APRESENTADA AO INSTITUTO DE  
GEOCIÊNCIAS DA UNIVERSIDADE ESTADUAL DE  
CAMPINAS PARA OBTENÇÃO DO TÍTULO DE DOUTOR  
EM CIÊNCIAS NA ÁREA DE GEOLOGIA E RECURSOS  
NATURAIS

THESIS PRESENTED TO THE INSTITUTE OF  
GEOSCIENCES OF THE UNIVERSITY OF CAMPINAS TO  
OBTAIN THE DEGREE OF DOCTOR IN SCIENCES IN  
AREA OF GEOLOGY AND NATURAL RESOURCES

ORIENTADOR: PROF. DR. ALEXANDRE CAMPANE VIDAL

ESTE EXEMPLAR CORRESPONDE À VERSÃO FINAL  
DA TESE DEFENDIDA PELO ALUNO GUILHERME  
FURLAN CHINELATTO E ORIENTADA PELO PROF. DR.  
ALEXANDRE CAMPANE VIDAL.

CAMPINAS

2020

Ficha catalográfica  
Universidade Estadual de Campinas  
Biblioteca do Instituto de Geociências  
Marta dos Santos - CRB 8/5892

C441a Chinelatto, Guilherme Furlan, 1987-  
Análise petrofísica em coquinas abordando o conceito de tafofácies /  
Guilherme Furlan Chinelatto. – Campinas, SP : [s.n.], 2020.

Orientador: Alexandre Campane Vidal.  
Tese (doutorado) – Universidade Estadual de Campinas, Instituto de  
Geociências.

1. Tafonomia. 2. Carbonatos. 3. Petrofísica. 4. Porosidade. 5.  
Permeabilidade. I. Vidal, Alexandre Campane, 1969-. II. Universidade Estadual  
de Campinas. Instituto de Geociências. III. Título.

Informações para Biblioteca Digital

**Título em outro idioma:** Petrophysical analysis in coquinas addressing the concept of taphofacies

**Palavras-chave em inglês:**

Taphofacies

Carbonates

Petrophysics

Porosity

Permeability

**Área de concentração:** Geologia e Recursos Naturais

**Titulação:** Doutor em Geociências

**Banca examinadora:**

Alexandre Campane Vidal [Orientador]

Giorgio Basilici

Fresia Soledad Torres Branco

Paulo César Boggiani

Moises Calazans Muniz

**Data de defesa:** 14-02-2020

**Programa de Pós-Graduação:** Geociências

**Identificação e informações acadêmicas do(a) aluno(a)**

- ORCID do autor: <https://orcid.org/0000-0002-8691-5871>

- Currículo Lattes do autor: <http://lattes.cnpq.br/4166653992330551>



UNIVERSIDADE ESTADUAL DE CAMPINAS  
INSTITUTO DE GEOCIÊNCIAS

**AUTOR:** Guilherme Furlan Chinelatto

ANÁLISE PETROFÍSICA EM COQUINAS ABORDANDO O CONCEITO DE  
TAFOFÁCIES

PETROPHYSICAL ANALYSIS IN COQUINAS ADDRESSING THE CONCEPT OF  
TAPHOFACIES

**ORIENTADOR:** Prof. Dr. Alexandre Campane Vidal

Aprovado em: 14 / 02 / 2020

**EXAMINADORES:**

Prof. Dr. Alexandre Campane Vidal - Presidente

Prof. Dr. Giorgio Basilici

Profa. Dra. Fresia Soledad Ricardi Torres Branco

Prof. Dr. Paulo César Boggiani

Prof. Dr. Moises Calazans Muniz

**A Ata de defesa com as respectivas assinaturas dos membros encontra-se disponível no SIGA - Sistema de Fluxo de Tese e na Secretaria de Pós-graduação do IG.**

Campinas, 14 de fevereiro de 2020.

## SÚMULA/BIOGRAFIA

Olá, meu nome é Guilherme, nasci em Americana-SP e hoje tenho 32 anos. Ingressei no curso de geociências (Ciências da Terra) pela Unicamp no ano de 2009 e me formei em 2013. No último ano de graduação, participei de um grupo de pesquisa que estudavam rochas carbonáticas análogas aos depósitos do pré-sal, as coquinas da Formação Morro do Chaves localizadas na Bacia de Sergipe-Alagoas. A pesquisa me atraiu bastante e logo após me graduar vi a possibilidade de dar continuidade desse estudo na pós-graduação. O tema do mestrado foi sobre a interpretação deposicional das coquinas (Morro do Chaves) segundo aspectos tafonômicos. Conclui o mestrado em 2016 e ingressei no doutorado com intuito de compreender a variação dessas coquinas com a qualidade de reservatório. Em 2018 surgiu a possibilidade de realizar uma pesquisa em parceria com a empresa Equinor com ênfase no estudo petrofísico dos depósitos carbonáticos do pré-sal, dessa forma foi possível ter acesso a algumas amostras de coquinas da Formação Itapema localizada na Bacia de Santos. Hoje me dedico ao estudo petrofísico de rochas carbonáticas do pré-sal (fase rifte e sag), e durante o tempo livre me dedico a vida musical.

## **DEDICATÓRIA**

*Dedico esse trabalho primeiramente a meus pais, Claudia e João Carlos, as minhas irmãs Julia e Raquel e a todos que lutam pelo desenvolvimento da ciência e conhecimento.*

## **AGRADECIMENTO**

Agradeço primeiramente aos meus pais, foram eles que sempre me aconselharam a seguir nos estudos e me ampararam durante minha infância e adolescência para poder me dedicar e ingressar em uma universidade pública. Agradeço a todos os familiares e amigos que sempre me apoiaram, em especial a Camila, minha companheira nessa grande jornada, a todos os meus amigos do Lab MGRe meu orientador e amigo Vidal. Agradeço também a todos os professores que me ensinaram ao longo dessa jornada, sem o esforço e dedicação deles eu não estaria aqui. Também quero agradecer a todo apoio e financiamento promovido pela Coordenação de Aperfeiçoamento de Pessoal de Nível Superior (CAPES)- Código de Financiamento 001, Equinor e Unicamp ao longo desses anos.

A todos vocês, “aquele abraço”!

“Há mil maneiras pra se poder vencer, há mil maneiras pra poder continuar, enquanto o tempo voa, o seu sonho ecoa e você não pode parar!”

(Guilherme Furlan Chinelatto: Pérola Nuvem – Epifania)

## RESUMO

Coquina é um termo utilizado para referir rochas sedimentares compostas principalmente por conchas e seus fragmentos. Esse tipo de rocha pode apresentar como matriz grãos carbonáticos ou siliciclásticos resultando em uma diversa combinação de seus componentes texturais. Sabe-se que as condições do ambiente de sedimentação e alterações diagenéticas influenciam diretamente na preservação ou modificação de grãos carbonáticos resultando em uma grande heterogeneidade textural, afetando diretamente na preservação ou não do sistema poroso e consequentemente influenciando na permeabilidade. O estudo apresentado tem como objetivo a interpretação do sistema deposicional para diferentes tipos de acumulações de coquinas depositadas durante a fase rifte nas bacias de Sergipe-Alagoas e Santos compreendendo as Formações Morro do Chaves e Itapema, e qual a sua relação com a porosidade e permeabilidade. Através das características tafonômicas, que estão diretamente ligadas ao estado de preservação, empacotamento e orientação das conchas, essas rochas foram classificadas como tafofácies de alta e baixa energia e interpretadas dentro de um modelo deposicional. Para a classificação da porosidade foram utilizados dos seguintes métodos: i) o uso de lâmina delgada de rocha, ii) análise de tomografia de raio-x de testemunho de rocha, iii) análise de tomografia de alta resolução de plugues de rochas e iv) análise de ressonância magnética nuclear (RMN). Com esse tipo de dado foi possível segmentar o sistema poroso e dividi-lo de acordo com: a) tafofácies com predominância de poros primários, b) tafofácies com valores equivalentes de poros primários e secundários e 3) tafofácies com poros predominantemente secundários. Como resultado, observa-se que tafofácies de alta energia apresentam em maior quantidade a porosidade primária preservada devido aos processos de remoção de material fino associados a processos de retrabalhamento e seleção, enquanto que nas fácies de baixa energia, onde esses processos apresentam menor intensidade, o sistema poroso se dá principalmente pela atuação da diagênese criando uma diversidade de poros secundários como móldicos e vugulares. Com relação à permeabilidade as tafofácies de alta energia apresentam os valores mais altos, geralmente acima de 150 milliDarcy (mD) pois os poros apresentam boa conectividade devido a preservação de poros primários assim como a criação de canais, favorecendo a movimentação de fluidos. As tafofácies de baixa energia apresentam valores inferiores de permeabilidade, geralmente próximos a 150 mD devido à ocorrência de poros isolados, normalmente vugulares e móldicos como também da ocorrência de microporosidade. Coquinas depositadas em ambientes com alto grau de seleção, quando favorecidas pela diagênese, representam as melhores qualidades de rochas reservatórias enquanto que as de baixo grau de seleção apesar de apresentar bons resultados de porosidade, possuem os menores valores para a permeabilidade.

**Palavras-chave:** tafofácies, coquina, petrofísica, porosidade, permeabilidade.

## ABSTRACT

Coquina is a term used to sedimentary rocks composed mainly by shells and their fragments. This type of rock can have carbonate or siliciclastic grains as matrix, resulting in a diverse combination of its textural components. It is known that the conditions of the sedimentation environment and diagenetic process directly influence the preservation or modification of carbonate grains resulting in a great textural heterogeneity, directly affecting the preservation or not of the porous system and consequently influencing the permeability. The present study aims to interpret the depositional system for different types of coquina accumulations deposited during the rift phase in the Sergipe-Alagoas and Santos basins, comprising the Morro do Chaves and Itapema Formations, and what is their relation with porosity and permeability. Through the taphonomic characteristics, which are directly linked to the state of preservation, packaging and orientation of the shells, these rocks were classified as high and low energy taphofacies and interpreted within a depositional model. To porosity classification, the following methods were used: i) the use of thin sections, ii) x-ray tomography analysis from cores, iii) high resolution tomography from plugs and iv) nuclear magnetic resonance analysis (NMR). Through this data it was possible to segment the porous system and divide it according to: a) taphofacies with predominance of primary pores, b) taphofacies with equivalent values of primary and secondary pores and 3) tapofacies with predominantly secondary pores. As a result, it is observed that high energy taphofacies present the preserved primary porosity due to the removal of thinner grains, and associated with rework and selection processes. In the low energy facies, where the reworking processes is not effective, the porous system occurs mainly through the action of diagenesis that creates a diversity of secondary pores such as moldic and vugular. Regarding the permeability, the high energy taphofacies have the highest values, usually above 150 milliDarcy (mD) because the pores present good connectivity due to the preservation of primary pores as well as the creation of channels, favoring the fluid movement. Low-energy taphofacies have lower permeability values, usually below 150 mD due to the occurrence of isolated pores, vugular and moldic, as well as the occurrence of microporosity. Coquinas deposited in environments with high energy and high sorting degree, when favored by diagenesis, represent the best qualities of reservoir rocks while those of low degree of sorting, despite presenting good porosity results, have the lowest values for permeability.

**Keywords:** taphofacies, coquinas, petrophysics, porosity, permeability.

## SUMÁRIO

1.	INTRODUÇÃO .....	14
1.1.	Contextualização geológica e estratigráfica.....	16
1.1.1.	Bacia de Segipe-Alagoas.....	16
1.1.2.	Bacia de Santos .....	17
1.2.	Estrutura da tese .....	18
2.	RELAÇÃO ENTRE BIOFÁBRICA E POROSIDADE, COQUINAS DA FORMAÇÃO MORRO DO CHAVES (BARREMIANO/APTIANO), BACIA DE SERGIPE-ALAGOAS, NE-BRASIL .....	22
2.1.	INTRODUÇÃO .....	25
2.2.	CONTEXTO GEOLÓGICO REGIONAL E ÁREA DE ESTUDO .....	26
2.2.1.	Formação Morro do Chaves .....	27
2.3.	MATERIAIS E MÉTODOS .....	28
2.3.1.	Descrição de afloramento e coleta de amostras .....	28
2.3.2.	Análise de laboratório: descrição petrográfica e classificação da biofábrica .....	29
2.3.3.	Quantificação e classificação da porosidade.....	31
2.3.4.	Redes neurais: Self organizing Map .....	32
2.4.	RESULTADOS E DISCUSSÃO .....	33
2.4.1.	Análise de fácies.....	33
2.4.2.	Redes neurais e biofábrica .....	36
2.5.	RELAÇÃO ENTRE BIOFÁBRICA, AMBIENTE DEPOSICIONAL E POROSIDADE .....	41
2.6.	CONCLUSÃO .....	43
2.7.	REFERÊNCIAS.....	45
3.	A TAPHOFACIES INTERPRETATION FOR SHELL CONCENTRATIONS AND THEIR RELATIONSHIP WITH PETROPHYSICS: A CASE STUDY OF COQUINAS IN THE ITAPEMA FORMATION, SANTOS BASIN-BRAZIL.....	51
3.1.	INTRODUCTION .....	53
3.2.	GEOLOGICAL SETTING .....	54
3.2.1.	The Itapema Formation.....	55
3.3.	METHODS .....	56

3.3.1.	Taphofacies Classification .....	57
3.3.2.	Measurement and classification of porosity through thin sections .....	58
3.3.3.	Porosity from CT and H-CT scan .....	58
3.3.4.	Experimental analysis.....	58
3.4.	RESULTS.....	59
3.4.1.	Taphofacies characterization .....	59
3.4.2.	Diagenesis - General Aspects .....	65
3.4.3.	Porosity and permeability .....	67
3.5.	DISCUSSION.....	76
3.5.1.	Taphofacies Interpretation .....	76
3.5.2.	Origin of porosity .....	81
3.5.3.	NMR log comparison.....	85
3.6.	CONCLUSIONS .....	88
3.7.	REFERENCES .....	90
4.	RELATIONSHIP BETWEEN BIOFABRIC AND PETROPHYSICS IN COQUINAS, INSIGHTS ON BRAZILIAN BARREMIAN-APTIAN CARBONATES OF SANTOS AND SERGIPE-ALAGOAS BASINS.....	96
4.1.	INTRODUCTION .....	98
4.2.	COQUINAS SAMPLES .....	99
4.3.	METHODS.....	101
4.3.1.	Laboratorial analysis and H-CT acquisition .....	101
4.3.2.	Biofabric and porosity description .....	102
4.3.3.	Fluid flow properties .....	102
4.4.	RESULTS.....	102
4.4.1.	Biofabric characterization .....	102
4.4.2.	Porosity and permeability relationship.....	107
4.4.3.	Pore Network Modeling and Global Hydraulic Elements.....	109
4.5.	DISCUSSION.....	111
4.5.1.	Biofabric texture and porosity .....	111
4.5.2.	Porosity control, PNM and GHU.....	113
4.6.	CONCLUSION .....	119
4.7.	ACKNOWLEDGEMENTS .....	120
4.8.	REFERENCES .....	121

5. CONCLUSÃO .....	126
6. REFERÊNCIAS.....	128

## 1. INTRODUÇÃO

Nas últimas décadas, diversas notícias e artigos científicos foram publicados a respeito das descobertas dos reservatórios carbonáticos do pré-sal encontrados nas bacias de Campos e Santos, localizadas na porção offshore da costa leste brasileira, devido sua importância econômica (Abrahão e Warme, 1990; Mohriak et al., 1990; Guardado et al., 2000; Chang et al., 2008; Riccomini et al., 2012; Thompson et al., 2015). Dados da Agência Nacional do Petróleo referentes ao mês de novembro de 2019 (ANP, 2019) revelam que, a produção de petróleo e gás oriundos do pré-sal corresponderam a 65.5% do total produzido pelo Brasil, totalizando 2,588 milhões de barris de óleo equivalente por dia (MMboe/d). Essa produção recebeu um grande salto a partir das descobertas dos grandes campos localizados na Bacia de Santos, que hoje é responsável por mais da metade da produção do petróleo nacional, tendo como destaque o campo de Lula, com uma produção média de 1 MMboe/d (ANP, 2019).

Esses reservatórios são compostos por rochas sedimentares carbonáticas formadas durante a fase do rompimento do supercontinente Gondwana, que ocorreu entre o Jurássico superior e Cretáceo inferior, e resultou na separação do continente sul-americano e africano e na abertura do Oceano Atlântico Sul (Chang et al., 1992; Cainelli and Mohriak, 1999; Chang et al. 2008; Mohriak et al., 2008). Parte dessas rochas carbonáticas que compõe esse grande sistema petrolífero são os depósitos de coquinas pertencentes à Formação Coqueiros na Bacia de Campos, identificadas como rochas reservatório nos campos de Badejo e Linguado (ANP, 2017), e à Formação Itapema na Bacia de Santos, localizadas no campo de Libra (Carlotto et al., 2017).

O termo coquina se refere a rochas sedimentares cujo constituinte principal é representado por conchas de moluscos e seus fragmentos, e podem apresentar como constituintes secundários uma diversidade de grãos carbonáticos e/ou siliciclásticos (Kidwell, 1991). Esse tipo de rocha carrega uma diversidade de informações que podem ser utilizadas tanto por geólogos na correlação lateral de camadas e interpretação de ambientes deposicionais como também por paleontólogos no estudo de fósseis e reconstrução da paleoecologia. Na indústria petrolífera a importância de estudar os diferentes tipos de acumulação de coquinas (*shell beds ou shell concentrations*), é com relação ao entendimento de como essas rochas se distribuem em uma bacia sedimentar e quais os fatores geológicos envolvidos durante o seu processo de formação, assim como a variação de suas características petrofísicas.

Coquinas são amplamente descritas e interpretadas na geologia, principalmente em ambientes marinhos como apontado por Kidwell(1991) e apresentam uma grande diversidade

textural e espacial dentro de um ambiente deposicional. No entanto, publicações sobre a origem de coquinas de ambiente lacustre na proporção que ocorre nos reservatórios do pré-sal, é escassa. Além disso, afloramentos das formações que compõe as rochas do pré-sal não são observados ao longo das bacias, dificultando a compreensão de como esses depósitos se distribuem e quais as heterogeneidades envolvidas na qualidade de reservatório.

Na tentativa de compreender como são formados os depósitos do pré-sal, se faz necessário a utilização de afloramentos análogos, ou seja, aqueles que apresentam características similares quanto ao processo de formação ou, através da análise de testemunhos de sondagem obtidos durante o processo de perfuração de um poço de petróleo. Alguns trabalhos foram publicados abordando o ponto de vista do modelo deposicional como também sua variação petrofísica através do uso de afloramentos análogos, como os da Formação Morro do Chaves na Bacia de Sergipe-Alagoas (Figueiredo, 1981; Tavares et al., 2015; Corbett et al., 2016; Luna et al., 2016; Belila et al., 2018; Chinelatto et al., 2018), como também através da análise de testemunho das rochas reservatório da Formação Coqueiros na Bacia de Campos (Carvalho et al., 2000; Herlinger et al., 2017; Mizuno et al., 2018; Muniz e Bosence, 2018; Oliveira et al., 2019). Muitos desses trabalhos utilizam das características tafonômicas e sedimentares, que descrevem a biofábrica das coquinas, como também as estratigráficas para a interpretação de como foram formados. Essas características são consideradas as mais importantes para a interpretação de concentrações conchíferas como apontado por Kidwell (1991).

Como resultado, essas coquinas foram interpretadas como depósitos localizados em plataformas carbonáticas de águas rasas, geralmente associadas a ambientes de alta energia, com ação de ondas e correntes de fundo, que retrabalham as conchas e formam concentrações com características texturais distintas. Os depósitos apresentam diferentes tipos de grãos carbonáticos e siliciclásticos, com diversidade granulométrica, como também uma grande variação de seleção e de processos diagenéticos.

A variedade dos grãos carbonáticos, como também a variação do ambiente deposicional e diagenético, influencia diretamente na complexidade do sistema poroso e consequentemente na permeabilidade resultando em uma grande heterogeneidade petrofísica (Lucia, 1999; Lønøy, 2006). Autores como Corbett et al. (2016, 2017), Luna et al. (2016), Herlinger et al. (2017), Belila et al. (2018) e Zielinski et al. (2018) abordam a variação dos parâmetros petrofísicos nas coquinas, como a variação e distribuição de tamanho de poros, garganta de poro e conectividade entre eles. No entanto, pouco debate é apresentado

sobre qual é relação entre os processos sedimentares e diagenéticos nas coquinas que resultam em um determinado tipo de biofábrica e qual sua relação com a porosidade e permeabilidade.

Nesse contexto, essa tese de doutorado visa a interpretação dos depósitos de coquinas através da tafonomia e sua relação com as características petrofísicas. Nesse trabalho foram utilizadas amostras do afloramento da Formação Morro do Chaves (Bacia de Sergipe-Alagoas) e de testemunho de sondagem da Formação Itapema (Bacia de Santos), a fim de reconhecer quais os processos deposicionais e diagenéticos resultam em diferentes tipos de biofábricas e quais os fatores que controlam a variedade dos tipos de poro e consequentemente as respectivas permeabilidades.

### **1.1. Contextualização geológica e estratigráfica**

As bacias de Sergipe-Alagoas e de Santos, foram formadas durante o processo de rompimento do supercontinente Gondwana entre o Jurássico superior e Cretáceo inferior (Chang et al., 1992; Cainelli and Mohriak, 1999; Chang et al. 2008; Mohriak et al., 2008). Essa separação ocorreu em diversos processos de intensa atividade e quiescência tectônica apresentando uma variedade de sistemas deposicionais e litotipos. Durante o processo de separação dos continentes, ocorreu o afinamento da crosta terrestre gerando um sistema de falhas e fraturas formando estruturas tectônicas como horsts e grâbens, e também intenso vulcanismo na região sul e sudeste (Cainelli and Mohriak, 1999; Mohriak et al., 2008). Esse período é caracterizado tectonicamente como o estágio rifte e ocorre em todas as bacias da margem leste brasileira. Nesse período em que as Formações Morro do Chaves e Itapema, objeto do estudo, estão inseridas, depositadas entre as idades do Barremiano e Aptiano.

#### **1.1.1. Bacia de Sergipe-Alagoas**

A Bacia de Sergipe-Alagoas está localizada na região nordeste do Brasil compreendendo os estados de Sergipe, Alagoas e Pernambuco, cobrindo uma área equivalente a 44.370 Km<sup>2</sup>(ANP, 2013), apresenta seu limite norte com a Bacia de Pernambuco-Paraíba pelo alto de Maragogi e a sudoeste com a Bacia de Jacuípe (Campos-Neto et al., 2007). A bacia foi subdividida em quatro estágios tectônico-estratigráficos (mega-sequências) bem definidos, sendo eles: i) sinéclise, ii) pre-rifte, iii) rifte e, iv) margem passiva – pós rifte - drifte (Campos-Neto et al., 2007).

Sob condições intracratônicas, duas Formações foram depositadas durante a fase de sinéclise, a Formação Batinga, representadas por rochas siliciclásticas depositadas em ambiente glacial subaquoso e, a Formação Aracaré, representada por depósitos siliciclásticos de ambientes desérticos, litorâneos e deltaico. A fase pré-rifte apresenta os depósitos de folhelhos vermelhos lacustres da Formação Bananeiras, arenitos fluvio-deltaicos da Formação Candeeiro como também arenitos fluviais da Formação Serraria. A fase rifte apresenta os seguintes depósitos: lacustres-deltaicos da Formação Feliz Deserto, fluviais e aluviais da Formação Penedo, aluvias da Formação Pitanga, lacustres da Formação Morro do Chaves, fluvio-deltaico da Formação Coqueiro Seco, deltaico lacustre da Formação Barra de Itiúba e alívio-deltaicos da Formação Maceió. A fase pós rifte foi instaurado condições de golfo restrito seguido por mar aberto, compreendendo os depósitos aluvio-deltaicos, sabkha e de plataforma carbonáticas das Formações Muribeca e Riachuelo, seguido pelos depósitos de rampa carbonáticas da Formação Cotinguba. Com o rebaixamento do nível do mar, com transição de depósitos profundos a costeiros, foram depositadas as rochas do Grupo Piaçabuçu com ocorrência de transição de plataforma carbonáticas para siliciclástica.

### **1.1.2. Bacia de Santos**

A Bacia de Santos está localizada na região sudeste da margem continental brasileira, compreendendo o litoral dos estados do Rio de Janeiro, São Paulo, Paraná e Santa Catarina, cobrindo uma área equivalente a 350.000 Km<sup>2</sup>. O seu limite norte se dá com a Bacia de Campos pelo alto de Cabo Frio e ao sul com a Bacia de Pelotas pela Plataforma de Florianópolis (Moreira et al., 2007). Diferente da Bacia de Sergipe-Alagoas, a Bacia de Santos foi subdividida em três estágios tectônico-estratigráficos sendo eles: i) rifte, ii) pós rifte/Sag e iii) drifte (Moreira et al., 2007).

A base da sequência rifte é caracterizada pelos derrames basálticos da Formação Camboriú, seguidos pelos depósitos de conglomerados, arenitos, siltitos e folhelhos da Formação Piçarras como também pela sequência de coquinas e folhelhos da Formação Itapema. A sequência pós-rifte é marcada pela ocorrência de um ambiente transicional composta pelos carbonatos da Formação Barra Velha seguido pelos evaporitos da Formação Ariri. A sequência drifte é representada pelos depósitos carbonáticos e siliciclásticos dos Grupos Camboriú, Fraude e Itamambuca que representam sedimentos marinhos e não marinhos associado a eventos transgressivos e regressivos (Moreira et al., 2007).

## 1.2. Estrutura da tese

Essa tese de doutorado é organizada na forma de três artigos que serão descritos a seguir. O artigo 1 aborda a influência da biofábrica com o tipo de porosidade das coquinas da Formação Morro do Chaves. No total foram utilizadas 20 amostras de coquinas das quais tiveram uma das faces cortadas para classificação da biofábrica em uma escala macroscópica, como também a confecção de lâmina delgada das quais foram utilizadas para classificação da biofábrica em escala microscópica como também para a classificação da porosidade. Utilizando de dados tafonômicos e de porosidade foi possível realizar o agrupamento das amostras utilizando técnicas de Redes Neurais conhecida como SOM (*Self-Organizing Map / Mapa Auto Organizável*). Como resultado, três grandes grupos foram identificados de acordo com o valor de porosidade, sendo eles baixa, média e alta porosidade.

No grupo de baixa porosidade, foram identificadas coquinas com características tafonômicas e sedimentares produtos de ambientes deposicionais de baixa energia, sendo classificados como packstones e wackestones. De maneira geral, as amostras apresentaram baixa seleção, alto conteúdo de matriz fina, alto grau de preservação de conchas e pouca ou nenhuma ocorrência da porosidade primária, onde a maior parte dos poros são produtos da dissolução de conchas e fraturas. Os grupos de média e alta porosidade são representados por amostras que apresentaram características de ambientes de maior energia. Essas amostras são representadas por grainstones e rudstones, com conchas que apresentaram alto grau de fragmentação e abrasão, características observadas em ambientes onde há retrabalhamento e maior seleção. Nesses grupos a porosidade primária é preservada devido a remoção de materiais finos no espaço entre as valvas e amplificada pela ação da diagênese, onde são criados poros móldicos e vugulares.

O artigo 2 aborda um estudo de caso para as coquinas da Formação Itapema da Bacia de Santos. Esse trabalho faz uma interpretação de ambiente deposicional usando do conceito de tafofácies relacionando-o com dados petrofísicos. Foram disponibilizados aproximadamente 12 metros de testemunho com 40 lâminas delgadas e 10 plugues para análise. Para o estudo petrofísico utilizou-se de dados de lâmina delgada, ressonância magnética nuclear (RMN) de plugue e poço, porosidade e permeabilidade a gás e imagens de tomografia e tomografia de alta resolução de testemunho e plugues. Seis tafofácies foram propostas nesse trabalho e posteriormente agrupadas como coquinas bem selecionadas, compostas principalmente por conchas inteiras e seus fragmentos das mal selecionadas, que

apresentaram outro tipo de grão carbonático inferior a 0.2 mm, como peloids, ostracodes e micrita.

De maneira geral, coquinas que passaram por um processo de retrabalhamento, associados a ambientes de maior energia, como em regiões de praia por exemplo, foram classificadas como tafofácies bem selecionadas. Esse tipo de rocha pode ser encontrada nas regiões proximais nas bordas de lago e formam depósitos como barras de coquinas ou bermas que podem ser depositadas durante eventos de tempestade. Esse grupo apresenta um controle da porosidade que varia de deposicional a híbrido. A preservação da porosidade primária nesse grupo está associada aos processos deposicionais que favorecem a seleção dos grãos e remoçãodos grãos finos. A atuação da diagênese contribui ainda mais com o aumento do espaço poroso, permitindo uma melhor comunicação entre os poros primários e secundários influenciando diretamente nos altos valores de permeabilidade.

As coquinas que foram agrupadas com baixo grau de seleção, foram interpretadas como sendo produtos de depósitos cuja energia não foi suficiente para remover os materiais finos, geralmente associados a regiões próximas a fundo de lago ou áreas protegidas. Nesse grupo de amostras a porosidade varia de controle híbrido a diagenético, pouca porosidade primária é preservada devido ao baixo grau de seleção, como também pela cimentação por calcita.No entanto, poros móldicos e vugulares ocorrem,contribuindo com altos valores de porosidade. Devido à baixa conectividade associada tanto aos processos deposicionais e diagenéticos, esse grupo de amostras apresentou os menores valores de permeabilidade. Por fim, realizamos uma comparação dos resultados de RMN obtidos em cada tipo de biofábrica com perfil de ressonância de poço (RMN) a fim de identificar a variação da porosidade e permeabilidade em um reservatório real.

O artigo 3 é um conjunto de dados obtidos a partir dos dois primeiros, abordando a relação da biofáfrica com parâmetros petrofísicos. Esse artigo tem como objetivo o agrupamento das coquinas da Formação Morro do Chaves e Itapema e buscar dentre elas o padrão do controle da porosidade em diferentes tipos de biofábrica. Nesse trabalho foram utilizados dados de porosidade e permeabilidade a gás como também análise de imagens de tomografia de plugues de coquina, em alta resolução. As amostras foram agrupadas de acordo com as características de sua biofábrica e de acordo com o controle da porosidade.

Como resultado observamos que o controle da porosidade varia de deposicional a diagenético e sugerimos uma equação de tendência para a relação "porosidade vs. permeabilidade" para grupo como também, sua distribuição dentro de unidades de fluxo denominadas como *Global Hydraulic Elements (GHE)*. Como produto final, utilizando a

segmentação da porosidade em tomografia de alta resolução, foi possível segmentar o sistema poroso e observar como se distribui os poros e gargantas de poro e relacionar o tipo de biofábrica com a porosidade total e permeabilidade.

Biofábricas que apresentaram um controle deposicional da porosidade apresentam uma boa relação entre porosidade e permeabilidade, onde os altos valores estão relacionados tanto às características de boa seleção como também preservação da biofábrica e da porosidade primária. Amostras que apresentaram baixos valores estão relacionadas com os processos deposicionais e diagenéticos, onde há baixa seleção e ocorrência de cimentação e compactação. Biofábricas com controle híbrido a diagenético podem conter biofábricas com alto ou baixo grau de seleção como também de preservação. No geral as amostras que apresentaram os melhores valores de porosidade e permeabilidade foram aquelas com maior preservação de porosidade primária, devido as condições do ambiente deposicional, como também o alargamento da porosidade por dissolução. Rochas com alto valores de porosidade e baixos valores de permeabilidade geralmente foram associados a biofábricas com baixo grau de seleção, alto grau de cimentação e, alto grau de dissolução de conchas, que resultou em poros mólicos e vugulares isolados. Esse grupo de amostras apresenta baixa conectividade como também alta frequência de gargantas de poros apertadas, influenciando diretamente nos baixos valores de permeabilidade.

O título e autores dos artigos, assim como sua situação até a data de 10/01/2020 são apresentados a seguir:

**Artigo 1: Relação entre biofábrica e porosidade, coquinas da Formação Morro do Chaves (Barremiano/Aptiano), Bacia de Sergipe-Alagoas, NE-Brasil**

*Guilherme Furlan Chinelatto, Michelle Chaves Kuroda, Alexandre Campane Vidal.*

Artigo publicado em: *Geologia USP, série científica, v. 18(4), p. 57-72 – dezembro de 2018.*

**Artigo 2: A taphofacies interpretation of Shell Concentrations and their relationship with petrophysics: A case study of Barremian-Aptian Coquinas in the Itapema Formation, Santos Basin-Brazil.**

*Guilherme Furlan Chinelatto, Aline Maria Poças Belila, Mateus Basso, João Paulo Ponte Souza, Alexandre Campane Vidal.*

Artigo aceito: *Marine and Petroleum Geology.*

**Artigo 3:Relationship between biofabric and petrophysics in coquinas, insights on Brazilian Barremian-Aptian carbonates of Santos and Sergipe-Alagoas Basins.**

*Guilherme Furlan Chinelatto, Aline Maria Poças Belila, Mateus Basso, João Paulo Ponte Souza, Alexandre Campane Vidal.*

**Artigo será submetido**

**2. RELAÇÃO ENTRE BIOFÁBRICA E POROSIDADE, COQUINAS DA FORMAÇÃO MORRO DO CHAVES (BARREMIANO/APTIANO), BACIA DE SERGIPE-ALAGOAS, NE-BRASIL.**

*Biofabric and porosity relationship in coquinas, Morro do Chaves Formation  
(Barremian/Aptian), Sergipe-Alagoas Basin, Brazil-NE.*

Relação entre biofábrica e porosidade em coquinas.

Guilherme Furlan Chinelatto<sup>1</sup>, Michelle Chaves Kuroda<sup>1</sup>, Alexandre Campane Vidal<sup>1</sup>

<sup>1</sup>Universidade Estadual de Campinas - UNICAMP, Departamento de Geologia e Recursos Naturais, Centro de Estudos do Petróleo (DGRN - CEPETRO), Rua 6 de Agosto, 50, 1º andar, Reitoria V, CEP 13083-873, Barão Geraldo, Campinas, SP, BR

(gfchinelatto@gmail.com; mckuroda@gmail.com; [yidal@ige.unicamp.br](mailto:yidal@ige.unicamp.br))

Recebido em 10 de novembro de 2017; aceito em 1º de outubro de 2018

<https://doi.org/10.11606/issn.2316-9095.v18-140513>

**RELAÇÃO ENTRE BIOFÁBRICA E POROSIDADE, COQUINAS DA FORMAÇÃO  
MORRO DO CHAVES (BARREMIANO/APTIANO), BACIA DE SERGIPE-  
ALAGOAS, NE-BRASIL.**

**RESUMO**

As coquinas da Formação Morro do Chaves são consideradas rochas análogas aos reservatórios da fase rifte do pré-sal nas bacias de Campos e Santos, são compostas principalmente por conchas e fragmentos de bivalves revelando uma grande variedade da biofábrica e do sistema poroso que possibilita o uso da tafonomia para relacionar o ambiente deposicional dessas rochas com as características de porosidade. Os principais atributos tafonômicos abordados nesse trabalho são: orientação das valvas; empacotamento das conchas; granulometria e seleção; e grau de fragmentação, abrasão e arredondamento. A interpretação dos dados teve como objetivo agrupar as amostras com relação às diferentes características tafonômicas e a porosidade, tendo como ferramenta auxiliar o método de redes neurais artificiais (Self-Organization Map — SOM). A análise dos dados resultou em três agrupamentos: A1 com altos valores de porosidade (entre 11 e 23%), cujas características tafonômicas revelam ambientes de alta energia; A2 com valores intermediários de porosidade (entre 7 e 15%), cujas características tafonômicas indicam um ambiente de transição entre alta e baixa energia; por fim, o grupo A3 com menores valores de porosidade (entre 0 e 7%), cuja tafonomia indica ambientes de baixa energia. Como resultado final, as características tafonômicas revelam a energia do ambiente deposicional e é possível associar ambientes de alta energia com as altas porosidades para as coquinas da Formação Morro do Chaves.

Palavras-chave: Tafonomia, Coquina, Porosidade, Formação Morro do Chaves.

## ABSTRACT

Coquinas of Morro do Chaves Formation are analogous rocks of pre-salt reservoirs of Campos and Santos basins; they are mainly composed by shells and fragments of bivalves that present a great variability of biofabric and porous system, which allows the use of taphonomy to relate their depositional environment. The main taphonomic attributes in this work are: valve orientation; shell packing; granulometry and selection; degree of fragmentation, abrasion and roundness. The interpretation of data had as objective grouping the samples according to different taphonomic patterns and porosity, using the artificial neural networks method (Self-Organization Map — SOM) as auxiliary tool. The analysis of data resulted in 3 clusters: A1 with high porosity values (between 11 and 23%) whose taphonomic characteristics reveal a high energy environment; A2 with intermediate values of porosity (between 7 and 15%) whose taphonomic characteristics indicate a transition environment between high and low energy; finally, group A3 with lower values of porosity (between 0 and 7%) whose taphonomy indicates low energy environments. As a final result, the taphonomic characteristics reveal the energy of the depositional environment and it is possible to associate high energy environments with the high porosities for the Coquinas of the Morro do Chaves Formation.

Keywords: Taphonomy, Coquina, Porosity, Morro do Chaves Formation.

## 2.1. INTRODUÇÃO

Os reservatórios carbonáticos constituem aproximadamente 50 - 60% de toda reserva de hidrocarbonetos no mundo (Ramakrishnan et al., 2001; Bust et al., 2011; Burchette, 2012), são de uma natureza diversa com relação a sua formação e podem apresentar um complexo sistema poroso. De maneira geral, esses reservatórios se diferenciam dos siliciclásticos devido ao tipo de produção de sedimentos e da reatividade química de minerais carbonáticos (Ehrenberg e Nadeau, 2005), resultando em rochas com grande diversidade textural e petrofísicas.

Nas últimas décadas, reservas de petróleo em carbonatos foram encontradas em águas ultra profundas na margem continental brasileira, abrangendo as bacias de Campos e Santos (Chang et al., 2008; Riccomini et al., 2012). Alguns desses reservatórios foram descobertos abaixo da sequência de evaporitos, denominados de pré-sal, e são compostos por rochas carbonáticas lacustres, predominantemente coquinas e microbialitos (Baumgarten et al., 1988; Carvalho et al., 2000; Riccomini et al., 2012; Muniz e Bosence, 2015). O acesso a essas rochas é feito por meio de furos de sondagens por conta da ausência de afloramentos em superfície e, por esse motivo, o uso de depósitos análogos pode auxiliar na compreensão desses reservatórios. As coquinas da Formação Morro do Chaves são consideradas análogas às coquinas do pré-sal na Bacia de Campos (Abrahão e Warme, 1990). Entender como se formaram, como se distribuem e quais os principais fatores que controlam suas características petrofísicas pode auxiliar na exploração das reservas do pré-sal.

A caracterização das propriedades petrofísicas em coquinas é um grande desafio para a indústria petrolífera devido sua heterogeneidade geológica referente aos processos de sedimentação (Carvalho et al., 2000; Thompson et al., 2015; Tavares et al., 2015; Corbett et al., 2016), além das alterações provocadas pela diagênese (Tavares et al., 2015; Corbett et al., 2016).

De maneira geral, os trabalhos que buscam relacionar as características geológicas e petrofísicas, em arenitos e carbonatos, têm como foco a caracterização da porosidade e da permeabilidade em função de características texturais, deposicionais e diagenéticas (Scherer, 1987; Ferm et al., 1993; Makhlofiet et al., 2013).

A tafonomia é um ramo da ciência que estuda os processos de fossilização, com enfoque no *habitat*, nos processos de transporte, na sedimentação e na diagênese dos organismos. Por meio das características tafonômicas e sedimentares é possível interpretar as condições de energia e paleoambientais envolvidas nos processos de sedimentação.

Com referência às coquinas, as assinaturas tafonômicas são utilizadas de forma rotineira para a caracterização geológica dessas rochas, sendo importante as informações sobre tamanho, orientação, fragmentação e abrasão das conchas, como também quantidade de matriz (Kidwell, 1986; Kidwell et al., 1986; Kidwell e Holland, 1991; Fürsich e Oschmann, 1993).

Como forma de avaliar a correlação entre propriedades geológicas e petrofísicas, este trabalho buscou avaliar a influência de algumas assinaturas tafonômicas sobre a porosidade macro (amostra de mão) e meso (lâmina delgada) de amostras de coquinas da Formação Morro do Chaves.

## **2.2. CONTEXTO GEOLÓGICO REGIONAL E ÁREA DE ESTUDO**

A Formação Morro do Chaves está inserida na Bacia de Sergipe-Alagoas, uma bacia da margem passiva brasileira, localizada na região Nordeste do Brasil entre os paralelos 9 e 11° sul. O limite norte da bacia é atribuído ao Alto Maragogi e o sul, ao sistema de falhas Vaza Barris; conta com uma área de aproximadamente 33 mil km<sup>2</sup>: 13 mil km<sup>2</sup> em sua área emersa e 20 mil km<sup>2</sup> referente à submersa (Feijó, 1994).

A bacia desenvolveu-se durante a separação do supercontinente Gondwana com diferentes estágios de evolução tectônica. As fases de separação da bacia se deram em sinéclise, pré-rifte, rifte e margem passiva (drifte) (Campos Neto et al., 2007). A Formação Morro do Chaves depositou-se durante a fase rifte da bacia.

Essa formação é constituída por sedimentos carbonáticos do tipo coquina e siliciclásticos representados por folhelhos e arenitos, caracterizando um sistema lacustre desenvolvido em um semi-gráben durante a fase rifte (Figueiredo, 1981; Feijó, 1994; Souza-Lima et al., 2002; Campos-Neto et al., 2007)

No intervalo estratigráfico referente à fase rifte, a bacia é compartimentada por um sistema em meio-gráben mergulhando para sudeste, sendo constituída de um conjunto de falhas normais N-S interceptado por falhas E-W e NE-SW, resultando em uma configuração NE-SW *en-échelon* (Ojeda e Fugita, 1976 *apud* Souza-Lima et al., 2002; Lana e Milani, 1986; Van Der Ven et al., 1989).

A bacia conta com altos e baixos estruturais, nos quais os altos são de dois tipos: *horsts* e estruturas dônicas. Os horsts são alongados na direção N-S cujas falhas separam o meio-gráben, as estruturas dônicas se mostram arqueadas como produto de esforços associados ao cisalhamento (Lana e Milani, 1986; Lana, 1990).

O preenchimento sedimentar ocorreu por meio das diferentes fases tectônicas que atuaram na bacia; cada compartimento sofreu processos de soerguimento ou subsidência de modo desigual ao longo do tempo, o que resultou em uma distribuição espacial bastante complexa das unidades estratigráficas (Aquino e Lana, 1990).

### **2.2.1. Formação Morro do Chaves**

A Formação Morro do Chaves apresenta coquinas de bivalves como litologia predominante, intercaladas com folhelhos e arenitos depositados em diferentes pulsos tectônicos (Campos Neto et al., 2007). Essas rochas carbonáticas são interpretadas como depósitos lacustres rasos em razão da ausência de fósseis marinhos (Petri, 1962; Figueiredo, 1981) e da ocorrência de ostracodes não marinhos (*Hourcqia africana*). No entanto, estudos recentes sugerem certa influência marinha por conta da descoberta de fósseis típicos desse ambiente (Gallo et al., 2010; Garcia, 2012, 2016; Thompson, 2013). Os depósitos foram acumulados em altos estruturais em um sistema de rampa suave, onde extensas camadas de bivalves foram depositadas em ambiente raso e de alta energia (Figueiredo, 1981; Kinoshita, 2010; Tavares et al., 2015; Chinelatto et al, 2018).

O contato superior entre a Formação Morro do Chaves e a Formação Coqueiro Seco é erosivo ou gradacional para depósitos clásticos na sub-bacia de Sergipe, enquanto na sub-bacia de Alagoas é marcado pela ocorrência de um calcário gredoso (chalky). Em direção à margem da bacia, a unidade migra lateralmente para os depósitos da Formação Rio Pitanga (Schaller, 1969).

As coquinas da Formação Morro do Chaves têm sido alvo de diversos estudos (Kinoshita, 2010; Belila, 2014; Tavares et al., 2015; Corbett et al., 2016; Menezes et al., 2016; Chinelatto et al., 2018). Entre esses trabalhos, alguns são voltados à utilização de dados tafonômicos para interpretação do ambiente deposicional e explicar a evolução dos depósitos (Tavares et al., 2015; Chinelatto et al., 2018).

Com a interpretação de tafofácies, esses trabalhos ilustram a evolução das coquinas como depósitos rasos, profundos e de tempestade variando suas características texturais. As coquinas interpretadas como de ambiente raso não apresentam material argiloso, são compostas por conchas de bivalves e fragmentos de conchas; os bioclastos são arranjados preferencialmente concordantes com o acamamento e apresentam um empacotamento denso. É possível observar conchas com sinais de abrasão e a micritização dos bioclastos é baixa. Acumulações profundas apresentam matriz argilosa, diferente das coquinas rasas; estas apresentam menor concentração de bioclastos fragmentados caracterizando um

empacotamento frouxo a disperso. É comum a ocorrência de valvas fechadas e bordas bem micritizadas. Os depósitos de tempestade podem ou não conter matriz argilosa, as conchas de bivalves não apresentam uma orientação preferencial e, de maneira geral, os bioclastos são desarticulados, embora valvas fechadas possam ocorrer. Fragmentos de conchas são comuns e o empacotamento pode variar de frouxo a denso. Nesse tipo de acumulação, é comum a ocorrência de superfícies erosivas na base.

### **2.3. MATERIAIS E MÉTODOS**

#### **2.3.1. Descrição de afloramento e coleta de amostras**

O afloramento utilizado para o estudo está localizado na pedreira CIMPOR Cimentos, na cidade de São Miguel dos Campos, Alagoas, com acesso por meio da Rodovia Governador Mario Covas (AL-220), km 135. A cava da pedreira tem extensão norte-sul de aproximadamente 1 km e seção vertical próxima a 60 m. O embasamento na área de estudo compreende paragnaisse e migmatitos do Complexo Arapiraca. Depósitos sedimentares pós-proterozoicos do Grupo Coruripe são aflorantes, principalmente a Formação Coqueiro Seco (Cretáceo Inferior), depositada concomitantemente à Formação Morro do Chaves. Acima dessas unidades, depósitos do Grupo Barreiras ocorrem assim como sedimentos aluvionares do quaternário (Figura 1).

Na etapa de campo, foram levantadas seções geológicas identificando as principais litologias utilizando da classificação de Dunham (1962) e Embry e Klovan (1971), onde diferentes fácies de coquinas foram amostradas e encaminhadas ao laboratório. As características utilizadas para diferenciar os tipos de coquina foi com relação ao estado de preservação das conchas, à quantidade de matriz e à qualidade do espaço poroso. As amostras são representativas da variabilidade da biofábrica das coquinas encontrada em afloramento, principalmente com relação ao grau de fragmentação e orientação das conchas, à granulometria média e ao tipo de matriz. Para esse trabalho foram coletadas 20 amostras com volume próximo a 2.000 cm<sup>3</sup> cada e orientadas em relação ao acamamento e à direção do topo.

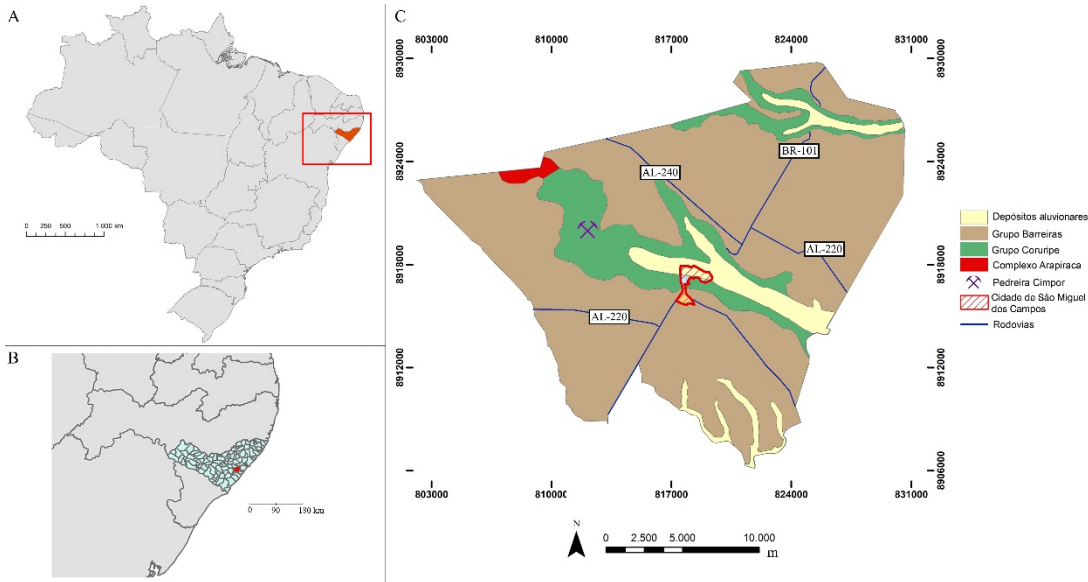


**Figura 1.** (A) Mapa dos estados brasileiros (em destaque o estado de Alagoas); (B) municípios do estado de Alagoas (em destaque a cidade de São Miguel dos Campos); (C) mapa geológico do município de São Miguel dos Campos (modificado de CPRM, 2009).

### 2.3.2. Análise de laboratório: descrição petrográfica e classificação da biofábrica

A análise petrográfica se baseou na descrição de lâminas delgadas e na análise de imagens escaneadas de rocha, onde foi possível desenhar e quantificar as conchas observadas. Esse processo foi realizado utilizando do *software* editor de imagem *Inkscape*. As imagens foram obtidas por meio de cortes perpendiculares em relação ao plano do topo/base de cada amostra e posteriormente analisadas em escala macro de alta resolução (1.200 dpi).

Para a classificação da biofábrica foram utilizados os parâmetros sugeridos por Kidwell e Holland (1991) e Kidwell (1991) de granulometria, seleção, densidade de empacotamento das conchas, orientação das valvas, e grau de fragmentação.

Os parâmetros tafonômicos foram quantificados a partir das imagens digitalizadas da rocha; 50 – 100 bioclastos vizinhos/adjacentes foram computados para o levantamento dos dados. A análise petrográfica foi utilizada também para a obtenção de parâmetros tafonômicos, principalmente na determinação do grau de fragmentação e abrasão das conchas.

#### Orientação das valvas

A classificação da orientação das valvas segue o modelo proposto por Kidwell (1991), que a divide nas seguintes categorias:

1. concordante;
2. oblíquo;
3. vertical em relação ao plano de acamamento.

Dessa forma, conchas que apresentam concavidade voltada para baixo ou para cima e são paralelas ao acamamento são consideradas concordantes; quando dispostas inclinadas, são consideradas oblíquas; e quando inclinadas próximas a 90 graus ao acamamento, são definidas como verticais (Figura 2A). Biofábrica que apresentasse conchas empilhadas ou aninhadas (*nested*, em inglês) também foi mencionada, no entanto não foi quantificada individualmente.

Rochas que apresentam mais de 45% de conchas concordantes ao acamamento foram classificadas como coquinas com biofábrica concordante, e as demais como coquinas com biofábrica caótica.

#### *Granulometria, seleção e densidade de conchas*

De acordo com Kidwell e Holland (1991), a seleção varia entre três parâmetros: bem selecionada, bimodal e mal selecionada, dentro da escala granulométrica *phi* (Figura 2B). Rochas bem selecionadas são aquelas que apresentam por volta de 80% da concentração de bioclastos entre 1 – 2 escalas adjacentes de granulometria. Seleção bimodal pode aparentar uma boa seleção, no entanto apresentam ocorrências de granulometrias muito distantes umas das outras dentro da escala granulométrica, por exemplo, uma rocha com domínio de granulometria em -1 e -4 *phi* seria considerada uma distribuição bimodal. Rochas com má seleção são aquelas que apresentam 80% de sua distribuição granulométrica entre 3 ou mais classes.

Quanto à densidade de conchas, Kidwell e Holland (1991) classificam como empacotamento denso, frouxo e disperso (Figura 2C). O empacotamento denso representa rochas bioclasto suportadas, onde o contato bioclasto-bioclasto é comum, normalmente observado em *rudstones* e *grainstones*. O empacotamento frouxo representa rochas cujo contato bioclasto-bioclasto é menor e o espaçamento entre eles é pequeno (menor que o seu tamanho de corpo); normalmente, os bioclastos encontram-se flutuantes na matriz e podem ser representados por *packstones* e *wackestones*. O empacotamento disperso representa rochas onde os bioclastos estão dispersos na matriz, espaçados por uma distância maior que o comprimento máximo das valvas e podem ser representados por *wackestones* e *mudstones*.

#### *Grau de fragmentação*

Três classes foram propostas neste trabalho para classificar a fragmentação das conchas em coquinas: baixa (0), média (1) e alta (2) (Figura 2D), com base na análise visual da biofábrica. O baixo grau de fragmentação (0) corresponde a conchas bem preservadas em uma matriz micrítica ou esparítica, onde há pouco fragmento de concha e predomínio de conchas inteiras. O grau de fragmentação médio (1) corresponde a conchas parcialmente

preservadas em uma matriz com menor densidade de fragmentos bioclásticos, há o predomínio de conchas inteiras em relação a fragmentadas. Por último, o alto grau de fragmentação (2) corresponde a bioáfricas que apresentam conchas bem fragmentadas, onde parte da matriz é composta por fragmentos de concha e ocorrem raras valvas totalmente preservadas.

Para a classificação de abrasão/arredondamento também foi proposto três categorias (Figura 2D): valvas sem sinais de abrasão com bordas de conchas preservadas (0), valvas com pouco sinal de abrasão, cujas bordas apresentam ligeiros sinais de arredondamento e desgaste (1) e valvas bem arredondadas (2).

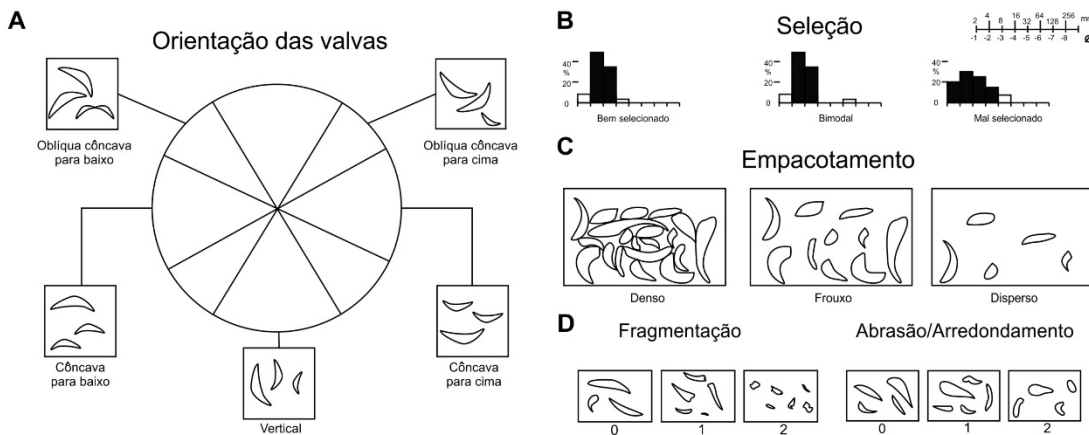


**Figura 2.** Características tafonômicas (adaptado de Kidwell e Holland, 1991). (A) Orientação das valvas; (B) seleção; (C) empacotamento das conchas; (D) fragmentação, abrasão e arredondamento das valvas..

### 2.3.3. Quantificação e classificação da porosidade

A quantificação da porosidade foi realizada a partir das imagens de lâminas delgadas através do software *Imago*. Esse software é capaz de isolar o espaço poroso dos sólidos resultando em uma imagem binarizada em dois tons, geralmente branco e preto, onde é possível quantificar em porcentagem o espaço poroso. A binarização pode ser realizada das seguintes maneiras: por meio de histogramas RGB, HSI ou por meio das redes neurais. Utilizou-se o método de redes neurais no processo de binarização, no qual o usuário seleciona o campo de cores que corresponde a poro e não poro. As imagens digitais foram obtidas a partir de câmera fotográfica acoplada a um microscópio petrográfico com aumento de 10 vezes. Diversos pesquisadores utilizam o método de binarização para quantificar a porosidade

em rochas (Anselmetti et al., 1998; Mazurkiewicz e Mlynarczuk, 2013; Rego e Bueno, 2015; Datta et al., 2016).

A classificação da porosidade segue o modelo proposto por Choquette e Pray (1970), que classifica o espaço poroso em categorias seletivas ou não seletivas quanto à fábrica.

#### **2.3.4. Redes neurais: Self organizing Map**

Neste trabalho, o método de redes neurais SOM (*Self-Organizing Map* — Mapa Auto-Organizável) foi aplicado para avaliar a relação entre as propriedades tafonômicas e a porosidade. Desenvolvido por Kohonen (2001), SOM não requer conhecimento prévio para identificação de classes. A técnica é formada por nós conectados, também chamados de neurônios, que formam uma rede, dando nome ao algoritmo (Figura 3).

O método tem como objetivo ajustar a localização dos neurônios na malha, adaptando a rede aos dados de entrada por meio da distância Euclidiana entre eles. Assim, o método aproxima os nós das amostras de entrada mais próximas e, portanto, semelhantes, e os distâncias das divergentes, mais distantes. Visto que o método adapta não só o neurônio mais próximo da amostra de entrada, mas também os seus vizinhos, a rede mantém a topografia do mapa.

Uma vez que a saída do algoritmo é uma malha de neurônios em duas dimensões, é possível avaliar visualmente os agrupamentos por meio do mapa de distâncias entre os neurônios, chamado de Matriz-U. Nesta matriz, as cores quentes representam maiores distâncias e estão associadas a neurônios com padrões distintos, enquanto cores frias representam neurônios próximos com padrões similares. Além disso, os mapas das projeções das variáveis de entrada auxiliam o intérprete na identificação das características dos grupos identificados pela técnica. Detalhes do funcionamento da rede neural estão presentes no trabalho de Kohonen (2001).

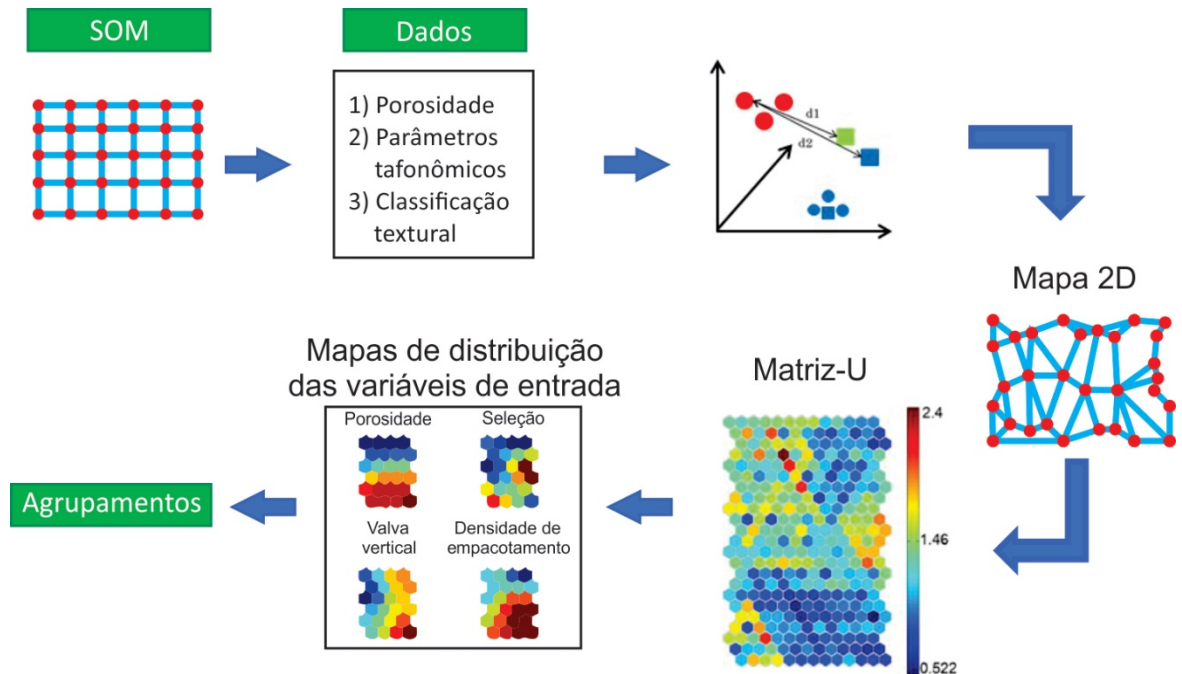


**Figura 3.** Fluxograma do algoritmo Self-Organization Map treinado com dados de porosidade e parâmetros tafonômicos. O método calcula as distâncias Euclidianas entre os nós da rede e as amostras de entrada e rearanja a localização dos nós, aproximando os neurônios da amostra mais próxima. A distância entre os neurônios é visualizada por meio da Matriz-U que guia o intérprete na identificação de grupos. Além dessa matriz, os mapas de distribuição das variáveis de entrada auxiliam a caracterização de cada um dos grupos e os limites entre eles.

## 2.4. RESULTADOS E DISCUSSÃO

### 2.4.1. Análise de fácies

O levantamento do perfil estratigráfico está apresentado na Figura 4. As principais litologias descritas foram rudstones, grainstones e packstones, e em menor quantidade, wackestones e mudstones. As litologias carbonáticas são compostas principalmente por bioclastos de bivalves e variam quanto ao grau de preservação e orientação das valvas, apresentando normalmente granulometrias entre 2 e 6 mm. Camadas com valvas bem fragmentadas cuja granulometria é inferior a 2 mm também ocorrem.

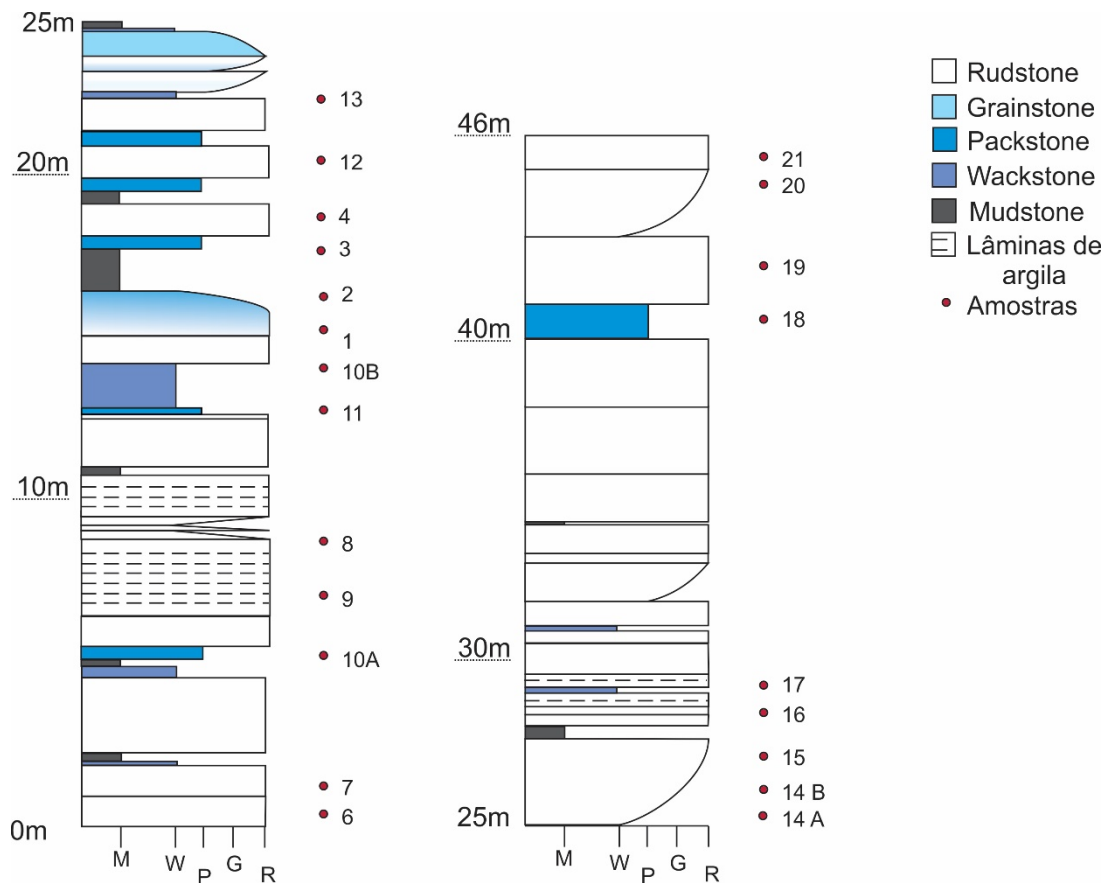


**Figura 4.** Seção estratigráfica esquemática da distribuição de fácies carbonáticas da Formação Morro do Chaves. As litologias são compostas principalmente por bioclastos de bivalves.

As coquinas do tipo *rudstone* são compostas de bioclastos de bivalves com granulometria entre 4 e 6 mm, apresentam grau de fragmentação intermediário e grau de empacotamento denso. O arranjo das conchas varia de concordante a aleatório e são predominantemente desarticuladas, apresentando sinais de abrasão e arredondamento. Alguns *rudstones* podem apresentar grãos de quartzo na matriz e arranjo caótico das conchas, com padrões de empilhamento e aninhamento.

De maneira geral, essas camadas podem variar de 0,3 – 3 m de espessura, possuem geometria tabular e extensão lateral com mais de dezenas de metros (> 100 m). Camadas que apresentam arranjo caótico dos bioclastos tendem a apresentar contato com base erosiva (Figuras 5A e 5B).

Os *packstones/floatstones* são compostos por bioclastos preservados e fragmentos de conchas, a granulometria de valvas bem preservadas varia de 2 a 4 mm, enquanto os fragmentos possuem valores inferiores a 1 mm, apresentam grau de fragmentação intermediário e o grau de empacotamento varia de denso a frouxo. O arranjo das conchas varia de concordante a aleatório, são predominantemente desarticuladas, embora ocorram raros

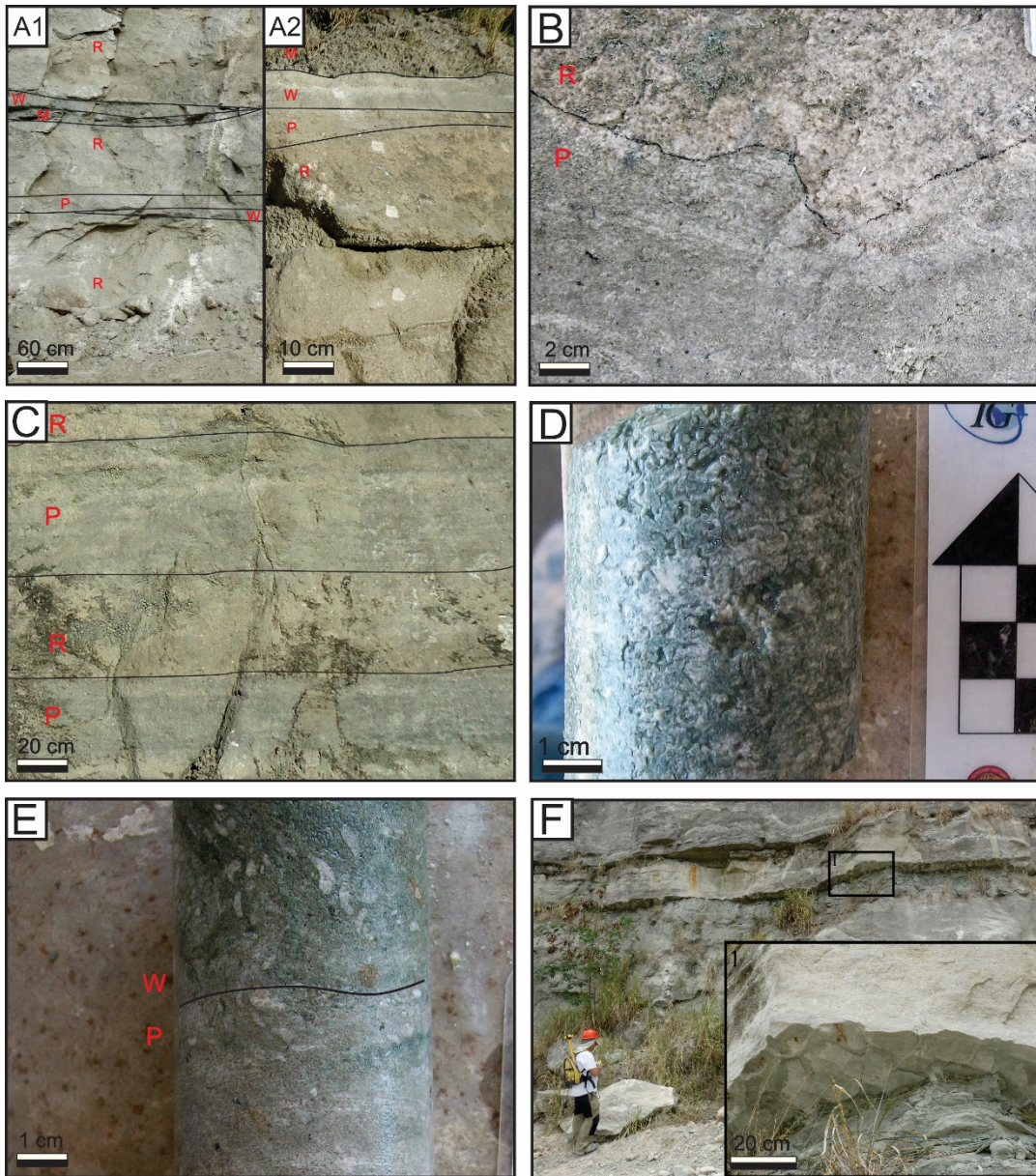
casos de valvas fechadas. Sinais de abrasão também são observados em algumas valvas. A matriz dessas rochas pode conter argila, silte, grãos de quartzo e pequenos fragmentos de conchas. Em alguns *packstones*, é possível encontrar conchas aninhadas e empilhadas.

Essas camadas variam de 0,3 – 1 m de espessura e possuem geometria tabular ou em forma de cunha (Figuras 5A e 5C), com extensão lateral de mais de 100 m. Assim como nos *rudstones*, biofábricas com arranjo caótico das conchas apresentam contato erosivo na base.

Coquinas do tipo *wackestone/floatstone* são compostas de bivalves com granulometria média de 2 mm, porém, em alguns casos, as valvas podem alcançar 6 mm, as conchas apresentam grau de fragmentação intermediário a baixo e grau de empacotamento disperso. O arranjo das conchas é caótico, pode haver ocorrências de valvas articuladas e intermediário a baixo grau de abrasão e arredondamento. A matriz apresenta grãos de quartzo, pequenos fragmentos de conchas e predomínio de argilas (Figuras 5D e 5E).

As camadas apresentam espessura máxima de 0,3 m, geralmente intercaladas com *mudstones*, apresentam forma de cunha e extensão lateral inferior às litologias anteriores. Na base dessa litologia, é comum encontrar superfícies erosivas.

Os *mudstones* podem ou não apresentar bioclastos. De maneira geral, os bioclastos são pequenos, menores que 2 mm, com pouca ocorrência de valvas fragmentadas, sem sinais de abrasão, e podem conter valvas de bivalves fechadas ou abertas em formato borboleta. De maneira geral, são camadas tabulares com espessuras que variam entre 0,1 – 1 m e podem apresentar ou não superfícies erosivas no topo ou estruturas de dessecação tipo *mud-cracks* (Figura 5F).



R: rudstones; W: wackestones; M: mudstones; P: packstones.

**Figura 5.** (A1-2) Seção aflorante dos principais litotipos, geometria das camadas e contatos; (B) contato erosivo entre packstone e rudstone; (C) contato plano paralelo entre packstone (abaixo) e rudstone (acima); (D-E) testemunho de sondagem exibindo wackestones com disposição caótica das conchas; (F) mudstone laminado com gretas de dessecação (mud□cracks).

#### 2.4.2. Redes neurais e biofábrica

No total foram analisadas 20 amostras de coquinas, compreendendo *rudstones*, *grainstones*, *packstones* e *wackestones*. Em todas as amostras nove variáveis foram obtidas: 1) Porosidade; 2) Seleção; 3) Orientação das conchas em relação ao acamamento - Valva concordante; 4) Valva oblíqua; 5) Valva vertical; 6) Grau de empacotamento das conchas; 7)

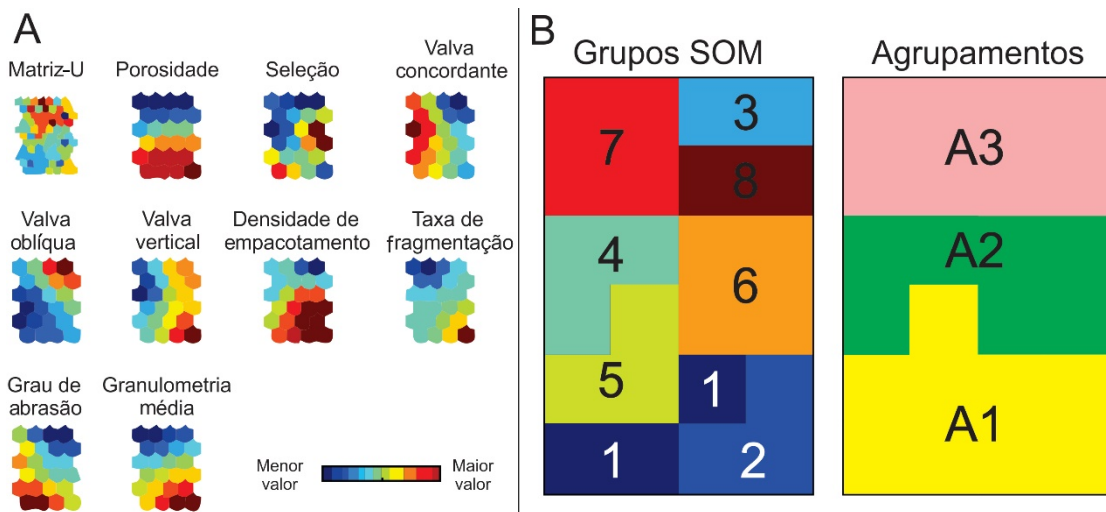
Grau de fragmentação; 8) Abrasão/Arredondamento; 9) Granulometria média das valvas. A tabela 1 apresenta os dados levantados para cada amostra coletada.

Tabela 1: Dados de porosidade e parâmetros tafonômicos das amostras coletadas

Amostra	Porosidade (%)	Seleção	V.C. (%)	V.O. (%)	V.V. (%)	Densidade	Fragmentação	Abrasão	Granulometria	Grupo SOM
Coq 6	11,6	2	35,5	47,4	17,1	1	1	3	5	1
Coq 7	18	2	42,0	43,2	14,8	1	1	2	4	1
Coq 4	23,5	0	35,3	45,1	19,6	1	1	1	4	1
Coq 19	15,8	2	42,1	30,3	27,6	1	1	2	6	2
Coq 14 a	15,9	0	30,3	45,5	24,2	1	2	1	5	2
Coq 14 b	22,1	0	24,6	45,6	29,8	1	2	1	5	2
Coq 12	2	1	27,0	47,6	25,4	0	1	0	3	3
A 2	3	0	27,6	53,3	19,0	0	1	0	3	3
A 3	3,4	0	12,6	65,5	21,8	0	1	1	3	3
Coq 17	6,6	0	51,1	38,3	10,6	0	1	1	4	4
Coq 9	7,6	0	52,9	36,8	10,3	1	1	2	3	4
Coq 8	14,3	0	45,1	35,2	19,7	1	1	0	4	5
Coq 13	17	2	47,6	31,7	20,7	0	1	1	4	5
Coq 15	18,6	0	44,2	38,5	17,3	1	1	2	4	5
Coq 11	6,2	2	31,6	44,3	24,1	1	1	1	4	6
Coq 10 b	11,1	2	35,7	45,5	18,8	1	1	1	4	6
Coq 10 a	12,2	2	37,8	42,9	19,4	1	1	1	4	6
Coq 1	16,5	2	32,0	48,0	20,0	1	1	1	4	6
Coq 16	3,5	2	45,3	47,7	7,0	0	1	2	3	7
Coq 2	2	0	35,8	41,5	22,6	1	0	0	2	8

V.C.: valva concordante; V.O.: valva oblíqua; V.V.: valva vertical.

O método SOM identificou oito padrões no conjunto de dados amostrais que definiram os grupos apresentados na Figura 6. O resultado dos agrupamentos está representado por meio do mapa particionado (Figura 6A), realizado a partir da análise visual da Matriz-U, e interpretados com auxílio dos mapas de influência de cada uma das variáveis que definiram a intensidade de valor para cada grupo (Figura 6B).



**Figura 6.** (A) A Matriz-U está representada no canto superior esquerdo, mostrando as distâncias entre os neurônios que deram origem ao agrupamento de (B), e os mapas de cada variável utilizada para o treinamento da rede neural. Por meio dos valores dos mapas de (A), é possível inferir as características de cada grupo definido em (B); (B) resultado do Self-Organization Map, que encontrou oito padrões distintos representados na malha da Matriz-U, e agrupamentos A1 – A3.

Segundo análise da classificação assistida realizada com SOM, observa-se que os grupos de maior porosidade são os de número 1, 2 e 5, denominados de Agrupamento 1 (A1); os de porosidade intermediária são representados pelos grupos de número 4 e 6, denominados de Agrupamento 2 (A2); e os de baixa porosidade são os grupos de número 3, 7 e 8, denominados de Agrupamento 3 (A3).

Com base na Figura 6, as variáveis que possuem maior correlação com a porosidade são: densidade de empacotamento, grau de fragmentação, grau de abrasão e granulometria média das valvas. Por outro lado, a seleção e a orientação das valvas com relação ao acamamento não apresentaram correlação com a porosidade.

A Tabela 2 a seguir resume as principais características dos grupos de 1 a 8 com relação à porosidade e às características tafonômicas.

Tabela 2: Resumo das principais características tafonômicas e porosidade.

Mediana				
Grupos SOM	Porosidade (%)	V.C. (%)	V.O. (%)	V.V. (%)
1	18.0	35.5	45.1	17.1
2	15.9	30.3	45.5	27.6
3	3.0	27.0	53.3	21.8
4	7.1	52.0	37.5	10.5
5	17.0	45.1	35.2	19.7
6	11.7	33.9	44.9	19.7
7	3.5	45.3	47.7	7.0
8	2.0	35.8	41.5	22.6
Classes majoritárias de cada grupo				
Seleção	Densidade	Fragmentação	Abrasão	Granulometria
2	1	1	2	4
0	1	2	1	5
0	0	1	0	3
0	0	1	1	3
0	1	1	1	4
2	1	1	1	4
2	0	1	2	3
0	1	0	0	2

V.C.: Valva concordante      V.O.: Valva oblíqua      V.V.: Valva vertical

#### *Agrupamento 1: Amostras com alta porosidade*

Os grupos de maior porosidade apresentam como principais características tafonômicas: grau de empacotamento denso, alto a intermediário grau de fragmentação, alto a intermediário grau de arredondamento e alta granulometria, com conchas superiores a 4 mm.

Os principais litotipos que compõe esse agrupamento são coquinas do tipo *rudstones*. As amostras contidas em A1 apresentam valvas de bivalves com granulometrias superiores a 4 mm, que podem ser encontradas dispostas de forma caótica — representada pelo grupo 2 — ou concordante com o acamamento — como representado pelo grupo 1. De maneira geral,

apresentam uma matriz composta de fragmentos de conchas e grãos de quartzo e ocorrência de cimento espártico. Os bioclastos encontram-se neomorfisados com preservação da estrutura aragonítica original da concha (Figura 7A). Em algumas amostras, há ocorrência de alto grau de dissolução das valvas, cimento e matriz, onde é quase imperceptível identificar os limites entre valvas e cimento.

A porosidade é predominantemente do tipo interpartícula, intrapartícula, móldica e vugular (Figuras 7A e 7B); em menor quantidade, observa-se porosidade por canal e por fratura, e variam de 11 a 23%. As porosidades encontram-se conectadas onde é comum a interação dos poros primários com os secundários.

#### *Agrupamento 2: Amostras com porosidade intermediária*

As principais características tafonômicas de A2 são grau de empacotamento frouxo a denso, grau intermediário de fragmentação, grau intermediário de arredondamento e granulometria entre 3 – 4 mm.

O principal grupo de amostras que compõe A2 são *rudstones* e *packstones*. Assim como no grupo A1, as amostras contidas em A2 apresentam valvas de bivalves dispostas de forma caótica ou concordante com o acamamento com granulometrias entre 2 – 4 mm, variando de bem selecionada a bimodal, ocorrendo valvas de maior tamanho (Figuras 7C e 7D). De maneira geral, A2 apresenta uma matriz composta por fragmentos de conchas, grãos de quartzo, material fino micrítico recristalizado em forma de cimento e ocorrência de cimento espártico que obstrui grande parte da porosidade. Assim como A1, os bioclastos encontram-se neomorfisados. A porosidade nessas amostras é predominantemente do tipo interpartícula, intrapartícula (Figuras 7C e 7D) e, em menor quantidade, móldica.

As porosidades desse grupo de amostras variam de 7 a 15% e encontram-se interconectadas; poucas amostras possuem poros isolados sem conectividade.

#### *Agrupamento 3: Amostras de baixa porosidade*

A3 apresenta as seguintes características tafonômicas: baixo grau de empacotamento das conchas, baixo grau de fragmentação, baixo grau de arredondamento e baixa granulometria.

As principais amostras desse agrupamento são *packstones* e *wackestones*. A3 apresenta valvas de bivalves dispostas de forma caótica ou concordante com o acamamento com granulometrias que variam entre 2 – 3 mm. A matriz dessas rochas é composta

principalmente por fragmentos de conchas, grãos de quartzo e alta quantidade de material fino micrítico, com ocorrência de cimento espático de calcita mosaico em drusa (Figuras 7E e 7F).

Assim como A1 e A2, os bioclastos encontram-se neomorfisados. As porosidades nessas amostras são predominantemente do tipo interpartícula, intrapartícula e, em raras ocorrências, móldica. As porosidades desse grupo de amostras variam de 0 a 7%, normalmente são conectadas por dutos de dissolução ou fraturas.

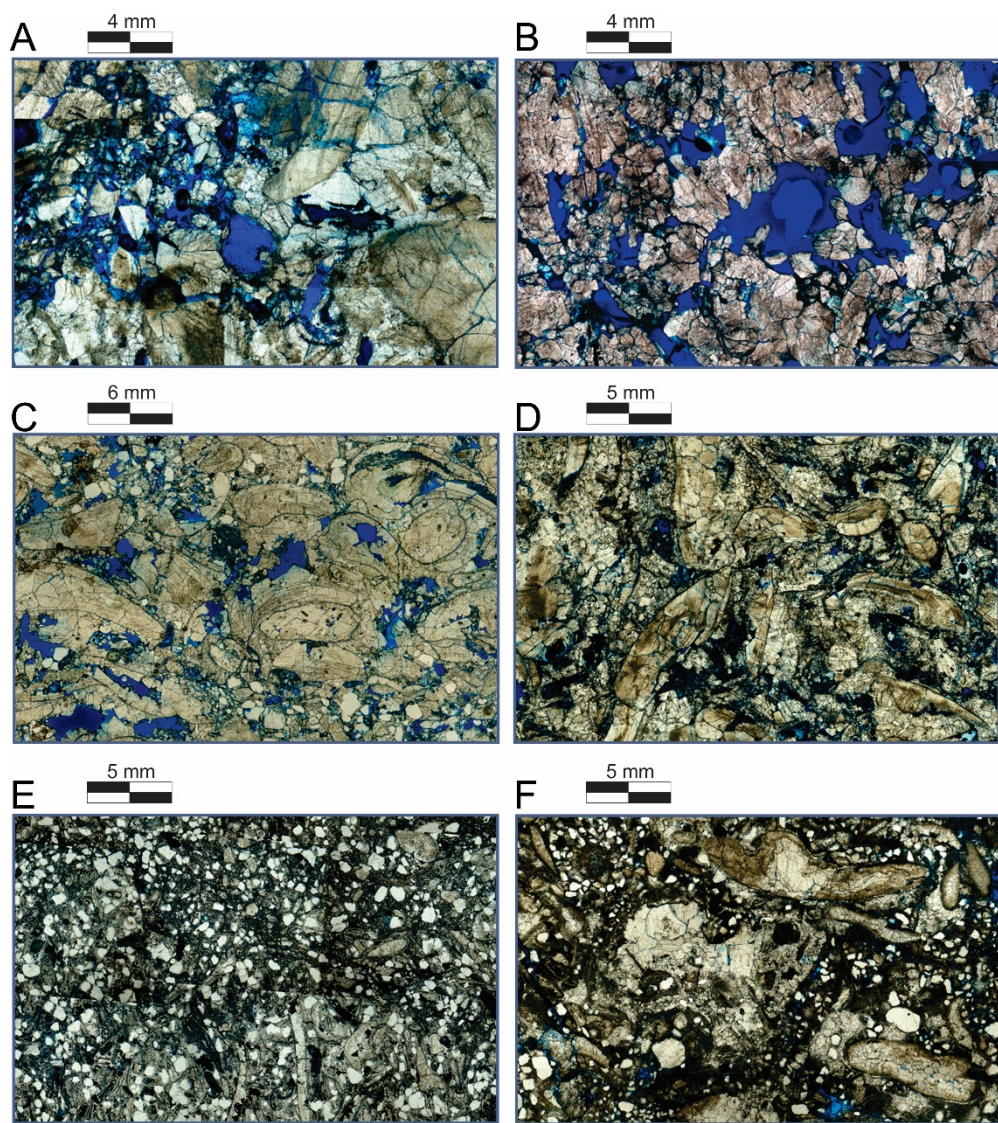


**Figura 7.** Lâminas delgadas dos agrupamentos A1 – A3. (A-B) Amostras de A1 com ênfase nos poros móldicos, interpartícula e vugulares; (C-D) amostras de A2 com ênfase nos poros interpartícua e ocorrência de cimento e finos que obstruem os poros; (E-F) amostras de A3 com pouca porosidade e alta concentração de finos e cimento obstruindo os poros (cristais de pirita também estão presentes).

## 2.5. RELAÇÃO ENTRE BIOFÁBRICA, AMBIENTE DEPOSICIONAL E POROSIDADE

Acumulações conchíferas podem ocorrer em diversos ambientes deposicionais, como rios, lagos, mares e oceanos, e com base nas condições de preservação e acumulação das valvas é possível interpretar as características energéticas de cada depósito. Como apresentado por alguns autores (Fürsich e Oschmann, 1986, 1993; Kidwell, 1986, 1991; Kidwell e Holland, 1991), acumulações conchíferas geradas em ambientes de alta energia tentem a apresentar valvas fragmentadas, desarticuladas, com sinais de abrasão e ausência de material fino, como micrita na matriz. Exemplos em lagos recentes apontam que o retrabalhamento das conchas está vinculado diretamente à lâmina d'água, ou seja, apresentam maior grau de fraturamento nas porções rasas cujo ambiente é de maior energia (McGlue et al., 2010; Hassan et al., 2014). Além disso, a ausência de valvas fechadas e a ocorrência de conchas com sinais de abrasão são um indício de que essas conchas foram retrabalhadas (Tietze e Francesco, 2014). Já nos ambientes de menor energia, os bioclastos se encontram mais preservados, articulados, podendo ser encontrados até mesmo em condições de vida nas quais muitas vezes ocorre matriz argilosa.

Com base nessas características, podemos concluir que as coquinas do tipo grainstone e rudstone são produtos de um ambiente de maior energia comparadas às coquinas do tipo packstone e wackestone. Os depósitos de ambiente de alta energia na Formação Morro do Chaves apresentam o retrabalhamento por correntes de fundo e/ou ondas durante períodos de tempo bom ou eventos de tempestade que removem o material fino, resultando em acumulações conchíferas com valvas bem fragmentadas, elecionadas e com sinais de abrasão (Tavares et al., 2015; Chinelatto et al., 2018). Algumas amostras do A1 e do A2 apresentam características de coquinas formadas em ambiente de tempestade proximal, cujas principais características são o empacotamento denso, a disposição caótica, aninhada ou empilhada das conchas, com grau médio de fragmentação e raras ocorrências de valvas articuladas, além de apresentar contatos erosivos na base (Tavares et al., 2015; Chinelatto et al., 2018). As coquinas do A3 são as de menor energia, localizadas abaixo do nível de onda bom e são interpretadas como acumulações de eventos de tempestade de baixa energia (Tavares et al., 2015; Chinelatto et al., 2018).

Por meio da análise das características tafonômicas de cada agrupamento, podemos observar que o grupo de coquinas com alta porosidade são aqueles interpretados como sendo produtos de ambientes de maior energia, como apresentado pelo A1 e pelo A2, enquanto as

rochas do A3, que apresentam características de ambientes de baixa energia, apresentam os menores valores de porosidade.

A porosidade primária interpartícula de A1 e A2 pode ser resultado do retrabalhamento, do transporte das valvas e do joeiramento do material mais fino que pode ser ocasionado por ondas, correntes ou eventos periódicos de tempestade. Esse tipo de porosidade é controlado pelo tamanho da partícula, pela seleção e pelo volume de cimento (Lucia, 2007). A3, no entanto, é o grupo que apresenta menor valor de porosidade primária, os poros estão praticamente preenchidos por micrita e pseudoesparita. Nesse caso, a porosidade desse grupo se resume a poros móldicos, por fratura ou pequenos canais de dissolução.

A porosidade secundária é comum em todos os agrupamentos e são predominantemente dos tipos móldica e vugular. A porosidade móldica é controlada pela granulometria das conchas, pois quanto maior o bioclasto maior será o molde gerado. No caso de A1 e A2, há o predomínio de empacotamentos densos de alta granulometria que, associados com alta taxa de dissolução, resultam em alta quantidade de poros móldicos e vugs. Além disso, os poros primários podem facilitar a percolação de água não saturada em calcita, resultando na criação de vugs. No caso de A3, a quantidade de conchas é menor, além de sua granulometria ser inferior, se comparada a dos outros grupos, o que resulta em uma rocha com menor quantidade de poros móldicos e vugulares. Devido à ausência de poros primários em A3, a dissolução e a criação de vugs são menores comparadas a A1 e A2.

Analizando A1 e A2, nota-se que a intensidade da cimentação e a presença de material fino variam. Grande parte da porosidade primária encontra-se obstruída por microesparita e pequenas quantidades de micrita, resultado da mudança da energia deposicional do ambiente e pela precipitação de cimento.

As porosidades por dissolução (intrapartícula, móldica e vugs) são formadas durante as diferentes fases diagenéticas. Durante a eodiagenese temos o neomorfismo das conchas, no qual temos a substituição dos cristais originais de aragonita por calcita de forma que esse preenchimento possa ocorrer de forma incompleta preservando porosidades do tipo intrapartícula. Os exemplos do A1 (Figuras 7A e 7B) e do A2 (Figuras 7C e 7D) apresentam dissolução de conchas inteiras e de seus fragmentos como também do cimento intergranular, resultando em uma porosidade secundária. A cimentação inicial por calcita no espaço poroso primário sustenta o arcabouço da rocha, limitando a redução dos poros por compactação, no entanto a cimentação diminui o volume do poro.

Em A1, a porosidade por dissolução tem maior destaque comparado aos outros grupos, o alto grau de fragmentação das conchas combinado com um fluido capaz de dissolver os

bioclastos são uma combinação importante para favorecer a formação de porosidade secundária (quanto mais fragmentadas as conchas, mais fácil será a dissolução). No A2, a diagênese pode contribuir ou obliterar a porosidade. Nas amostras com menor porosidade (valor próximo a 7%), a cimentação obstrui grande parte do sistema poroso inicial e ocorre pouca dissolução tanto das conchas como do cimento, enquanto nas amostras de maior porosidade (valor superior a 14%) a cimentação é baixa, preservando porosidades primárias, nas quais a dissolução é capaz de remover pequenos grãos e cimento gerando vugs ou porosidades parcialmente móldicas.

A3 é o grupo de menor porosidade. Como dito anteriormente, grande parte da porosidade está obstruída por material fino e cimento. Durante a diagênese, o pouco espaçoporoso pode ser completamente obstruído por cimento de calcita e a micrita chega a se recristalizar formando cimento microesparítico. As conchas não sofrem processo de dissolução e a pouca porosidade móldica é rara e ocorre parcialmente em bioclastos ou pequenos fragmentos de conchas. Nesse grupo, a porosidade pode ser controlada pela ocorrência de pequenas fraturas que podem ser alargadas pela dissolução.

## **2.6. CONCLUSÃO**

Analizando as características da biofábrica (porosidade, seleção, orientação das conchas, grau de empacotamento, grau de fragmentação, abrasão/arredondamento e granulometria média das valvas) e diagenéticas das coquinas da Formação Morro do Chaves, podemos concluir que há uma diferença entre o valor da porosidade de coquinas formadas em ambientes de alta e baixa energia.

As coquinas depositadas em ambientes de alta energia apresentam os maiores valores de porosidade, pois a ação de ondas e/ou correntes favorecem a preservação da porosidade interpartícula, pois promove o joeiramento de material fino. Essas coquinas vão apresentar uma biofábrica com conchas bem fragmentadas, orientadas ou não, com sinais de arredondamento e desarticuladas.

Coquinas depositadas em ambientes de baixa energia (por exemplo, fundo de lago) possuem maior quantidade de material fino entre os bioclastos, obstruindo a porosidade primária e resultando em rochas com pouca ou nenhuma porosidade. Normalmente, a biofábrica apresentará bioclastos mais preservados, com poucos fragmentos, orientados ou não, e frequentes conchas articuladas.

Coquinas produtos de evento de tempestade, como observado em alguns casos de A1 e A2, podem apresentar condições favoráveis à preservação de porosidade, pois mesmo tempestades podem jear o material fino e depositar extensas camadas de coquinas em regiões onde normalmente prevalecem condições de baixa energia, abaixo do nível de ondas de tempo bom.

A diagênese também revela uma boa relação com a porosidade e com as características da biofábrica, principalmente com as coquinas que apresentam alto grau de fragmentação. Quando essas rochas são submetidas à dissolução, esses fragmentos são facilmente removidos, formando diversos poros móldicos e vugulares.

## **AGRADECIMENTOS**

Agradecemos ao Prof. Dr. Celso Peres Fernandes, a disponibilidade do software Imago; ao Departamento de Geologia e Laboratório de Laminação da Universidade Estadual de Campinas (Unicamp); ao financiamento promovido pelo Conselho Nacional de Desenvolvimento Científico e Tecnológico (CNPq) (Projeto nº 132487/2014-4) e pela Coordenação de Aperfeiçoamento de Pessoal de Nível Superior (Capes) (Projeto nº 1579147); aos amigos Mateus Basso e Aline Maria Poças Belila, que acompanharam as atividades de campo; e aos revisores anônimos as dicas e observações sugeridas. A todos, um forte abraço.

## 2.7. REFERÊNCIAS

- ABRAHÃO, D., WARME, J. E. (1990). Lacustrine and associated deposits in a rifted continental margin-Lower Cretaceous Lagoa Feia Formation, Campos Basin, off shore Brazil. In: B. J. Katz (Ed.), *Lacustrine Basin Exploration – Case Studies and Modern Analogs* (v. 50, 287-305). American Association of Petroleum Geologists Memoir.
- ANSELMETTI, F. S., LUTHI, S., EBERLI, G. P. (1998). Quantitative Characterization of Carbonate Pore Systems by Digital Image Analysis. *AAPG Bulletin*, 82(10), 1815-1836.
- AQUINO, G. S., LANA, M. C. (1990). Exploração na Bacia de Sergipe-Alagoas: O “Estado da Arte”. *Boletim de Geociências da Petrobras*, 4(1), 75-84.
- BAUMGARTEN, C. S., DULTRA, A. J. C., SCUTA, M. S., FIGUEIREDO, M. V. L., SEQUEIRA, M. F. P. B. (1988). Coquinas da Formação Lagoa Feia, Bacia de Campos: evolução da Geologia de Desenvolvimento. *Boletim de Geociências da Petrobras*, 2, 27-36.
- BELILA, A. M. P. (2014). Caracterização petrofísica dos carbonatos da Formação Morro do Chaves, Bacia de Sergipe-Alagoas. Dissertação (Mestrado). Campinas: Instituto de Geociências – Universidade Estadual de Campinas.
- BURCHETTE, T. P. (2012). Carbonate rocks and petroleum reservoirs: A geological perspective from the industry. Geological Society, London, Special Publications, 370(1), 17. <http://dx.doi.org/10.1144/SP370.14>
- BUST, V. K., OLETU, J. U., Worthington, P. F. (2011). The challenges for carbonate petrophysics in petroleum resource estimation. *SPE Reservoir Evaluation & Engineering*, 14(1), 25-34. <https://doi.org/10.2118/142819-PA>
- CAMPOS NETO, O. P. A. C., LIMA, W. S., CRUZ, F. E. G. (2007). Bacia de Sergipe-Alagoas. *Boletim de Geociências da Petrobras*, 15(2), 405-415.
- CARVALHO, M. D., PRAÇA, U. M., SILVA-TELLES Jr., A. C., JAHNERT, R. J., DIAS, J. L. (2000). Bioclastic carbonate lacustrine facies models in the Campos Basin (Lower Cretaceous), Brazil. In: E. H. Gierlowski-Kordesch, K. R. Kelts (Eds.), *Lake Basins Through Space and Time: AAPG Studies in Geology* (46, 245-256). Tulsa, Oklahoma: AAPG..
- CHANG, H. K., ASSINE, M. L., CORRÊA, F. S., TINEN, J. S., VIDAL, A. C., KOIKE, L. (2008). Sistemas petrolíferos e modelos de acumulação de hidrocarbonetos na Bacia de Santos. *Revista Brasileira de Geociências*, 38(2 Supl. 1), 29-46.

- CHINELATTO, G. F., VIDAL, A. C., KURODA, M. C., BASILICI, G. (2018). A taphofacies model for coquina sedimentation in lakes (Lower Cretaceous, Morro do Chaves Formation, NE Brazil). *Cretaceous Research*, 85, 1-19. <https://doi.org/10.1016/j.cretres.2017.12.005>
- CHOQUETTE, P. W., PRAY, L. C. (1970). Geologic nomenclature and classification of porosity in sedimentary carbonates. *The American Association of Petroleum Geologists Bulletin*, 54(2), 207-250.
- CORBETT, P. W. M., ESTRELLA, R., RODRIGUEZ, A. M., SHOEIR, A., BORGHI, L., TAVARES, A. C. (2016). Integration of Cretaceous Morro do Chaves rock properties (NE Brazil) with the Holocene Hamelin Coquina architecture (Shark Bay, Western Australia) to model effective permeability. *Petroleum Geoscience*, 22(2), 105-122. <https://doi.org/10.1144/petgeo2015-054>
- DATTA, D., THAKUR, N., GHOSH, S., PODDAR, R., SENGUPTA, S. (2016). Determination of porosity of rocks samples from photomicrographs using image analysis. *IEEE 6<sup>th</sup> International Conference on Advanced Computing*.
- DUNHAM, R. J. (1962). Classification of carbonate rocks according to depositional texture. In: W. E. HAM (Ed.), *Classification of carbonate rocks: American Association of Petroleum Geologists Memoir* (v. 1, 108-121). Tulsa, Oklahoma: AAPG.
- EHRENBERG, S. N., NADEAU, P. H. (2005). Sandstone vs. Carbonate petroleum reservoirs: A global perspective on porosity-depth and porosity-permeability relationships. *AAPG Bulletin*, 89(4), 435-445. <https://doi.org/10.1306/11230404071>
- EMBRY, A. F., KLOVAN, J. E. (1971). A Late Devonian reef tract on Northeastern Banks Island. NWT: *Canadian Petroleum Geology Bulletin*, 19(4), 730-781.
- FEIJÓ, F. J. (1994). Bacias de Sergipe e Alagoas. *Boletim de Geociências da Petrobras*, 8(1), 149-161.
- FERM, J. B., EHRLICH, R., CRAWFORD, G. A. (1993). Petrographic image analysis and petrophysics: analysis of crystalline carbonates from the Permian Basin, west Texas. *Carbonates and Evaporites*, 8(1), 90-108. <https://doi.org/10.1007/BF03175166>
- FIGUEIREDO, A. M. F. (1981). Depositional Systems in the Lower Cretaceous Morro do Chaves and Coqueiro Seco Formations, and their Relationship to Petroleum Accumulations, Middle Rift Sequence, Sergipe-Alagoas Basin, Brazil. Thesis (Doctorade). Austin: University of Texas.
- FÜRSICH, F. T., OSCHMANN, W. (1986). Storm shell beds of Nanogyra in the Upper Jurassic of France. *Neues Jahrbuch für Geologie und Paläontologie*, 172(2), 141-161.

- FÜRSICH, F. T., OSCHMANN, W. (1993). Shell beds as tools in basin analysis: the Jurassic of Kachchh, western India. *Journal of the Geological Society*, 150(1), 169-185. <https://doi.org/10.1144/gsjgs.150.1.0169>
- GALLO, V., CARVALHO, M. S. S., Santos, H. R. S. (2010). New occurrence of Mawsoniidae (Sarcopterygii, Actinistia) in the Morro do Chaves Formation, Lower Cretaceous of the Sergipe-Alagoas Basin, Northeastern Brazil. *Boletim do Museu Paraense Emílio Goeldi Ciências Naturais*, 5(2), 195-205.
- GARCIA, G. G. (2012). Análise do conteúdo palinológico da Formação Morro do Chaves, Bacia de Sergipe-Alagoas e seu significado bioestratigráfico e paleoambiental. Trabalho de Conclusão de Curso. Rio Grande do Sul: Instituto de Geociências – UFRGS.
- GARCIA, G. G. (2016). Análise palinológica em folhelhos da Formação Morro do Chaves e implicações na evolução paleogeográfica da fase rifte da Bacia de Sergipe-Alagoas. Dissertação (Mestrado). Rio Grande do Sul: Instituto de Geociências – UFRGS.
- GARCIA, G. G., GARCIA, A. J. V., HENRIQUES, M. H. P. (2018). Palynology of the Morro do Chaves Formation (Lower Cretaceous), Sergipe Alagoas Basin, NE Brazil: Paleoenvironmental implications for the early history of the South Atlantic. *Cretaceous Research*, 90, 7-20. <https://doi.org/10.1016/j.cretres.2018.03.029>
- HASSAN, G. S., TIETZE, E., CRISTINI, P. A., DE FRANCESCO, C. G. (2014). Differential Preservation of Freshwater Diatoms and Mollusks in Late Holocene Sediments: Paleoenvironmental Implications. *PALAIOS*, 29(12), 612-623. <https://doi.org/10.2110/palo.2014.016>
- KIDWELL, S. M. (1986). Models for fossil concentrations: paleobiologic implications. *Paleobiology*, 12(1), 6-24.
- KIDWELL, S. M. (1991). The stratigraphy of shell concentrations. In: P. A. Allison, D. E. G. Briggs (Eds.), *Taphonomy, releasing the data locked in the fossil record* (v. 9, 211-290). Nova York: Plenum Press. (Topics in Geobiology).
- KIDWELL, S. M., FÜRSICH, F. T., AIGNER, T. (1986). Conceptual framework for the analysis and classification of fossil concentrations. *PALAIOS*, 1(3), 228-238. <http://dx.doi.org/10.2307/3514687>
- KIDWELL, S. M., HOLLAND, S. M. (1991). Field description of coarse bioclastic fabrics. *PALAIOS*, 6(4), 426-434. <http://dx.doi.org/10.2307/3514967>

- KINOSHITA, M. E. (2010). Modelagem sísmica-geométrica de fácies dos carbonatos lacustres da Formação Morro do Chaves, Bacia de Sergipe-Alagoas. Boletim de Geociências Petrobras, 18(2), 249-269.
- KOHONEN, T. (2001). Self-Organizing Maps. Berlin: Springer-Verlag, 501 p.
- LANA, M. C. (1990). Bacia de Sergipe-Alagoas: uma hipótese de evolução tectono-sedimentar. In: G. P. R. Gablagia, E. J. Milani (1990). Origem e evolução das bacias sedimentares (311-332). Rio de Janeiro: Petrobras.
- LANA, M. C., MILANI, E. J. (1986). A microplaca no nordeste brasileiro - Um elemento dinâmico no rifteamanto Cretacico Inferior. XXXIV Congresso Brasileiro de Geologia, n. 3, 1131-1144. Goiânia: SBG.
- LUCIA, F. J. (2007). Carbonate Reservoir Characterization, An Integrated Approach. Berlin: Springer Science & Business Media. <https://doi.org/10.1007/978-3-540-72742-2>
- MAKHLOUFI, Y., COLLIN, P. Y., BERGERAT, F., CASTELEYN, L., CLAES, S., DAVID, C., MENÉNDEZ, B., MONNA, F., ROBION, P., SIZUN, J. P., RUDY, S., RIGOLLET, C. (2013). Impact of sedimentology and diagenesis on the petrophysical properties of a tight oolitic carbonate reservoir. The case of the Oolithe Blanche Formation (Bathonian, Paris Basin, France). Marine and Petroleum Geology, 48, 323-340. <http://dx.doi.org/10.1016/j.marpetgeo.2013.08.021>
- MAZURKIEWICZ, L., MLYNARCZUK, M. (2013). Determining rock pore space using image processing methods. Geology, Geophysics & Environment, 39(1), 45-54. <http://dx.doi.org/10.7494/geol.2013.39.1.45>
- MCGLUE, M. M., SOREGHAN, M. J., MICHEL, E., TODD, J. A., COHEN, A. S., MISCHLER, J., O'CONNELL, C. S., CASTAÑEDA, O. S., HARTWELL, R. J., LEZZARK, K. E., NKOTAGU, H. H. (2010). Environmental controls on shell-rich facies in tropical lacustrine rifts: a view from Lake Tanganyika's littoral: PALAIOS, 25(7), 426-438. <https://doi.org/10.2110/palo.2009.p09-160r>
- MENEZES, P. T. L., TRAVASSOS, J. M., MEDEIROS, M. A. M., TAKAYAMA, P. (2016). High-resolution facies modeling of presalt lacustrine carbonates reservoir analog: Morro do Chaves Formation example, Sergipe-Alagoas Basin, Brazil. Interpretation, 4(2), SE63-SE74. <https://doi.org/10.1190/INT-2014-0213.1>

- MUNIZ, M. C., BOSENCE, D. W. J. (2015). Pre-salt microbialites from the Campos Basin (offshore Brazil): image log facies, facies model and cyclicity in lacustrine carbonates. In: D. W. J. Bosence, K. A. Gibbons, D. P. Le Heron, W. A. Morgan, T. Pritchard, B. A. Vining (Eds.), Microbial Carbonates in Space and Time: Implications for Global Exploration and Production (418). Londres: Geological Society, Special Publications. <http://dx.doi.org/10.1144/SP418.1034>
- OJEDA, H. A. E., FUGITA, A. M. (1976). Bacia Sergipe/ Alagoas. Geologia Regional e Perspectivas Petrolíferas. XXVIII Congresso Brasileiro de Geologia, n. 1, 137-158. Porto Alegre: SBG.
- PETRI, S. (1962). Foraminiferos Cretaceos de Sergipe. Boletim Faculdade de Filosofia, Ciencias e Letras da Universidade de São Paulo, 20, 5-140. <https://doi.org/10.11606/issn.2526-3862.bffcluspgeologia.1962.121894>
- RAMAKRISHNAN, T. S., RAMAMOORTHY, R., FORDHAM, E., SCHWARTZ, L., HERRON, M., SAITO, N., RABAUTE, A. (2001). A model-based interpretation methodology for evaluating carbonate reservoirs. Society of Petroleum Engineers. <https://doi.org/10.2118/71704-MS>
- REGO, E. A., BUENO, A. D. (2015). Reservoir Rocks Image Binarization: a Comparative Study Between Neural Network Method and Otsu Variance. International Journal of Modelling and Simulation for the Petroleum Industry, 9(1), 31-36.
- RICCOMINI, C., SANT'ANNA, L. G., TASSINARI, C. C. G. (2012). Pré-sal: geologia de exploração. Revista USP, (95), 33-42. <http://dx.doi.org/10.11606/issn.2316-9036.v0i95p33-42>
- SCHALLER, H. (1969). Revisão estratigráfica da Bacia de Sergipe/Alagoas. Boletim técnico da Petrobras, 12(1), 21-86.
- SCHERER, M. (1987). Parameters influencing porosity in sandstones: a model for sandstone porosity prediction. The American Association Petroleum Geologists Bulletin, 71(5), 485-491.
- SERVIÇO GEOLÓGICO DO BRASIL (CPRM) (2009). Carta Geológica de Arapiraca. Escala 1:250.000: Folha SC.24-X-D. Brasil: Serviço Geológico do Brasil.
- SOUZA-LIMA, W., ANDRADE, E. J., BENGTSON, P., GALM, P. C. (2002). A Bacia de Sergipe-Alagoas: Evolução geológica, estratigráfica e conteúdo fóssil. Aracaju: Fundação Paleontológica Phoenix. 34 Edição especial.
- TAVARES, A. C., BORGHI, L., CORBETT, P., NOBRE-LOPES, J., CÂMARA, R. (2015). Facies and depositional environments for the coquinas of the Morro do Chaves Formation, Sergipe-Alagoas Basin, defined by taphonomic and compositional criteria. Brazilian Journal of Geology, 45(3), 415-429. <http://dx.doi.org/10.1590/2317-488920150030211>

THOMPSON, D. L. (2013). The stratigraphic architecture and depositional environments of non-marine carbonates from Barremian-Aptian Pre-Salt strata of the Brazilian continental margin. Thesis (Doctorade). Melbourne: Monash University, 277 p.

THOMPSON, D. L., STILWELL, J. D., HALL, M. (2015). Lacustrine carbonate reservoirs from Early Cretaceous rift lakes of Western Gondwana: Pre-Salt coquinas of Brazil and West Africa. *Gondwana Research*, 28(1), 26-51. <https://doi.org/10.1016/j.gr.2014.12.005>

TIETZE, E., FRANCESCO, C. (2014). Taphonomic Differences in Molluscan Shell Preservation in Freshwater Environments From the Southeastern Pampas, Argentina. *PALAIOS*, 29(10), 501-511. <https://doi.org/10.2110/palo.2014.019>

VAN DER VEN, P. H., CAINELLI, C., FERNANDES, G. J. F. (1989). Bacia de Sergipe-Alagoas: Geologia e Exploração. *Boletim de Geociências da Petrobras*, 3(4), 307-319.

**3. A TAPHOFACIES INTERPRETATION FOR SHELL CONCENTRATIONS AND THEIR RELATIONSHIP WITH PETROPHYSICS: A CASE STUDY OF COQUINAS IN THE ITAPEMA FORMATION, SANTOS BASIN-BRAZIL.**

Guilherme F., Chinelatto<sup>1a</sup>; Aline M.P., Belila<sup>1b</sup>; Mateus, Basso<sup>1c</sup>; João P.P., Souza<sup>1d</sup>; Alexandre C., Vidal<sup>1e</sup>

<sup>1</sup>Centro de Estudos do Petróleo (CEPETRO), Universidade Estadual de Campinas (UNICAMP), +55(19)3521-4659, Rua 06 de Agosto, n°50 - first floor, Campinas, Sp, Brazil.

e-mail: a) [gfchinelatto@gmail.com](mailto:gfchinelatto@gmail.com); b)[alinebelila@yahoo.com.br](mailto:alinebelila@yahoo.com.br);  
c) [bassomgeo@gmail.com](mailto:bassomgeo@gmail.com); d)[joao.ponte.souza@gmail.com](mailto:joao.ponte.souza@gmail.com); e)[acvidal@gmail.com](mailto:acvidal@gmail.com)

**Artigo aceito**

<https://doi.org/10.1016/j.marpetgeo.2020.104317>

**A TAPHOFACIES INTERPRETATION OF SHELL CONCENTRATIONS AND  
THEIR RELATIONSHIP WITH PETROPHYSICS: A CASE STUDY OF  
BARREMIAN-APTIAN COQUINAS IN THE ITAPEMA FORMATION, SANTOS  
BASIN-BRAZIL.**

The Itapema Formation in the Santos Basin is described as a carbonate coquina interval, a type of sedimentary rock composed mainly by shells and their fragments. These rocks have different textural characteristics related to depositional and diagenetic processes, which influence the pore system and consequently the permeability. Understanding how the different facies are distributed and their relationship with petrophysics is essential to preview the quality of a reservoir. In this study, we classify the shell beds of the Itapema Formation through taphonomic characteristics, applying the concept of taphofacies, where taphonomic patterns such as orientation of shells, degree of packing, fragmentation of shells, abrasion, rounding, and sorting (type of grains) are used to differentiate shell concentrations. Six taphofacies (Tf-1 to Tf-6) were described in a core interval of 12 m, which corresponds to the Itapema Formation. Taphofacies Tf-1 and Tf-2 are well-sorted and unsorted grainstones/rudstones with parallel-oriented and densely packed shells with a braded valves. Taphofacies Tf-3 and Tf-4 are well-sorted and unsorted grainstones/rudstones with oblique oriented shells, generally well-preserved but often with high shell dissolution. Taphofacies Tf-5 and Tf-6 are well-sorted and unsorted grainstones/rudstones with randomly oriented shells and densely packed deposits. In general, all the well-sorted taphofacies are composed mainly of shells and their fragments, do not show mud matrix or even shell fragments smaller than 0.2 mm, the size of valves varies from 0.5 to 5 mm and shell fragments are the smallest components. The unsorted taphofacies contain grains smaller than 0.2 mm, most of them peloids, and very small shell fragments. Through the analysis of thin sections, x-ray tomography (CT), high resolution tomography (H-CT) and Nuclear Magnetic Resonance (NMR) it was possible to quantify the porosity in the described taphofacies and classify them according to Choquette and Pray (1970) and Ahr (2008). In well-sorted taphofacies primary pores are preserved; the total porosity varies from 9% to 21% in thin sections, and mainly consists of interparticle, intraparticle, and moldic pores and vugs. The control of porosity varies from depositional to hybrid 1, according to Ahr (2008), and pores are generally connected. In unsorted taphofacies, preserved primary porosity is uncommon and most pores are moldic and vugs. The total porosity in this facies varies from 2 to 15%, although almost all values are between 10% and 15%. The control of porosity varies from hybrid 1 to diagenetic, based on Ahr (2008), and the connectivity varies. Despite these textural differences between well-sorted and unsorted taphofacies, in general, the porosity is good and varies between 10% and 25%. The permeability in well-sorted taphofacies varies from 0.3 to 8 D, the high values being associated with a connected porous system, whereas in unsorted taphofacies the permeability varies from 0.01 to 0.4 D due to the occurrence of isolated vugs and moldic pores. The well-sorted coquinas were interpreted as deposits influenced by storm-induced currents and waves where the energy was sufficient to winnow the finer grains and preserve the primary pores. The taphonomic characteristics indicate tempestites to shoreface deposits, whereas in unsorted taphofacies the energy was not sufficient to remove finer grains generally associated with distal tempestites and backshore deposits.

**Key words:** taphofacies, petrophysics, shell concentrations, coquina, itapema formation

### 3.1. INTRODUCTION

The petroleum reservoirs at the eastern margin of Brazil, commonly known as pre-salt, are among the most important discoveries of the last decade. The pre-salt play consists of rift- and sag-sourced oils related to the rifting of the supercontinent Gondwana, where carbonate deposits formed in lacustrine settings during the Barremian and Aptian time intervals (Baumgarten et al., 1988; Carvalho et al., 2000; Chang et al., 2008; Ricomini et al., 2012; Muniz and Bosence, 2015; Kattah, 2017). During the rift phase of the Gondwana break-up, a sedimentary fossiliferous condensed rock unit composed of shells and their fragments, known as coquinas, or shell concentrations, was deposited. These became an important target for exploration in the Campos and Santos basins, such as in the Búzios and Libra oil fields (Abrahão and Warme, 1990; Carvalho et al., 2000; Thompson et al., 2015; Kattah, 2017).

In general, coquinas have a textural heterogeneity that is related to the depositional environment and the diagenetic processes affecting the sediments, resulting in particular petrophysical conditions with complex pore systems and a high range of porosity and permeability (Tavares et al., 2015; Corbett et al., 2016; Herlinger et al., 2017; Chinelatto et al., 2018ab, Belila et al., 2018, Zielinski et al., 2018). In this context, it is necessary to understand how and where the different coquina facies were deposited, their relationship with diagenetic processes and, consequently, their petrophysical characteristics.

The interpretation of sedimentary processes in coquinas can be supported by a taphonomic analysis, in combination with sedimentary and stratigraphic aspects (Brett and Baird, 1986; Kidwell et al., 1986; Kidwell, 1991; Kidwell and Holand, 1991; Brett, 1995; Dattilo et al., 2008; Bressan and Palma, 2010; McGlue et al., 2010; Horodyski et al., 2019). The processes leading to shell concentrations influence the signature of skeletal elements and the biofabric (Fürsich and Oschmann, 1993; Fürsich, 1995), based on which it is possible to recognize deposits associated with high and low water energy (Bressan and Palma, 2010), deposits influenced by storms, tsunamis or mass movements (Quaglio et al., 2014; Puga-Bernabéu and Aguirre, 2017), or even whether these deposits formed *in situ* (Chen et al., 2010). Through taphonomy it is possible to establish a taphofacies model for an interval of shelly condensed deposits (Meldahl and Flessa, 1990; Fürsich and Oschmann 1993; Brett, 1995) and then correlate it with petrophysical parameters such as porosity and permeability.

In this paper, we propose a taphofacies interpretation for a coquina interval of the Itapema Formation, Santos Basin, based on taphonomic patterns such as the degree of shell

fragmentation, sorting, packing and orientation and, establish their relationship with the porosity and permeability.

### **3.2. GEOLOGICAL SETTING**

The Santos Basin is a passive margin basin located off the southeast coast of Brazil (Fig. 1A), between a latitude of 23° and 28° S, covering an area close to 350,000 km<sup>2</sup>. The northern boundary, with the Campos Basin, is formed by the Cabo Frio High and the southern border, with the Pelotas Basin, by the Florianopolis Platform (Moreira et al., 2007). The basin was developed during the rupture of the supercontinent Gondwana, throughout the Late Jurassic-Early and Cretaceous, when South America and Africa separated under an extensional tectonic regime, culminating in the opening of the South Atlantic Ocean (Macedo, 1990; Chang et al., 1992; Cainelli and Mohriak 1999; Milani and Thomaz Filho, 2000; Mohriak et al., 2008; Beasley et al., 2010).

The break-up of Western Gondwana started at the southern parts of the South American continent and advanced towards the north (Chang et al., 1992; Matos, 1992). In the southern basins, growing lithospheric stretching and faults promoted intense volcanism and the formation of half graben structures (Cainelli and Mohriak 1999; Mohriak et al., 2008). In the Santos Basin these volcanic rocks are represented by basalts of the Camboriú Formation (Mohriack et al., 2008) and represent the economic foundation of the basin (Moreira et al., 2007).

The stratigraphy of the Santos Basin (Fig. 1B) can be divided into three megasequences (Chang et al., 1992; Moreira et al., 2007). The first is a rift phase that occurred during the Early Cretaceous, between the Hauterivian to the Early Aptian (Moreira et al., 2007), characterized by continental deposits, mainly siliciclastic and lacustrine carbonates of the Piçarras and Itapema formations. The second stage is a post-rift/sag phase that occurred during the Late Aptian, with carbonates, Mg-clays and siliciclastic deposits of the Barra Velha Formation, overlapped by evaporites of the Ariri Formation. The last stage was the drift phase (Albian age to present) with carbonate and siliciclastic deposits of the Camburi, Fraude and Itamambuca groups, which represent marine and non-marine sediments associated with transgressive and regressive events (Moreira et al., 2007).

### 3.2.1. The Itapema Formation

The Itapema Formation, the focus of this paper, is characterized by the occurrence of lacustrine deposits, mainly carbonates and shales (Moreira et al., 2007). The coarse-grained carbonates are composed of dolomitized or silicified bivalve shells (coquinas), whereas shales are dark colored because of the high amount of organic matter. The base and top of the Itapema Formation are unconformities (Moreira et al., 2007; Quirk et al., 2013), at the base separating the Piçarras Formation, and at the top separating the Barra Velha Formation (sag). The top of the Itapema Formation marks the end of the rift phase (Moreira et al., 2007).

The Itapema Formation is regionally equivalent to the Coqueiros Formation of the Lagoa Feia Group in the Campos Basin (Moreira et al., 2007) which developed between the Barremian-Aptian, during the rift stage of the Gondwana break-up. The coquinas of the Coqueiros Formation have been interpreted as lacustrine deposits located at structural highs deposited under shallow, high-energy conditions, with facies varying between beaches, bars, bioaccumulated banks and storm deposits (Abrahão, 1987; Carvalho et al., 2000; Muniz, 2013; Thompson et al., 2015; Muniz and Bosence 2018; Mizuno et al., 2018; Oliveira et al., 2019). These coquinas are dominated by bivalves with occurrences of ostracods and gastropods, described as rudstones, grainstones, packstones, and wackestones, and exhibit very similar taphonomic, sedimentary, and stratigraphic characteristics with shell concentrations of the core described in this paper.

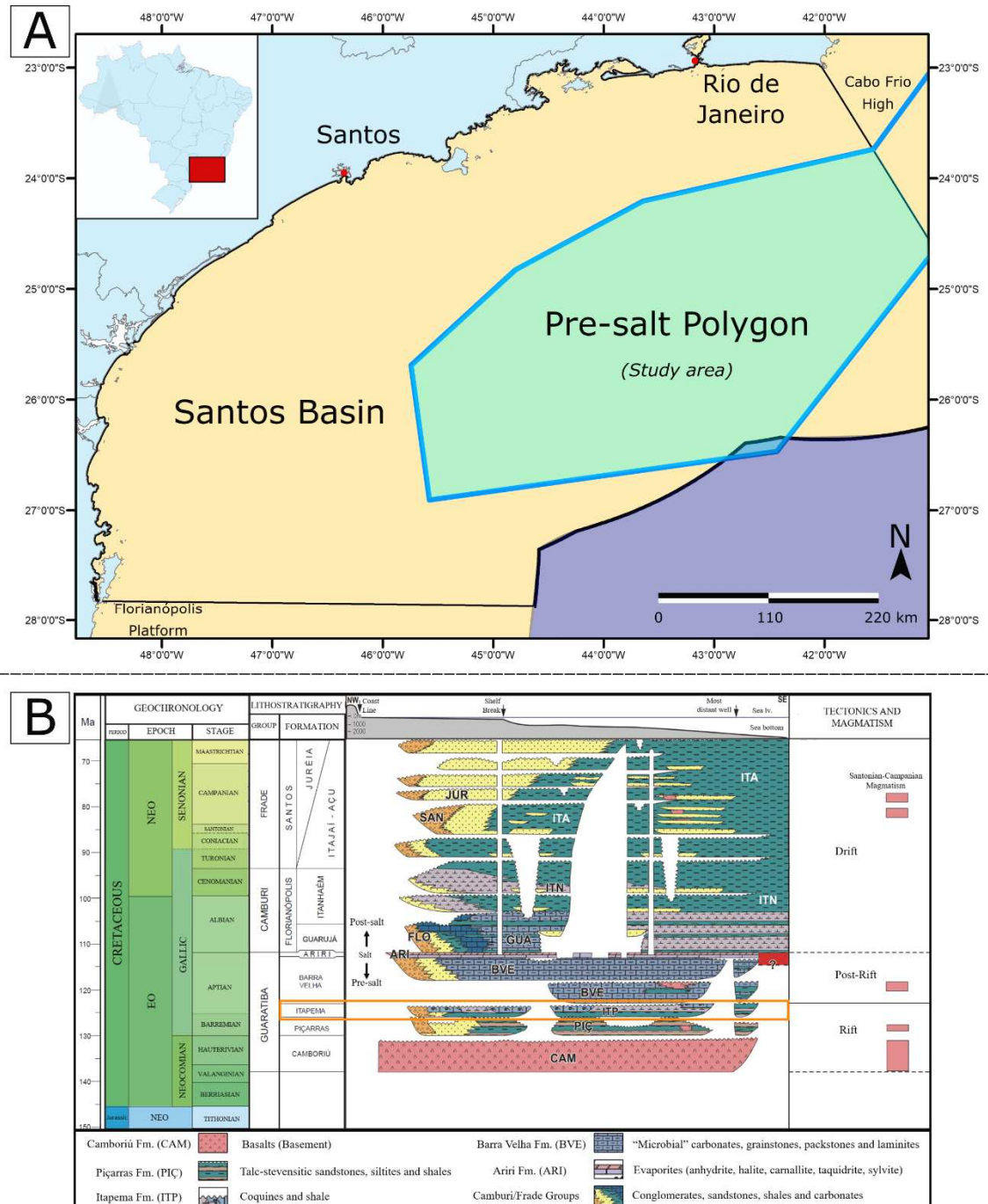


Fig. 1. A) Location of the Santos Basin and study area (in blue color). B) Stratigraphic section through the Santos Basin, the orange box highlights the Itapema Formation (adapted from Moreira et al., 2007).

### 3.3. METHODS

One vertical well core was available for geological description and taphofacies interpretation. A total of 11.55 m were described, from which 40 thin sections, spaced 20-30 cm apart, were analyzed. Subsequently, three meters of the core with 12 thin sections were

selected for laboratory analysis due to showing great facies variation. The thin sections were used to calculate the total porosity through digital image analysis and to perform a petrographic analysis of the diagenetic phase. Through the well core, a Computed Tomography scan (CT) was performed to assist in the interpretation of porosity along the facies distribution. Moreover, 10 plugs were designated for NMR analysis and High Resolution Computed Tomography scan (H-CT) to display the distribution of the porous system.

### **3.3.1. Taphofacies Classification**

Initially, a geological description and facies definition was performed through the analysis of well core and thin sections. The classification of carbonate rocks of Dunham (1962) and Embry and Klovan (1971) were used. However, these classifications do not take account of the small textural variations found in shell concentrations. Thus, a taphofacies model was developed following the classifications of Kidwell et al., (1986), Kidwell (1991) and Kidwell and Holland (1991), in which patterns as (i) orientation of valves, (ii) packing density, (iii) sorting, (iv) degree of fragmentation, (v) percentage of articulated valves, (vi) degree of abrasion/rounding and (vii) bioerosion/micritization are obtained and used to arrive at a taphofacies model. The taphonomic patterns were evaluated qualitatively. The orientation of shells is classified as concordant, oblique or perpendicular by the analysis of cross-section; the packing density (% volume of shells), fragmentation and abrasion by visual estimation through the use of charts and bioerosion/micritization by the thickness or micritized rims of valves. Shells with thin micritized rims are classified as hardly micritized whereas shells with thicker rims are stronger micritized. According to Kidwell and Holland (1991), sorting is related with the grain size distribution of coarse bioclastic fabrics, in this paper the concept of sorting is related with the grain components. Biofabrics composed mainly by shells and their fragments is classified as well-sorted whereas biofabrics that have high amount of ooids, peloids, ostracods, or other type of carbonate and/or siliciclastic grains are unsorted. Some sedimentary and stratigraphic features are described as sedimentary structures, physical contacts between layers and thickness of beds.

### 3.3.2. Measurement and classification of porosity through thin sections

The pore types were described according to the classifications of Choquette and Pray (1970) and Ahr (2008), and quantified through the analysis of thin sections images. The total porosity was obtained by the binarization method from the thin sections images, where it was possible to separate the porous system from the solids, represented by grains, matrix, and cement. Many authors use this method to obtain the total porosity from rocks, due the easy processing and fast analysis (Anselmetti et al., 1998; Mazurkiewicz and Mlynarczuk, 2013; Rego and Bueno, 2015; Datta et al., 2016). The obtained images of the thin-sections were produced with a transmitted light scanner with a resolution of 6400 dpi.

### 3.3.3. Porosity from CT and H-CT scan

The capturing of the CT image was performed by the Siemens tomography device, model SWFVD30C, with a potential of 10W and energy of 130kV. The obtained image size is 512x512 pixels with a resolution of 100 micrometers and a slice thickness capture of 1mm.

The Versa XRM-500 equipment was used to acquire the High resolution CT data (H-CT), operating with an optical lens of 0.4X and a potential of 10W and energy of 150kV. The obtained image size is 1024x1024 pixels, with a pixel resolution between 40-50 micrometers. The exposure time was 1s with steps of 0.225° and 360° rotation. After acquisition of the CT and H-CT images, the total porosity and connectivity was measured through PerGeos software and correlated with the interpreted taphofacies

### 3.3.4. Experimental analysis

**Porosity and Permeability:** The measure of porosity was performed by the UltraPoreTM 300 Helium Pycnometer System. The pore volume is measured by the expansion of a known gas under a pre-defined pressure using the Boyle law (Eq. 1):

$$\frac{p_1v_1}{T_1} = \frac{p_2v_2}{T_2} \quad (\text{Eq. 1}),$$

where p1, v1 and T1 are the initial pressure, volume and temperature and p2, v2 and T2 the final pressure, volume and temperature.

The permeability was calculated by UltraPermTM 500. The technique is based on the theory of Henri Darcy (Eq. 2):

$$Q = \frac{kA(Pb - Pa)}{\mu L} \quad (\text{Eq. 2})$$

where Q is the flux (cm), k is the permeability (Darcies), A is the cross-section area of the flow (cm<sup>2</sup>), Pb-Pa (pascals) is the total pressure drop,  $\mu$  is the viscosity (Centipoise) and L is the length (m). The equipment uses a nitrogen flux with a variable pressure (0-50psi) to obtain the permeability of samples.

**NMR analysis:** All plugs were saturated with deionized water for the experiment in GeoSpec 2-53/Maran DRX HF (2.24 MHz) equipment, manufactured by Oxford Instruments. The classical curve used for the interpretation of pore distribution is a relation between the amplitudes as a function of T<sub>2</sub> in logarithmic scale, obtained through a mathematical inversion in which each T<sub>2</sub> is related to the ratio between volume/surface of the pore (Eq. 3):

$$\frac{1}{T_2} = \frac{1}{T_{2bulk}} + p \frac{S}{V} + \frac{1}{T_{2D}} \quad (\text{Eq. 3})$$

where T<sub>2bulk</sub> = time of transverse relaxation of the fluid, p = surface relaxability, S/V = surface / volume ratio and T<sub>2D</sub> = diffusion of transverse relaxation time. The determination of T<sub>2</sub> cut-off was based on the Coates et al. (1999) method. For the porosity calculation from the NMR, the measured signal intensity was used, which is proportional to the magnetization of the nuclei. For the prediction of permeability, the Timur-Coates equation (Eq. 4) was used, commonly utilized in the literature to estimate permeability from the NMR data (Allen et al., 2001; Souza et al., 2005; Schuab et al., 2015). The Timur-Coates equation is based on a T<sub>2</sub> cutoff that separates the areas corresponding to the FFI (Free Fluid Index), relative to the larger pores (macropores), and BVI (Bulk Volume Irreducible), relative to the micropores.

$$K_{coates} = a \cdot \phi^b \cdot \frac{FFI^c}{BVI} \quad (\text{Eq. 4})$$

Subsequently, the NMR from plugs were compared with the NMR log of the analyzed interval.

### 3.4. RESULTS

#### 3.4.1. Taphofacies characterization

The coquinas described in the studied section consist of rudstones and grainstones. Their textural components are bivalve and gastropod shells that range between 0.5 to 5 mm, bone fragments generally 2 mm, intraclasts with a large size range (1-50 mm), peloids, ostracods, and stevensite ooids with shell fragments or ostracods as nuclei and rare occurrences of micrite. The thickness of beds varies from 10 to 90 cm, with either sharp and

planar or erosional bounding surfaces. These deposits were classified into six taphofacies (Tf-1 to Tf-6) based on taphonomic attributes and sedimentary structures. Then, the taphofacies were grouped into a well-sorted type (Tf-1, Tf-3 and Tf-5), mainly composed by shells and their fragments without the occurrence of finer particles (<0.2 mm), and unsorted (Tf-2, Tf-4 and Tf-6), with the occurrence of finer material such as very small shell fragments, ostracods, peloids, and micrite. The stratigraphic column of the described well section is shown in Figure 2.

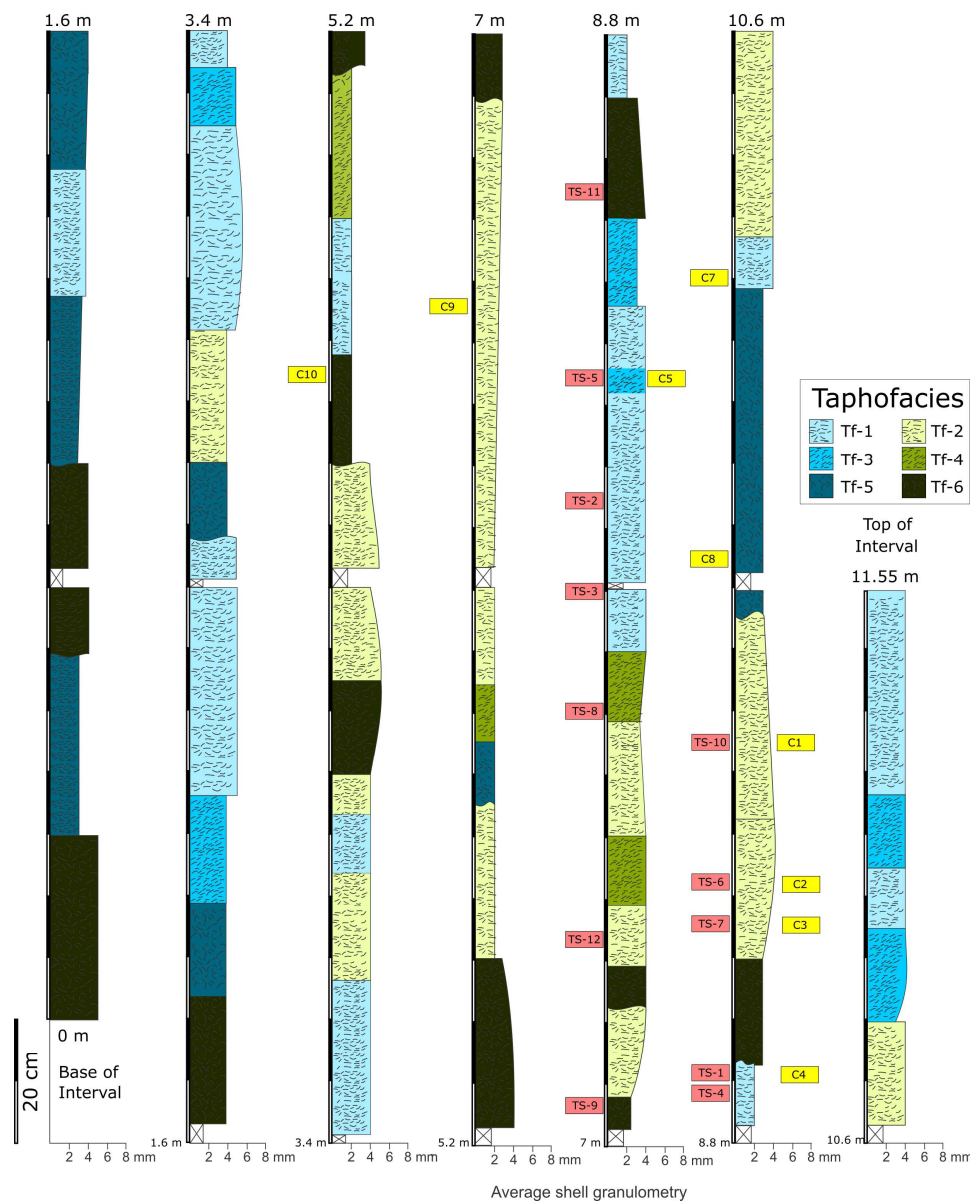


Fig. 2. Stratigraphic column of the described section. Yellow rectangles are the plug samples and red rectangles the thin sections.

**Taphofacies Tf-1: well-sorted rudstone/grainstone with oriented shells:** This taphofacies consists of rudstones and grainstones, whereby the rudstones exhibit bioclasts 2-5

mm across and a bimodal grain size distribution. The orientation of the valves is concordant to the bedding, a mix of concave-up and concave-down, and the smallest grains consist of shell fragments. In some Tf-1 samples, stevensite ooids with shell fragment nuclei and rare ostracods occur. The shells are abraded, the edges are more often rounded than chipped, but in some cases, shells with a low degree of abrasion occur. In the grainstones, the valves are very abraded and fragmented, whereas in the rudstones, shells larger than 2 mm are preserved. Articulated valves are not observed in these taphofacies and bioerosion/micritization occurs around the valves. Sedimentologically the deposits are densely packed with shell abundances of roughly 70-80%, without siliciclastic or muddy grains as matrix. Some beds of Tf-1 show millimetric planar lamination with 2-5 mm of thickness, composed by thinner shells (< 2 mm) and fragments. Randomly distributed intraclasts are common in these taphofacies. They are arranged parallel to bedding and 1-3 cm across. The intraclasts are composed of micrite, coquina, silicified coquina and laminated carbonate.

**Taphofacies Tf-2: Poorly-sorted rudstone/grainstone with oriented shells:** Tf-2 consists of rudstone and grainstone beds, which are very similar to taphofacies Tf-1 because they exhibit similar taphonomic characteristics (fragmentation, abrasion, valve orientation). However, articulated valves are rare, sorting is poor due to the occurrence of fine grains, bioerosion/micritization around shells is stronger, and occasionally they show a mix between shells enveloped by a thin layer of stevensite and shells with only a micritized rim. Tf-2 has a high concentration of fine material between the valves, mostly peloids, very small shells and their fragments (< 1 mm), and ostracods. Clay intraclasts are observed in some sections, varying from 0.5-3 cm. They are arranged concordant to bedding, and some are composed of mud and a peloidal matrix and ostracods. Dark brown laminae, 5-10 mm in thickness, are associated with abundant fine grains as peloids and micrite. Inverse grading from rudstone to grainstone is common, and the abundance of shells varies from 60-70%. Some samples exhibit laminae of micrite and some interparticle and moldic pores are partially filled with micrite and very small carbonate fragments.

**Taphofacies Tf-3: Well-sorted rudstone/grainstone with oblique shells:** This taphofacies is composed of rudstones and grainstones with bioclasts 1-4 mm across, with an unimodal to bimodal grain size distribution. The smallest grains are composed of shell fragments, the valves are obliquely oriented to the bedding and exhibit rounded edges due to abrasion. Articulated valves are absent and the degree of bioerosion/micritization is low, similar to that in Tf-1. Some rare stevensite ooids occur. Common sedimentological features include dense packing 70-80% volume of shells, and a lack of a siliciclastic matrix. Intraclasts

composed of micrite and grainstone-coquinas are common; they are arranged oblique to bedding and are 1-4 cm across. This Taphofacies is uncommon in the analyzed interval.

**Taphofacies Tf-4: Poorly-sorted rudstone/grainstone with oblique shells:** This taphofacies consists of grainstones and rudstones with bioclasts measuring 2-4 mm in size. Taphonomic characteristics are similar to taphofacies Tf-3, but peloids and shell debris occur whereas the micrite content is low. Sedimentological features are dense packing, 60-70% of shells, with rare micrite, and commons intraclasts are arranged oblique to bedding and 1-2 cm across. The intraclasts are composed of micrite and coquina. As in the case of Tf-3, the taphofacies is rare.

**Taphofacies Tf-5: Well-sorted rudstone without random valve orientation:** Tf-5 consists of rudstones with bioclasts measuring 3-5 mm, may display stevensite ooids, and exhibit a bimodal to unsorted grain size distribution. The valves are generally randomly arranged with fragmented and rounded shells chaotically distributed. Articulated valves are rare. Occasionally a mix of hardly abraded and fragmented valves and strongly abraded and fragmented shells occurs. Bioerosion/micritization is insignificant and occurs as a dark rim around shells, similar to the well-sorted taphofacies Tf-1 and Tf-3. Occasionally, a few shells exhibit a stevensite rim. The deposits are densely packed, with 70% shells, but without siliciclastic grains. In contrast, small shell fragments (<1mm) predominate. Intraclasts occur at the base of beds; they are randomly oriented and measure 0.5-2 cm across. The intraclasts consist of laminated carbonate and coquina.

**Taphofacies Tf-6: Poorly-sorted rudstone/grainstone with randomly oriented valve:** Tf-6 is composed of bioclastic rudstones and grainstones. The bioclasts are 2-4 mm in size. Taphonomic characteristics are similar to those of taphofacies Tf-5, but the taphofacies includes ostracods, peloids, and a low percentage of micrite. The taphofacies is a mixture of shells with a stevensite rim, strongly micritized and hardly micritized shells, and scattered silicified valves. Geopetal structures, such as concave-up oriented shells filled with peloids and fine shell occur. Sedimentological features are a dense packing, and 60-70% of shells. Intraclasts are 0.2-2 cm across and composed of peloidal grains in a muddy matrix.

The six taphofacies (Table 1) can be grouped in two types, well-sorted (Tf-1, Tf-3 and Tf-5) and unsorted (Tf-2, Tf-4 and Tf-6). A sketch of all taphofacies is represented in Figure 3, in addition to some examples of core and thin sections

Table 1: Characteristics of interpreted taphofacies

Taphofacies	Description	Taphonomic characteristics					
		Orientation	Sorting	Fragmentation	Abrasion	Articulated valves	Bioerosion/Micritization
Tf-1	Rudstones and grainstones, with densely packed shells; Some T1 exhibit intraclasts and stevensite ooids	Oriented shells concordant to the bedding	Well-sorted	High degree	Abraded shells	Absent	Low
Tf-2	Rudstone and grainstone with densely packed shells; high concentration of fine grains (peloids, very small shells, ostracods); some shells are enveloped by a thin layer of stevensite	Oriented shells concordant to the bedding	Unsorted	High degree	Abraded shells	Rare	Stronger
Tf-3	Rudstones and grainstones, with densely packed shells that exhibit rounded edges due to abrasion. Rare stevensite ooids occur.	Oblique shells	Well-sorted	High degree	Abraded shells	Absent	Low
Tf-4	Rudstone and grainstone with densely packed shells; high concentration of fine grains (peloids and shell debris) and low micrite content.	Oblique shells	Unsorted	High degree	Abraded shells	Absent	Low
Tf-5	Rudstones and grainstones, with densely packed shells; may display stevensite ooids. Occasionally exhibit a mix of hardly abraded and fragmented and strongly abraded and fragmented shells	Chaotically distributed	Well-sorted	High degree	Mix of hardly and strongly abraded shells	Rare	Low
Tf-6	Rudstone and grainstone with densely packed shells; includes ostracodes, peloids and a low percentage of micrite. Exhibit a mix of shells with stevensite border rim, strongly micritized and hardly micritized shells. Geopetal structures may occur.	Chaotically distributed	Unsorted	High degree	Mix of hardly and strongly abraded shells	Rare	Stronger

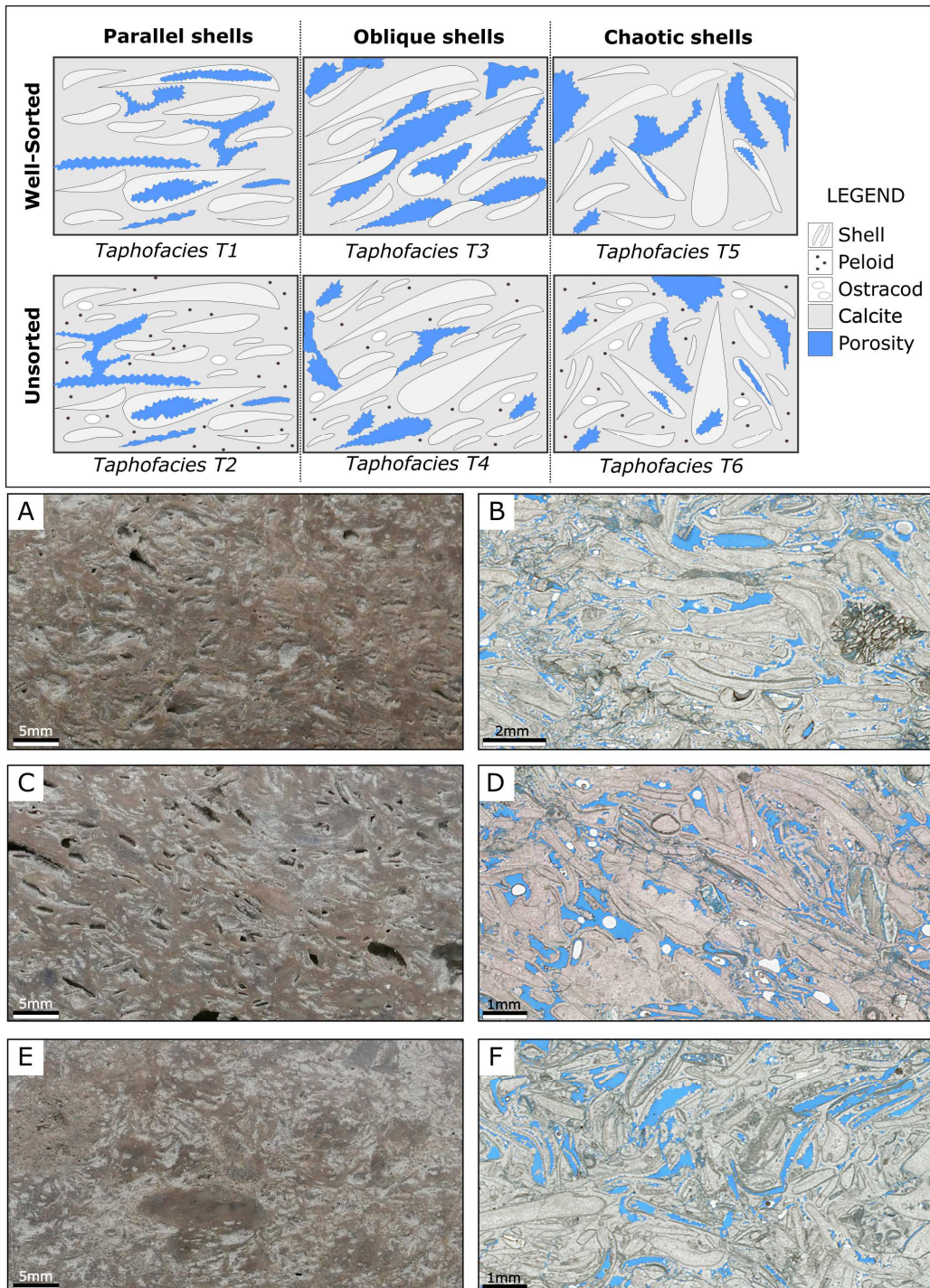


Fig. 3.Taphofacies based on shell orientation and sorting and some examples from core photographs and photomicrographs of thin sections. A-B) Shells oriented parallel to the bedding: taphofacies Tf-1-Tf-2, B) photomicrograph of Tf-1 composed of whole and fragmented shells and coquinas intraclasts. C-D) Shells with oblique orientation: taphofacies Tf-3-Tf-4; D) photomicrography of Tf-3, the white bubbles reflect the poor Epoxy impregnation. E-F) Shells with chaotic orientation: taphofacies Tf-5-Tf-6, F) photomicrograph of Tf-6 with peloids, small shell fragments and intraclasts.

### 3.4.2. Diagenesis - General Aspects

Calcite cementation is common in all taphofacies and with respect of filling the primary pores varies from partial to total. Dolomite and silica occur in the latest stages of cementation, but are less common. The types of calcite cement vary from circumgranular crusts and drusy (Fig. 4A-B), usually observed as interparticle cement or inside moldic pores, while granular cement is usually observed in the primary pore spaces. Some secondary pores, especially moldic pores, display drusy or dog-tooth calcite cement that reduces porosity (Fig. 4A-B). However, locally the cement does not completely fill the pore space, preserving an intraparticle/intercrystalline porosity (Fig. 4A-C, E). To a lesser amount, dolomite crystals occur as one of the last cementation stages in moldic, intraparticle and interparticle pores, usually superimposed on calcite crystals (Fig. 4D1, D2). This type of cementation is highlighted by the colorless dolomite crystals in Alizarin red. In some cases, the dolomite may show small signs of dissolution (Fig. 4D2). Silica cementation occurs as quartz rims around the micritized edges of bioclasts or inside moldic pores. In the molds, the silica crystallizes either with a partially to totally drusy texture (Fig. 4E), or as chalcedony (Fig. 4F). Generally, both dolomite or silica are not sufficient to occlude the pore spaces, and these occur as a minor constituent in all taphofacies without a preferential distribution. Neomorphism is common in all taphofacies, where aragonitic shells are partially or totally replaced by calcite. In some valves, it is possible to observe the original aragonitic growth structure of the shells (Fig. 4C). Micritization is common in all taphofacies and its intensity varies. In the case of well-sorted taphofacies (Fig. 4A, C), only a thin rim of the bioclasts is micritized, whereas in the unsorted taphofacies a slightly darker and thicker border occurs (Fig. 4G-H). Shell dissolution varies from partial to total in all taphofacies, resulting in moldic pores. When the dissolution is non-selective, vugs are created (Fig. 4H).

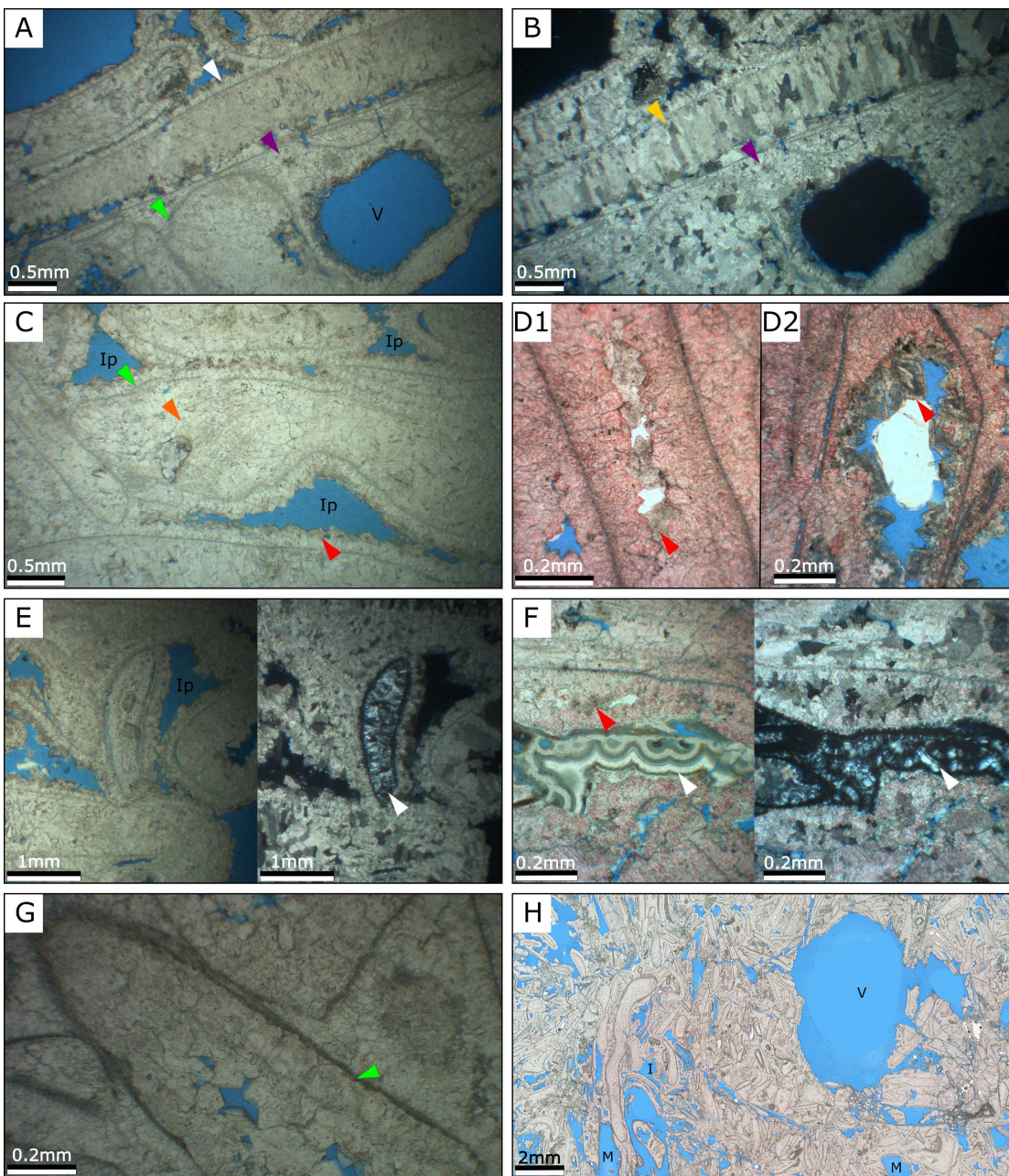


Fig. 4.General diagenetic features and porosity. A) Circumgranular calcite cement (white arrow), drusy calcite cement (purple arrow) micritized bioclasts (green arrow) and isolated vug pore (V). B) Dog-teeth inside bioclasts (yellow) and drusy calcite cement (purple) (XPL). C) Micritized grains (green arrow), original aragonitic microstructure (orange arrow), dolomite crystals (red arrow) as the last stage of cementation, and interparticle pores (Ip). D1-D2) Dolomite crystals inside dissolved shell. E) Silica cementation inside moldic pore and interparticle porosity (Ip). F) Chalcedony inside moldic pore. G) Dark border of micritized bioclasts of unsorted taphofacies (green arrow). H) Vug (V) and moldic (M) pores due to dissolution of carbonate grains and cement.

### 3.4.3. Porosity and permeability

The total porosity was obtained through the image analysis of thin sections, CT scans, H-CT scans, and also by gas injection into the plugs (Tables 2-4). The porosity in thin sections ranges between 2 and 22%, with an average of 12%, in the core CT it ranges between 1 to 8%, and in plugs it ranges between 2.3 to 15.5% in H-CT images and between 14 to 32%, with average of 21% in the case of gas injection. The permeability was measured only in plugs and varies from 18mD to 8D. The main pore types are interparticle, intraparticle, moldic and vugs (Fig. 5). The interparticle porosity is located between bioclasts and is a depositional product such as grain size, type of matrix, and by diagenetic alterations such as dissolution (Fig. 4C, E). The intraparticle porosity occurs inside grains as a result of dissolution of shells (Fig. 4G). The moldic pores are a result of intense leaching of valves and only a micrite envelope remained around the former grains (Fig. 4H). Vugs are pores that are fairly larger than grains and are associated with dissolution of both grains and cements (Fig. 4H). Compaction-fractures also contribute to the pore system through micro- and macro-fractures. Micro-fractures occur inside bioclasts, occasionally shifting parts of the grains, while macro-fractures can be seen cutting several grains and are commonly enlarged by dissolution.

Table 2. Results of porosity and permeability from experimental analysis and H-CT images.

<b>Samples</b>	<b>Taphofacies</b>	<b>Groups</b>	<b>Experimental Analysis</b>		<b>H-CT image analysis</b>
			<i>Porosity (%)</i>	<i>Permeability (mD)</i>	<i>Porosity (%)</i>
C1	Tf-2	Unsorted	16	18.12	12.7
C2	Tf-2	Unsorted	24	159.31	13.9
C3	Tf-2	Unsorted	13	-	2.3
C4	Tf-1	Well-sorted	32	3455.29	11
C5	Tf-1/3	Well-sorted	25	216.03	4.1
C6	Tf-1	Well-sorted	23	1440	-
C7	Tf-1	Well-sorted	14	128	6.5
C8	Tf-5	Well-sorted	24	8180	14.6
C9	Tf-2	Unsorted	24	67.6	9
C10	Tf-6	Unsorted	21	202	15.5

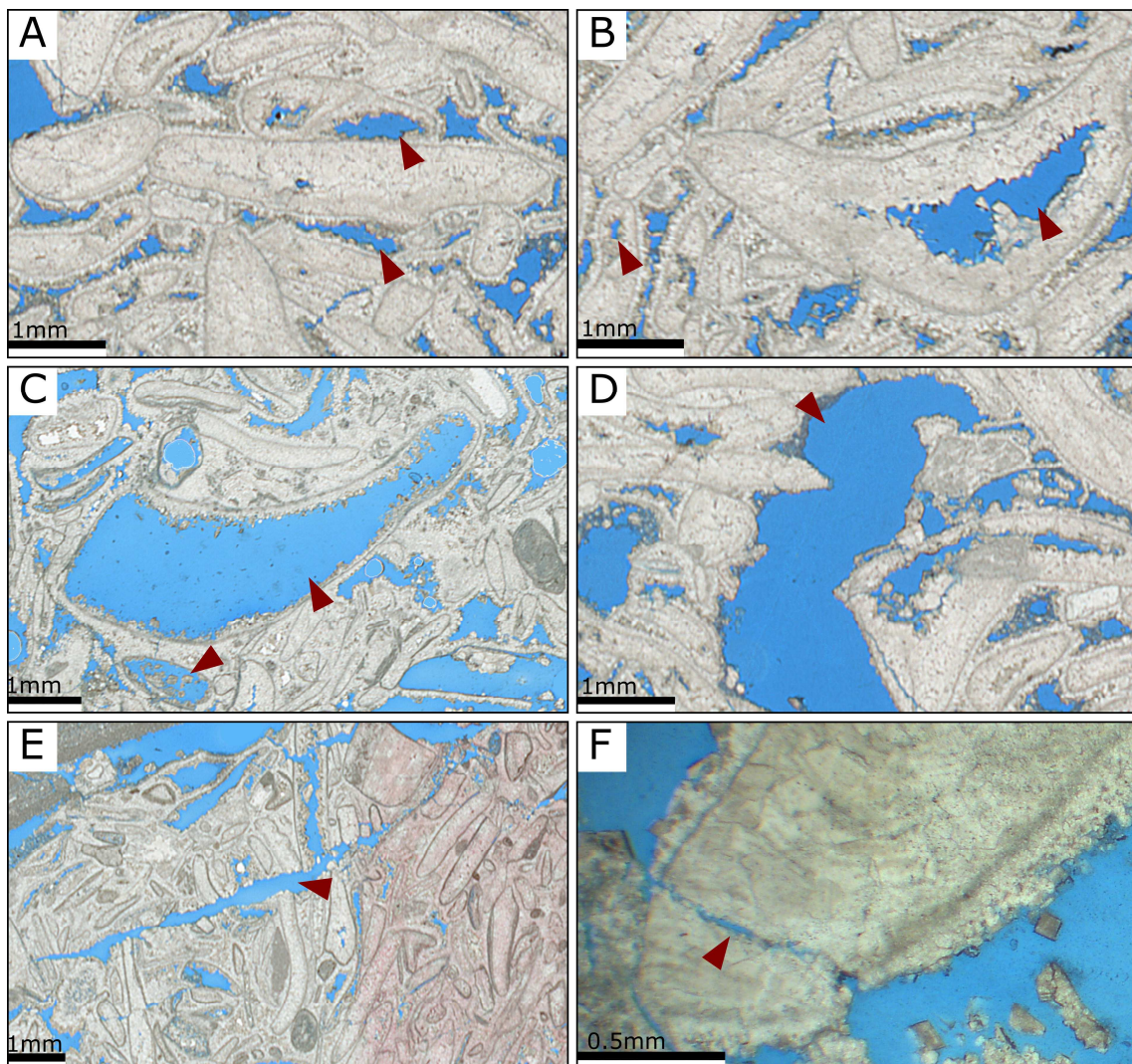


Fig. 5. The main pore types according to the Choquette and Pray classification: Fabric-selective pores: A) Interparticle, B) Intraparticle and C) moldic. Non-fabric-selective pores: D) Vugs, E) macro-fractures and F) micro-fractures.

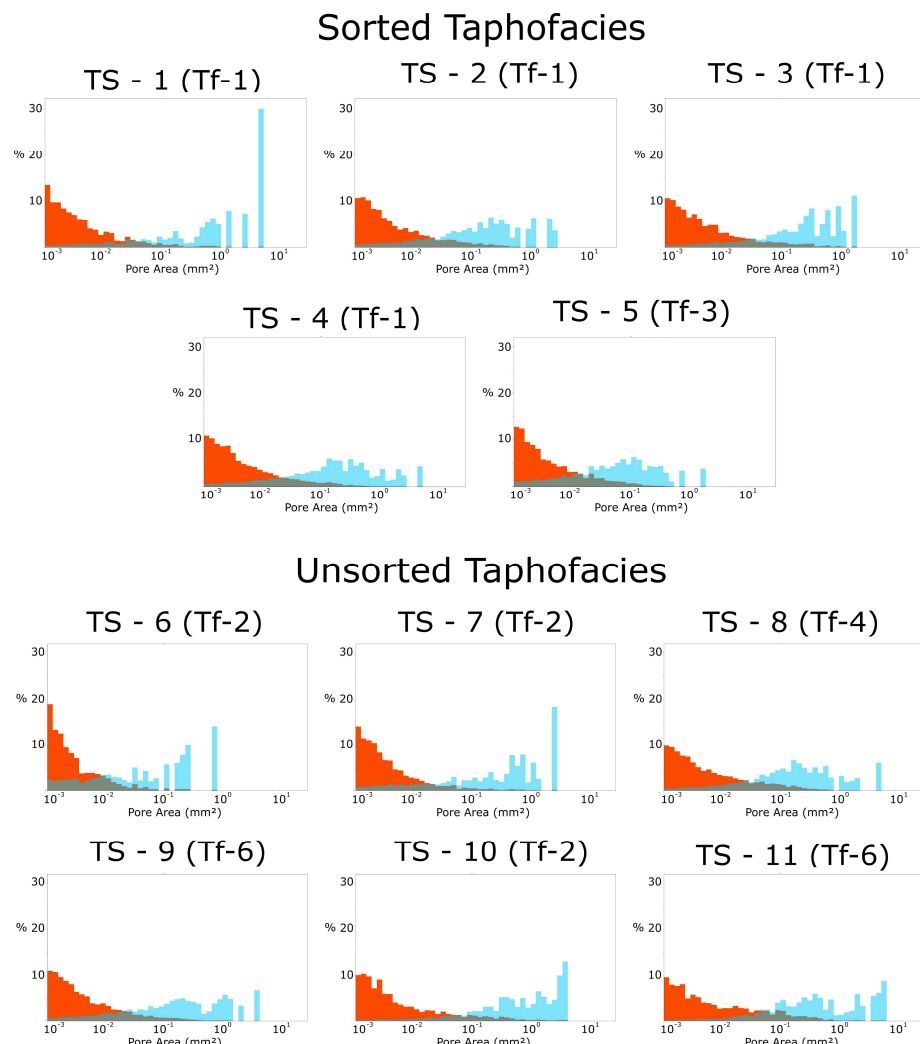
**Thin section pore segmentation:** The pore area obtained by the analysis of images of thin sections ranges between 0.1 and 7 mm<sup>2</sup>, where more than 50% of pore area corresponds to pores with values below 0.5 mm<sup>2</sup> (Fig. 6, 7). The factors of controlling porosity (Ahr, 2008) were obtained through pore-type segmentation (depositional or diagenetic) for well-sorted and unsorted taphofacies (Tables 3, 4), where samples with a majority of interparticle pores are classified as depositional, whereas vugs, molds, and intraparticle are classified as diagenetic. Samples with similar values between depositional and diagenetic were classified as Hybrid 1 (Ahr, 2008). In Figure 6, the orange bars represent the frequency of a pore area interval, whereas the blue bar correspond to the percentage contribution of each area interval to the total porosity.

Table 3. Total porosity and estimated types in well-sorted taphofacies.

ID	Taphofacies	Total porosity (%)	Estimated pore types	Porosity Group (Ahr, 2008)
TS-1	Tf-1	14.15	8% Vug, 6% inter-, intra-particle and moldic	Hybrid 1
TS-2	Tf-1	14.13	10% inter-particle, 3% vug, 1% moldic	Depositional
TS-3	Tf-1	12.47	4% inter-particle, 4% channel, 3% vug, 2% moldic	Hybrid 1
TS-4	Tf-1	21.32	Intense dissolution	Hybrid 1 / Diagenetic
TS-5	Tf-1/3	9.28	7% inter-particle, 1% moldic, 1% vug	Depositional

Table 4. Total and estimated segmented porosity in unsorted Taphofacies.

ID	Taphofacies	Total porosity (%)	Estimated pore types	Porosity Group (Ahr, 2008)
TS-6	Tf-2	1.4	moldic, vugs	Diagenetic
TS-7	Tf-2	11.26	5% moldic, 3% vugs, 3%inter-particle	Hybrid 1
TS-8	Tf-4	14.87	Moldic	Diagenetic
TS-9	Tf-6	10.26	3% moldic, 4% vug, 4% inter-particle	Hybrid 1
TS-10	Tf-2	12.25	6% moldic, 3% vug, 3% inter-particle	Hybrid 1
TS-11	Tf-6	15.25	10% moldic, vug, 5%inter-particle	Hybrid 1
TS-12	Tf-2	15.05	7% Vug, 7% moldic	Diagenetic

Fig. 6. Pore area results ( $\text{mm}^2$ ; x axis in logarithmic scale) of well-sorted (TS-1 to 5) and unsorted (TS-6 to 11) taphofacies based on thin section images. The orange bars represent the frequency of pore area and the blue bars correspond to the contribution of each pore area to the total porosity.

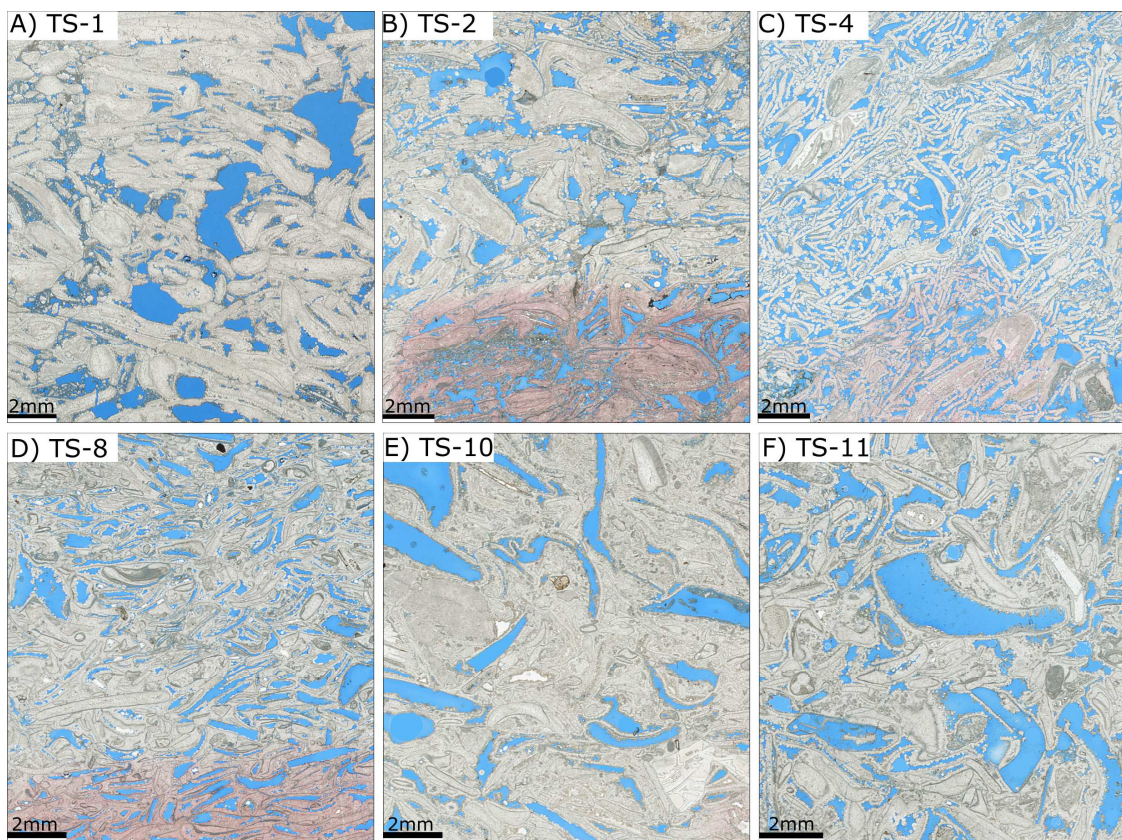
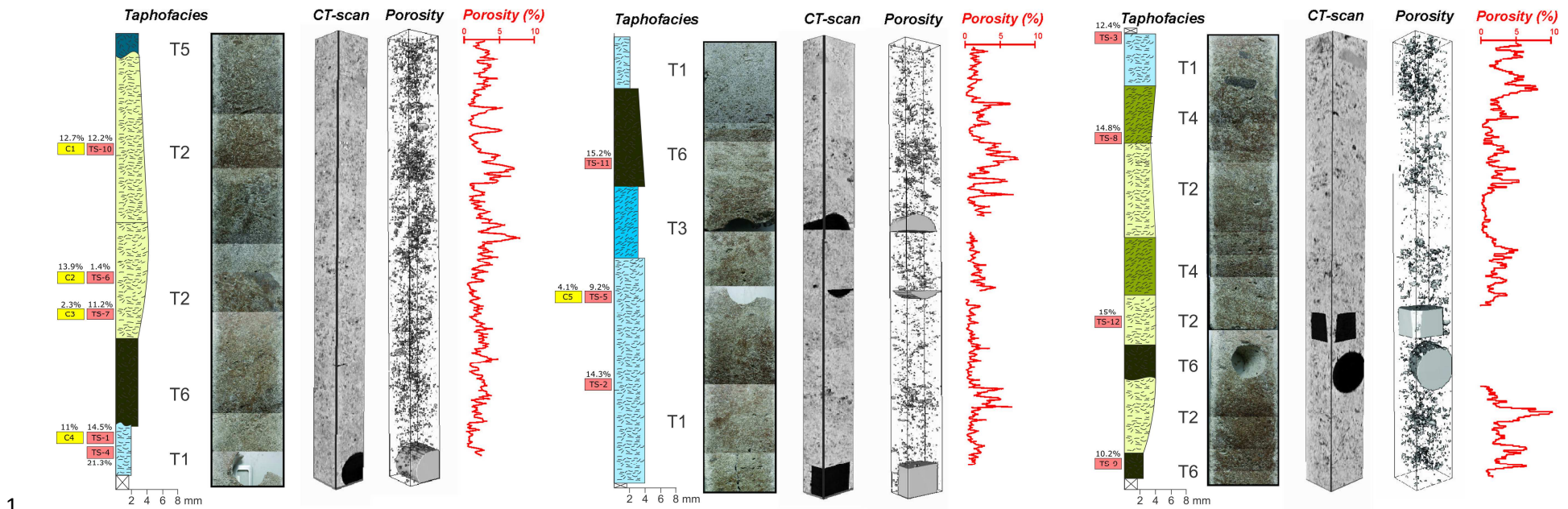


Fig. 7. Thin-section examples of well-sorted and unsorted taphofacies. A-C) Well-sorted taphofacies; and D-F) Unsorted taphofacies. Note that the largest pores in the area correspond to moldic pores and vugs, whereas the small pores are interparticle and intraparticle pores. More details concerning the total porosity are found in Tables 3 and 4.

**CT and H-CT analysis:** X-ray Computed Tomography (CT) was used for imaging the core volume. A total of 3 m were imaged at the resolution of 100  $\mu\text{m}$ , involving the six taphofacies and then segmented to porosity extraction (Fig. 8). The porosity in the core ranges between 1 and 8%. Furthermore, the pore size extracted from the main taphofacies was compared (Fig. 9). Ten sub-volumes (plugs) covering different taphofacies were selected (Tf-1, Tf-2, Tf-3, Tf-5 and Tf-6) for a H-CT scan analysis. As in the CT scan, the pores were segmented (Fig. 10) and, due to the high resolution of the analysis (40-50 micrometers), it was possible to determine the pore connectivity (coordination number - CN) and pore volume of samples (Fig. 11).



1  
2 Fig. 8. Porosity based on a tomography scan of the core (CT-scan). Generally, high values of porosity are related to the  
3 vugs and moldic pores. The low values are related to the  
4 low resolution of the CT-scan to capture the smaller pores. Yellow rectangles are the plug samples and red rectangles the thin sections (TS). All of them exhibit the measured porosity through image analysis (H-CT and TS images).

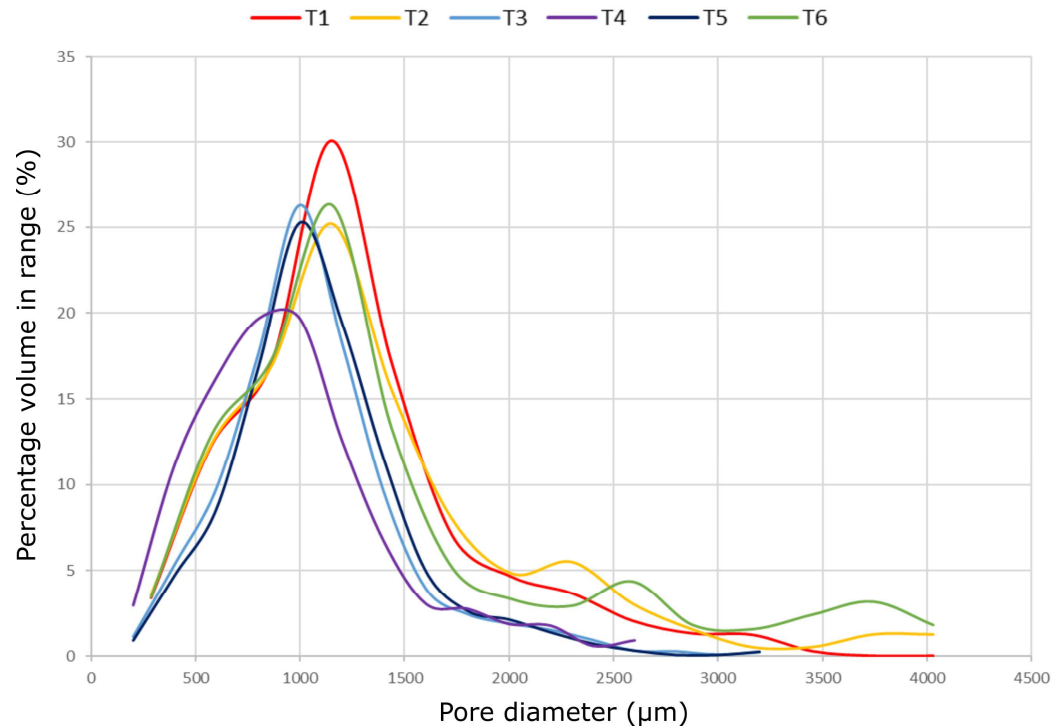


Fig. 9. Pore-size distribution based on tomography scan (CT-scan) of the core in taphofacies Tf-1-Tf-6. The values of pore size are very close in all taphofacies, ranging between 900-1200 micrometers. Unsorted taphofacies (Tf-2 and Tf-6) exhibit larger pores when compared to well-sorted taphofacies, having pore diameters larger than 2500 micrometers.

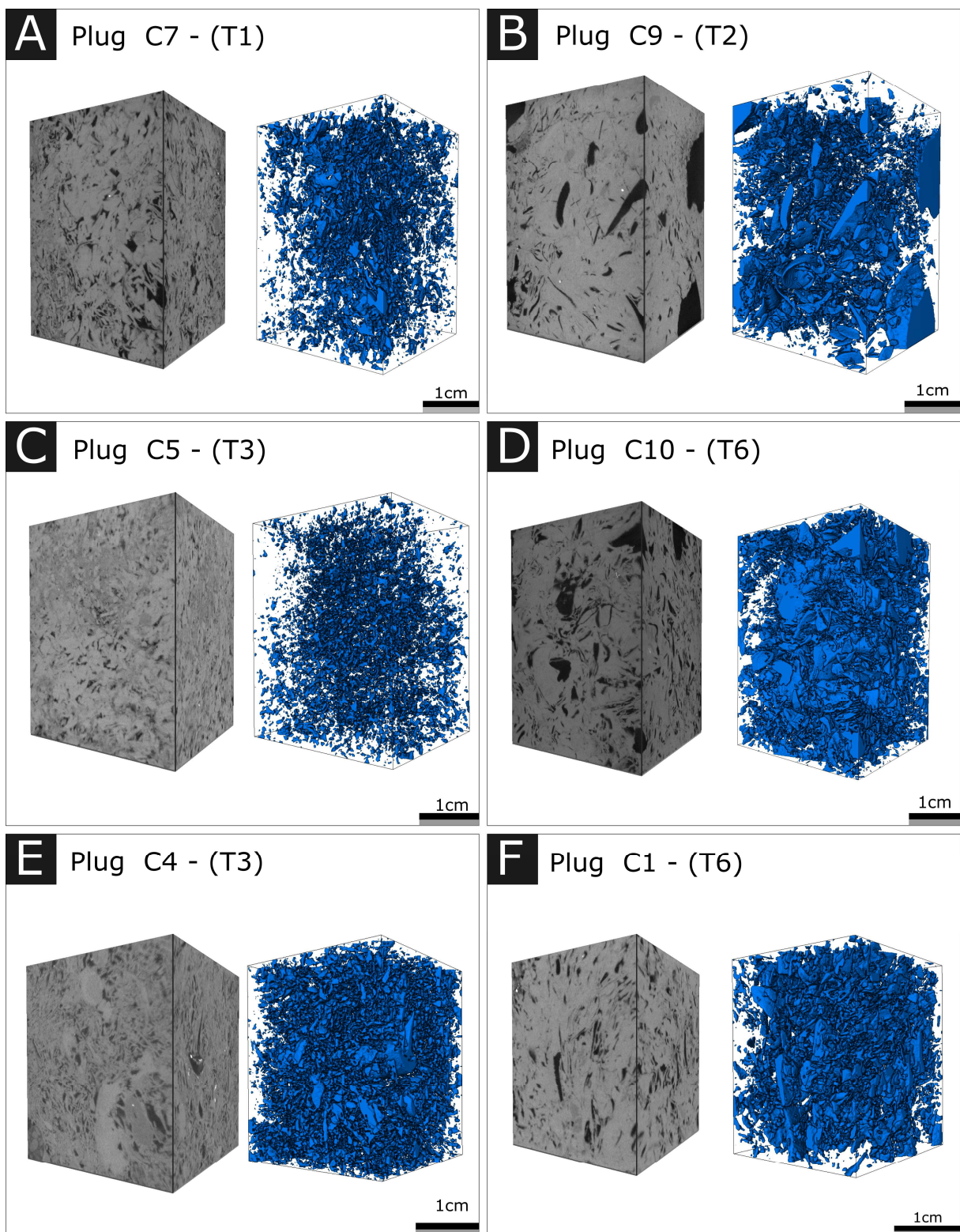
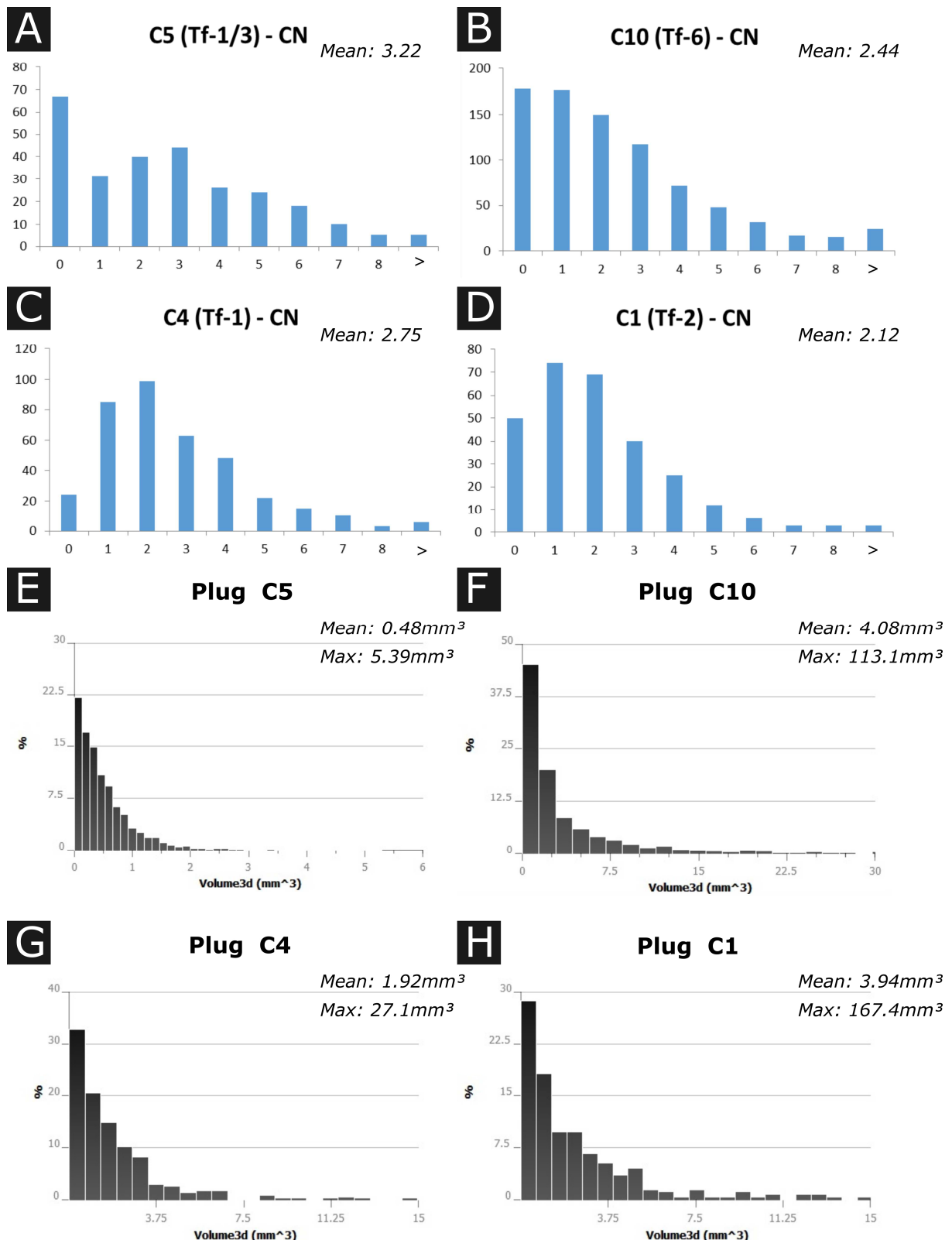


Fig. 10. Segmentation of pore space by H-CT images for well-sorted (A, C and E) and unsorted (B, D and F) taphofacies. Pores in well-sorted taphofacies are mainly of the interparticle and intraparticle type, whereas the unsorted taphofacies have moldic pores and vugs. The pore size in unsorted taphofacies is larger than in well-sorted taphofacies, due to the occurrence of moldic pores and vugs.



**NMR analysis:** Firstly, to validate the NMR analyses, the results of total porosity by gas injection and the results obtained by the NMR were compared. The data showed a good correlation ( $R^2 = 0.89$ , Fig. 12A). The high correlation indicates that the technique was able to capture the entire amplitude of pores in the rock. In order to determine a T2 cutoff that adequately separates the FFI and BVI areas – generally related to macro- and microporosity - the irreducible water saturation (Swir) was obtained by centrifuge method. However, it was not possible to quantify a reliable Swir because the samples fragmented during centrifugation, due to their high porosity and friability. Only few samples could be measured, indicating a cutoff of 70 ms. As just a few measurements are insufficient to represent the data set, the cutoff was determined by comparison with the experimental permeability data. Different cutoffs were tested in the Timur Coates equation in order to reach the best cutoff for permeability calculation. The best results came from a 100 ms cutoff, showing a correlation factor of 0,73 (Fig. 12B). In this ways the cutoff 0-100 ms indicate micropores and values between 100-3000 ms macropores. The results of the NMR for well-sorted and unsorted taphofacies is represented in Figure 13.

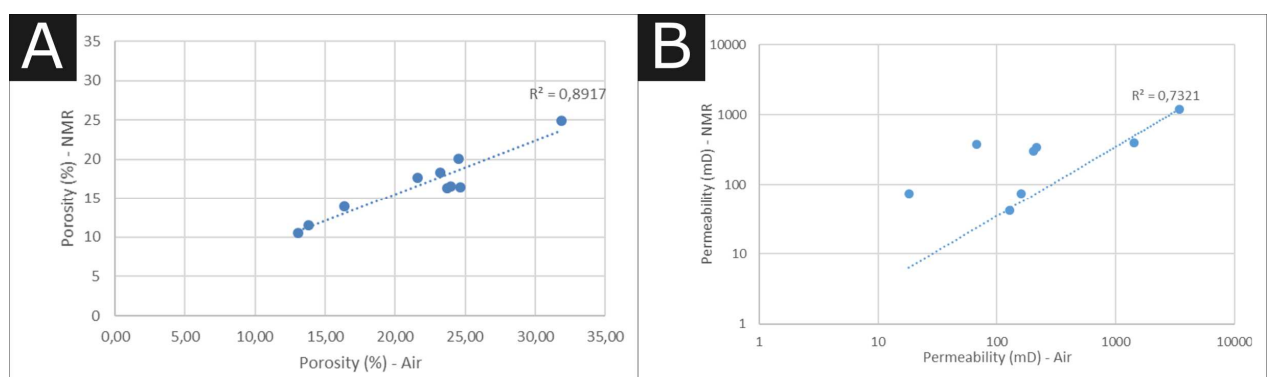


Fig. 12. A) Cross-plot of the NMR porosity vs. laboratory measurements. B) NMR permeability vs. laboratory measurements for samples from the Itapema Formation.

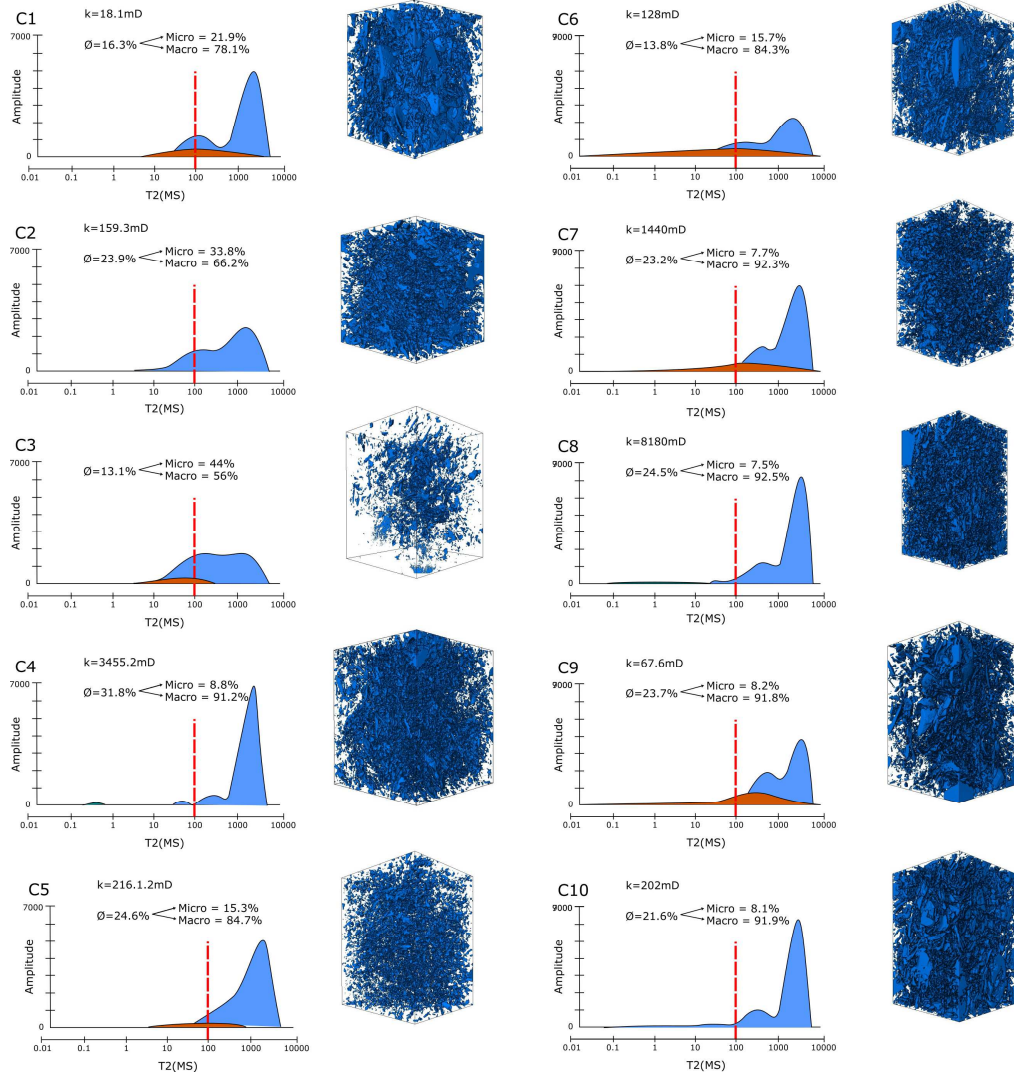


Fig. 13. Samples from the Itapema Formation. A) T2 curves for 100% (blue) and Swir (orange) saturations and the percentage of micro- and macropores calculated from T2 cutoff; B) H-CT scan of plugs.

### 3.5. DISCUSSION

#### 3.5.1. Taphofacies Interpretation

The analyzed interval of the Itapema Formation is mainly classified as grainstones and rudstones, with rare occurrences of micrite, presenting a dense packing of shells and common intraclasts. The orientation of the valves varies between concordant, oblique and chaotic with respect to bedding, in which plane-parallel structures and low angle cross-stratification can be observed.

The taphonomic features such as fragmented and non-articulated shells, abraded valves, and rare occurrence of finer grains point to a high-energy depositional environment (Brett et al., 1986; Kidwell et al., 1986; Kidwell, 1991; Fürsich and Oschmann, 1993). These taphonomic characteristics is a consequence of a high residence time at the sediment-water interface, reworking and transport. Aguirre and Farinati (1999) relate the abrasion and fragmentation with environment energy, time of exposure and particle size. They conclude that the high degree of fragmentation and abrasion are associated with reworking of the shells and the best attributes to differentiate in situ from transported deposits. Storm deposits may exhibit similar characteristics (Sanchez et al., 1991; Fürsich and Pandey, 1999; Li et al., 2007) where densely packed coquinas with broken and disarticulated shells are associated with allochthonous deposits. Taphonomic features such as shells with low degree of fragmentation and abrasion, as also the presence of closed valves or in life-position indicate low-energy environments and autochthonous / parautochthonous depositis (Brett et al., 1986; Kidwell et al., 1986; Kidwell, 1991; Fürsich and Oschmann, 1993). This pattern of accumulation was not observed in described section. Based on these characteristics, the interval of described coquinas can be interpreted as high energy deposits influenced by storms and reworked by currents and waves (Carvalho et al., 2000; Muniz, 2013; Muniz and Bosence, 2018; Mizuno et al., 2018; Oliveira et al., 2019).

In taphofacies Tf-1 and Tf-3 shells are oriented parallel and oblique to bedding, an effect of high energy environments which are influenced by waves and currents (Salazar-Jimenez et al., 1982; Fürsich and Pandey, 1999). The taphonomic characteristics support a scenario of reworked deposits located above the fair-weather wave-base as shoreface and foreshore deposits (Kidwell, 1991; Fürsich and Oschmann, 1993; Fürsich, 1995, Tavares et al., 2015; Chinelatto et al., 2018a, Muniz and Bosence, 2018; Oliveira et al., 2019). Furthermore, the presence of cross-bedding in Tf-3 may reflect high-energy bioclastic bars (Carvalho et al., 2000, Oliveira et al., 2019). In some rudstones, the few highly abraded and fragmented valves and silicified shell intraclasts, are indicative of time-averaging. This reveals that shells of different ages and environments were reworked and are possibly related to lake-level fluctuations and storm events (Fig. 14A).

Taphofacies Tf-2 and Tf-4, despite displaying taphonomic characteristics similar to Tf-1, show a high diversity of fine grains such as peloids, very small micrite intraclasts, shell debris, and ostracods. The high occurrence of these fine grains indicates a low-energy deposits, such as restricted deposits or storm deposits located below the fair-weather wave-base (Muniz and Bosence, 2018; Oliveira et al., 2019). However, in these taphofacies, some

taphonomic features, such as a high degree of fragmentation and abrasion are observed and indicate high energy conditions. The high amount of abraded and fragmented valves may point to washover or storm deposits with low sediment supply. In the first case, during storm surges, shells are removed from the shoreface and foreshore (zones where valves are in constant motion), and can be transported and deposited as coquina ridge (Jahnert et al., 2012). When the energy of currents is strong enough, the shells are reworked and deposited as washover deposits and a mixture of broken and abraded valves with small grains occurs, resulting in poorly-sorted deposits, as in the case of the Holocene coquinas of the Sharks Bay (Jahnert et al., 2012). In storm deposits, the presence of abrade and fragmented valves can be associate with a long residence time of shells on the sediment-water interface. The sedimentation rate and hardpart input control the time of exposition of valves (Kidwell, 1986; Tomašových et al., 2006). When the sediment supply or hardpart input is low, the shells are susceptible to a high residence time in the sediment-water interface and consequently to the process that lead the high degree of abrasion, fragmentation and bioerosion/micritization. Also, the presence of micrite laminae in taphofacies Tf-2 (Fig. 14B) indicate periods of calm water, which may occur in both settings following episodes of high energy (Dattilo et al., 2012). However, in storm deposits, the occurrence of erosional surfaces is common (Fürsich and Oschmann, 1993), a feature absent in taphofacies Tf-2. Furthermore, in some samples, fine grains such as micrite and very small carbonate fragments infiltrated the interparticle and moldic pores (Fig. 14C). These features indicate the vadose zone and could be associated with low water levels in shallow areas. Other features that support this interpretation are the occurrence of stevensite ooids with nuclei of ostracods and other shells, valves with a stevensitic and the presence of mudstone intraclasts (Fig. 14D-E). In lacustrine systems, the stevensite occurs in alkaline and saline waters as observed in Lake Turkana, in Kenya (Cerling, 1996) and Green River Formation of Central Utah (Bradley and Fahey, 1962; Tettenhorst and Moore, 1978). In the Campos and Congo basins, stevensite is interpreted as a product of magnesium-rich lake waters at sub-littoral zones (Wright, 2012; Tosca and Wright, 2015; Oliveira et al., 2019) where stevensite ooids and peloids are a product of shallow and slightly agitated water (Armelenti et al., 2016).The mudstone intraclasts (Fig. 14E) are from fine-grained sediments at the lake border or the product of eroded and transported microbial mats (microbial intraclasts), as highlighted by Muniz (2013) in the coquinas of the Coqueiros Formation in the Campos Basin.

Taphofacies Tf-5 and Tf-6 are interpreted as storm-induced concentrations, supported by the chaotic arrangement of shells, occurrence of ostracods and an erosional base of the

beds (Fürsich and Oschmann, 1993; Simões and Torello, 2003). Furthermore, the bioerosion/micritization in these taphofacies is higher compared to the others. Some samples exhibit a mix between very micritized and well-preserved shells (Fig. 14F), a feature of low-energy environments (Fürsich and Oschmann, 1993). The mixture of well-preserved and abraded, fragmented and micritized bioclasts corroborates time averaging, indicating a low sediment input in the system (Kidwell, 1986) and, consequently, the absence of some features such as fine-grained sediments in graded storm deposits.

Recently, Fick et al., (2018) simulated the formation of shell concentrations in flume experiments under fair-weather- and storm-wave conditions. They conclude that waves, storm-induced currents, the breaker and the shoaling zone control the distribution of shell concentration. Figure 15 provides the taphofacies interpretation of the analyzed deposits, indicating the limits of the breaker zone and zone of winnowing during fair-weather (Fig. 15A, C) and storm conditions (Fig. 15B, D).

During fair-weather conditions, taphofacies Tf-1 and Tf-3 formed at the shoreface and foreshore, while Tf-2 occurred below the winnowing zone where peloids could settle. At the same time, in restricted areas, peloids, seteensis ooids and shells with stevensite coatings are formed. At the lake margin, microbialites and mudstones may occur. During storm surges, the zone of reworking is wider and storm waves and currents are capable of eroding previously deposited taphofacies (red lines in Fig. 15D). Foreshore and shoreface coquinas may be eroded, transported and deposited as washover deposits with a mixture of old and fresh shells, whereas at the lake margin, the waves are capable of removing and transporting clay and microbialites clasts. In the deepest areas of the lake, mudstones may have been deposited even though they were not observed in the core section analyzed.

According to the analyzed interval the coquinas occur between the foreshore to offshore transitional, mainly as bioclastic bars and washover fans, because no marginal or deep lake facies were encountered, which may only be represented by a few carbonate intraclasts.

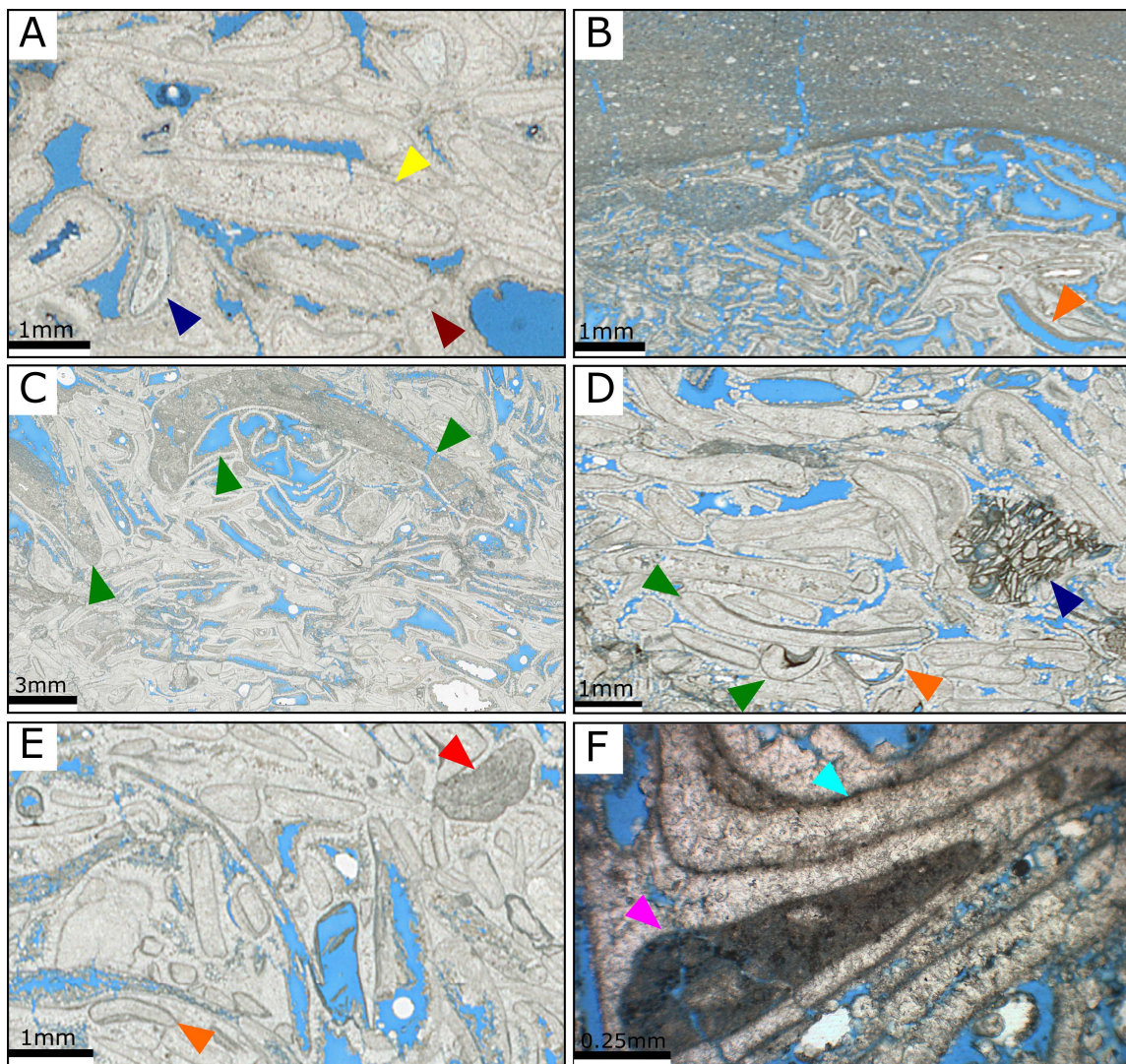


Fig. 14. A) Mix of fragmented (dark red arrow), well rounded (yellow arrow) and silicified (blue arrow) valves in taphofacies Tf-1. B) Laminae of clay and small carbonate grains (Tf-2). – The orange arrow points to a dissolved shell with preserved stevensite border. C) Clay infiltration in interparticle and moldic pores (green arrow) (Tf-2). D) Concave-up oriented shells with preserved micrite (green arrow), partially dissolved valve with stevensite border (orange arrow) and small intraclasts (blue arrow) (Tf-2). E) Microbialite Intraclast (red arrow) and abraded shell with stevensite border (orange arrow) (Tf-2). F) Mix of strongly micritized (pink arrow) and faintly micritized valves (blue arrow) in taphofacies Tf-6.

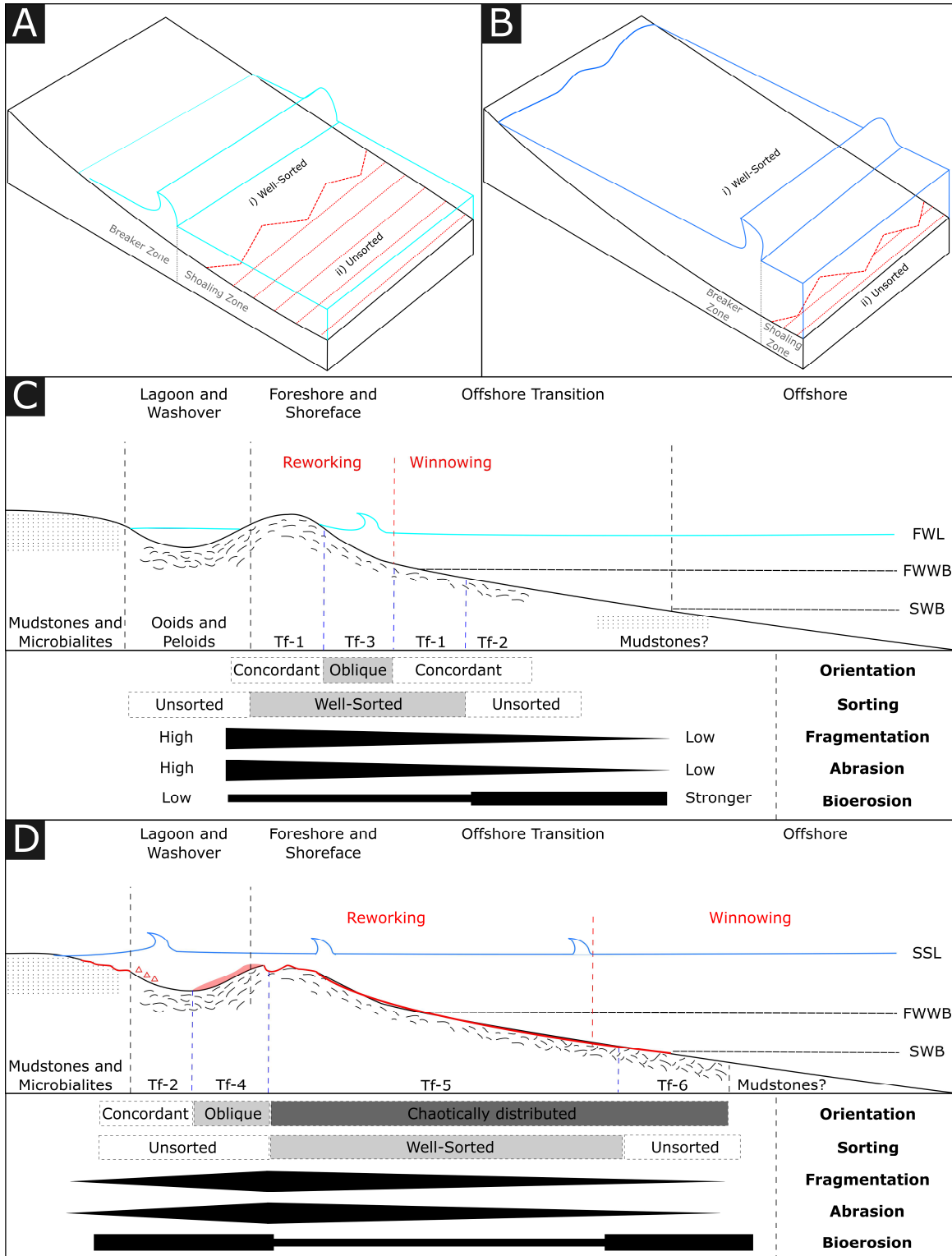


Fig. 15. Depositional interpretation of taphofacies under first wave breakpoint (Fick et al., 2018): A, C) Fair-weather conditions; B, D) Storm conditions.

### 3.5.2. Origin of porosity

Porosity varies between all taphofacies and in general do not exhibit a particular pattern but ranges from depositional to diagenetic with the great majority occurring as "Hybrid 1".

**Depositional porosity:** This type of porosity is represented by samples of the well-sorted taphofacies Tf-1, Tf-3 and Tf-5. The main pore type observed in this domain is interparticle pores, which are the result of depositional processes such as the action of waves, storm currents and winnowing. Due to the similar taphonomic characteristics of taphofacies Tf-1, Tf-3 and Tf-5, the porosity exhibit the same pore type and similar pore distribution in depositional type unlike taphofacies Tf-2, Tf-4 and Tf-6 that are unsorted. In this case the primary pore space is filled by finer grains reducing the depositional porosity close to zero. Diagenesis is incipient and is responsible for enhancing or reducing some interparticle pores. Cementation by circumgranular calcite is common and reduced the primary pores but did not fill it completely. Neomorphism and dissolution are high and are responsible for intraparticle pores. The degree of dolomitization and silicification varies from low to absent, and has little or no influence on porosity reduction. Analyzing thin sections and H-CT scan images, it can be shown that the pores with low area values correspond to the interparticle and intraparticle pores (Figs. 7, 10, 12), whereas some large pores represent rare moldic pores and vugs. The results of the NMR reveals that microporosity contributes to the total porosity (Fig. 13C5) but most of pores are macropores (84%). Interparticle pores can be very well identified by images of the H-CT scan, due to its high resolution (Figs. 10, 11). The well-sorted taphofacies generally exhibit low values of pore volume and the highest coordination numbers with mean values above 2.7, indicating that these facies, although having lower pore-volume values, exhibit the best of connectivity (Fig. 11 A, E). In general, this type exhibits a good pore connectivity that will influence the permeability directly.

**Hybrid 1 porosity:** This type of porosity is produced by depositional and diagenetic processes and porosity therefore varies between primary and secondary. In general, this type shows the following diagenetic characteristics: calcite cementation, dolomitization, neomorphism, micritization, and silicification. The main diagenetic difference in this group lies of the enhancement or reduction of porosity through dissolution and cementation. Coquinas with a higher degree of cementation are generally associated with Tf-2, Tf-4 and Tf-6 and tend to have a lower amount of interparticle pores, whereas a high dissolution of shells and cements generates moldic pores, channels and vugs. Differences in diagenetic processes are related to the occurrence of drusy calcite cements and the degree of dissolution. The taphofacies Tf-1, Tf-3 and Tf-5 exhibit calcite rims around the bioclasts reducing the primary porosity. Rare drusy calcite occurs obstructing the smallest interparticle pores decreasing the pore connectivity. The drusy cement post-dates circumgranular calcite that reduces interparticle porosity, while dissolution occurred at later stage, creating large vugs and moldic

pores. The taphofacies that exhibit drusy calcite followed by dissolution are Tf-2, Tf-4, Tf-5 and Tf-6 but commonly observed in Tf-2 and Tf-6. Based on the analysis of thin sections and H-CT scans (Fig. 11G, F) large pores can be correlated with the dissolution of shells and cements and areas with smaller pores with some interparticle and intraparticle pores. The NMR results of samples with high porosity values, due to the dissolution and preservation of primary pores (Fig. 13C1, C4), exhibit large quantities of macropores, mainly interparticle, moldics and vugs, whereas those with lower porosity, due to calcite cementation (Fig 13C3), exhibit a similar distribution of micro- and macropores (50% each). The “Hybrid 1” type can be identified in the CT-scan, due to the occurrence of larger pores ( $>100$  micrometers) and have a higher total porosity than samples with a depositional control of porosity. In general, this type exhibits a good pore connectivity, as observed in the H-CT scan (Fig. 11B, C), and high pore volume values as a result of shell dissolution (Fig. 11F, G). However, the pore system becomes tighter when calcite cementation is higher, reducing the interparticle pore space (Fig 13C3).

**Diagenetic porosity:** This type of porosity may be enhanced or reduced by diagenetic processes. In general, the group of samples that fit the diagenetic domain has, as main characteristic, an enhanced moldic and intraparticle porosity due to the dissolution of bioclasts, and the reduction of interparticle pores due to calcite cementation. The porosity in this type is related to isolated pores, connected either by small fractures or by rare interparticle porosity. Overall, the type displays dissolution, cementation, silicification, micritization, neomorphism and dolomitization. Samples of this type usually belong to the unsorted taphofacies Tf-2, Tf-4 and Tf-6. Diagenetic features that differ from other taphofacies are the absence of circumgranular calcite cement and the presence of only drusy or granular calcite, reducing interparticle pores to near zero. Dissolution and neomorphism occurred after the cementation processes and produced pores such as vugs and molds. Using thin sections, CT scans, and H-CT scans, it is possible correlate the large pores with vugs that reach close to  $160 \text{ mm}^3$  (Fig. 11H). Cases of intense dissolution were observed only in samples of well-sorted taphofacies where few shells are well-preserved (Fig. 7C). The NMR results exhibit a microporosity of one-third and a macroporosity of two-thirds (Fig. 13C2). The macropores resulted from the dissolution of shells that generated moldic and intraparticle pores. The permeability value is lower than in the depositional and hybrid types, due to the poor pore connectivity, and in some samples the coordination number is close to 2 (Fig. 11D).

Although the origin of porosity is different in each taphofacies, the values of total porosity are very similar (Tables 2-4), and the pore sizes differs little between depositional and diagenetic types (Figs. 6-7, 10, 11). Taphofacies whose porosity is controlled by sedimentary process will exhibit pores with a low area value (interparticle pores), whereas the Hybrid 1 to diagenetic types that have channels, moldic, and vug pores will have the largest values. In hybrid and diagenetic types, the moldic pores are easily identified in core section (Fig. 3A, C, E) due to the shell orientation. This pore orientation can be useful to identifying taphofacies Tf-1/2 (oriented shells concordant to the bedding), Tf-3/4 (oblique shells) and, Tf-5/6 (chaotically distributed shells).

Despite similar values of porosity, the permeability differs from all taphofacies. This is associated with the preservation of the primary pore space, pore throat and connectivity. Herlinger et al. (2017) studied coquinas of the Campos Basin and concluded that they vary between coquinas with preserved primary porosity with high permeability and coquinas with reduced primary porosity and low values of permeability.

The same pattern is observed in our analyzed section. The well-sorted coquinas represented by taphofacies Tf-1, Tf-3 and Tf-5, are coquinas with the best values of porosity and permeability. These taphofacies exhibit a porosity control between depositional to diagenetic. The preservation of primary pore space associated with the enhance of porosity by dissolution promotes the best values to porosity and permeability (Table 2 – C4-8). The unsorted taphofacies (Tf-2, Tf-4 and Tf-6) show few preserved primary pores and a hybrid to diagenetic porosity control. The porosity is enhanced by dissolution of the biofabric however, the low connectivity and tight pore throat reduce the values of permeability.

Figure 16 shows the influence of calcite cementation and dissolution between the depositional to diagenetic control of porosity, and the main pore type found in each group. In depositional control, taphofacies Tf-1, Tf-3 and Tf-5, will show great values of porosity and permeability comparable with the taphofacies Tf-2, Tf-4 and Tf-6 that exhibit finer grains between the shells reducing the interparticle space. In hybrid control the cementation and dissolution will controls the enhancement or reduction of porosity in all taphofacies. Generally, the high cementation is observed in all taphofacies, however, the samples that show great indices of dissolution was the taphofacies Tf-1, Tf-3 and Tf-5. In diagenetic control, the taphofacies Tf-2, Tf-4 and Tf-6 is dominant, the high cementation obstructs the primary pores, and only secondary porosity is observed. For these taphofacies the diagenesis reduces the primary pore, however, the dissolution of shells and matrix will promote the

moldic pores and vugs. Great dissolution was observed in Taphofacies Tf-1 and Tf-3, that represent the best value of porosity and permeability in our analyzed section.

Using a qualitative description for porosity and permeability (Ahr, 2008), it is possible to define the coquina deposits with a fair (10%) to an excellent (20% or more) values of porosity and a good (50-250 mD), very good (250-1000 mD) and excellent ( $> 1000$  mD) of permeability. All taphofacies will exhibit a range of fair to excellent for porosity whereas permeability will change. The taphofacies interpreted as storm-induced deposits of low winnowing, represented by Tf-2, Tf-4 and Tf-6, varies from good to very good permeability whereas the taphofacies Tf-1, Tf-3 and Tf-5 product of winnowed and reworked deposits varies between very good to excellent reservoir.

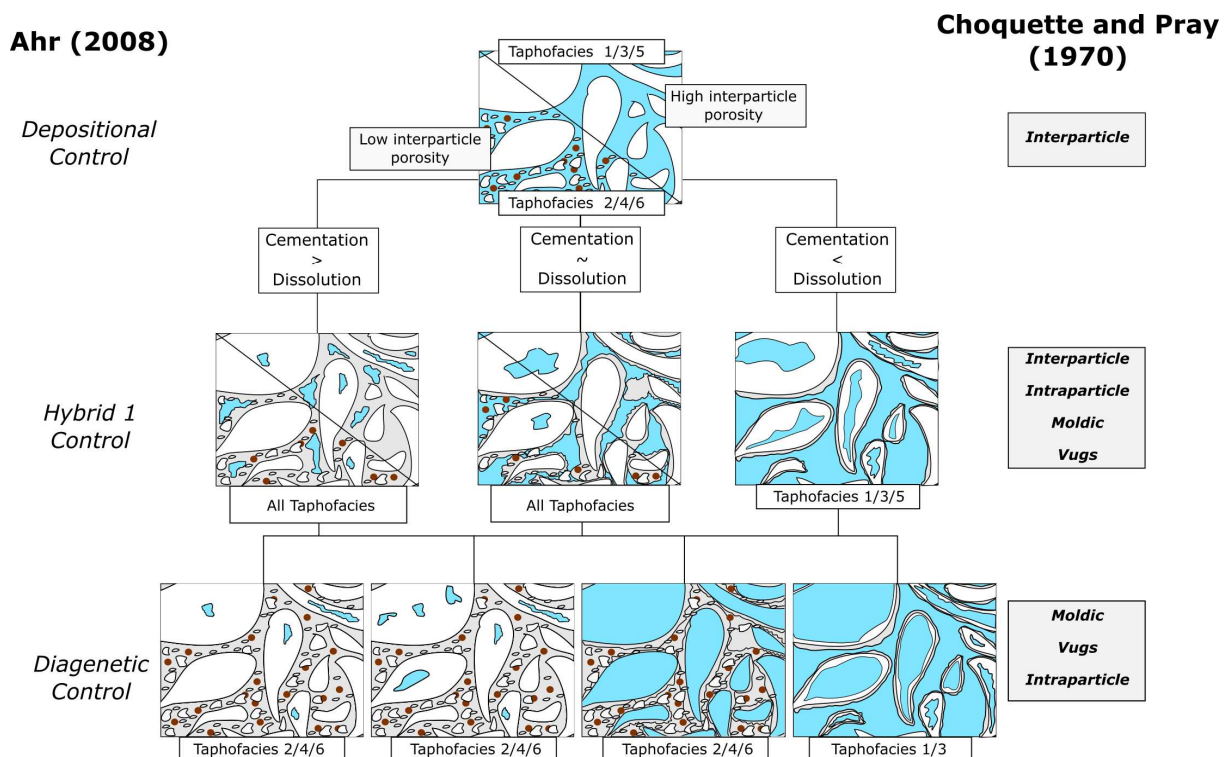


Fig. 16. Control of porosity according to Ahr (2008), the influence of calcite cementation (C) and dissolution (D), and main taphofacies found in each type. When the cementation prevails over dissolution ( $C > D$ ) interparticle pores are reduced, whereas  $C < D$ , vugs and molds are created.

### 3.5.3. NMR log comparison

When comparing permeability values from plugs (Table 2, Fig. 13) and the NMR well log (Fig. 17D), there is a good correlation between well-sorted and unsorted taphofacies using a T2 cutoff of 100 ms (Fig. 17E). The lowest values of permeability in the NMR perm log are

generally related to the unsorted taphofacies, due to the poor connectivity of pores, whereas the highest values are related to well-sorted taphofacies, as observed in laboratory measurements (Fig. 13). In the permeability log (Fig. 17D), a cutoff curve of 100 mD was used to categorize the interval. Plugs of well-sorted taphofacies fit in areas above this value, while unsorted taphofacies fit below (Fig. 17B).

Analyzing the pore distribution, the multiple T2 cutoff (Fig. 17C) varies along the section. Cutoff values between 0.3-100 ms (green color), indicate micro-porosity, whereas values from 100-3000 ms (blue color) correspond to the macropores. Micropores are present in well-sorted and unsorted taphofacies as shown by the laboratory NMR plug analysis (Fig. 13). However, these types of pores are abundant in unsorted taphofacies, as observed in samples C1, C2 and C3, with values ranging between 20-40%, whereas the well-sorted taphofacies generally exhibit values between 8-16% (samples C4 to C8). In Figure 16C, the micropore peaks fit in areas where the permeability is low and again are related to the unsorted taphofacies that display the lowest permeability values. The macropores are common in the entire section and reflect the macroporosity observed in all the taphofacies, generally associated with interparticle pores, vugs and moldic pores. Areas with high values of macropores but low values of permeability, may be associated with the unsorted taphofacies and their low pore connectivity due to cementation and isolated moldic pores (Figs. 7E, F, 13).

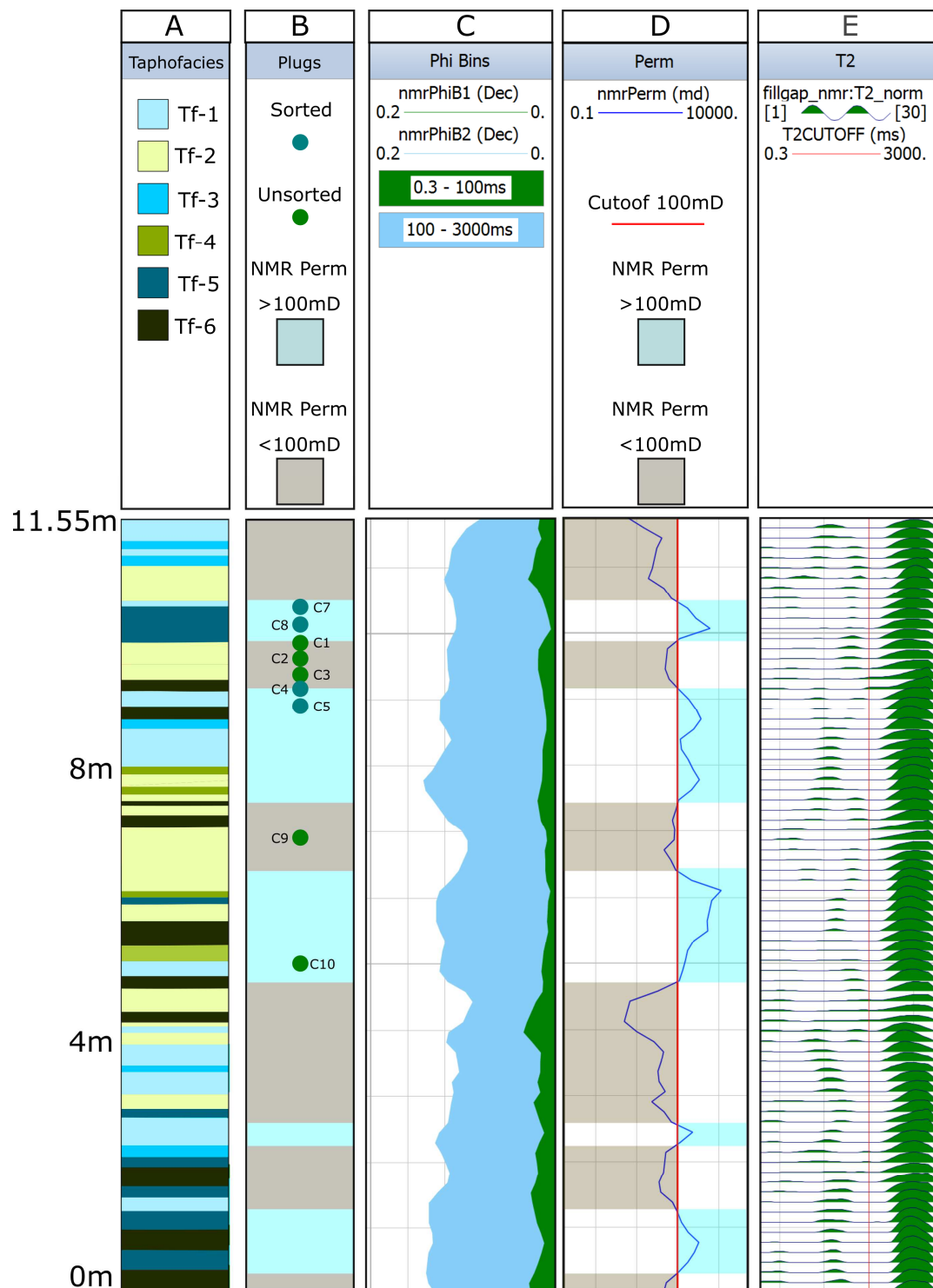


Fig. 17. NMR well log of analyzed interval (Fig. 2). A) Taphofacies groups divided. B) Location of analyzed plugs (C1 to C10, C6 is not available in this interval). C) Phi bins curves; in green the cut-off between 0.3-100 ms that corresponds to the micropores; in blue, the cutoff of 100-3000 ms that represents the macropores. D) Permeability curve obtained by the NMR analysis. E) T2 curve, the red line corresponding to a cutoff of 100 ms for permeability calculations.

### 3.6. CONCLUSIONS

The taphonomic features of the analyzed coquina interval varies greatly. In this study, six taphofacies are recognized and grouped into well-sorted and unsorted taphofacies. The samples were grouped in this way because sorting was the main taphonomic characteristic that influence the petrophysical parameters. The well-sorted taphofacies are interpreted as shallow-water coquinas, where currents and waves were capable of removing the finer grains (ostracods, peloids, small shell fragments, and micrite). The unsorted taphofacies are interpreted as low-energy deposits when compared with the well-sorted taphofacies, where waves and currents were not of sufficient strength to remove small grains. The origin of porosity in all taphofacies varies from depositional to diagenetic and is mainly classified as hybrid. In the well-sorted taphofacies, interparticle pores and a depositional to hybrid porosity origin is common, and cementation in these taphofacies is incapable of reducing the primary porosity to values close to zero. The porosity in well-sorted taphofacies varies from 9% to 21% according to thin-section analysis and 15-30% according to gas measurements, the pores being mainly interparticle, intraparticle, moldic, and vugs. In the unsorted taphofacies, the porosity origin varies from hybrid 1 to diagenetic. The primary porosity is reduced due to the presence of grains and cement, and the main pore types are moldic and vugs. The porosity in unsorted taphofacies varies from 2% to 15% according to thin-section analysis, although almost all values are between 10-15% and between 13-24% according to gas measurements. The laboratorial NMR results support the distribution of micro- and macropores. Generally, all taphofacies exhibit good macroporosity due to the occurrence of vugs and moldic pores. However, due to the occurrence of higher amounts of micropores, the unsorted taphofacies exhibit the lowest permeability values because of the poor pore connectivity compared to the well-sorted taphofacies. All taphofacies in the described interval are excellent to good reservoirs, due to the good values of porosity and permeability.

## Acknowledgements

The authors acknowledge financial support provided by CAPES. This study was financed in part by the “Coordenação de Aperfeiçoamento de Pessoal de Nível Superior - Brasil (CAPES)” - Finance Code 001. Thanks to all laboratory researchers from CEPETRO and LMPT and Agencia Nacional do Petróleo (ANP) for making data available. The authors are grateful for the reviewers Franz T. Fürsich and anonymous review, for their constructive comments and suggestions to improve the quality of the paper.

### 3.7. REFERENCES

- ABRAHÃO, D., 1987. Lacustrine and associated deposits in a rifted continental-margin: the Lagoa Feia formation, Lower Cretaceous, Campos Basin, offshore Brazil [MS Thesis]: Colorado School of Mines, Arthur Lakes Library, 207 p.
- ABRAHÃO, D., WARME, J.E., 1990. Lacustrine and associated deposits in a rifted continental margin-Lower Cretaceous Lagoa Feia Formation, Campos Basin, offshore Brazil. In: Katz, B.J. (Ed.), *Lacustrine Basin Exploration—Case Studies and Modern Analogs*. American Association of Petroleum Geologists Memoir, v. 50, p. 287–305.
- AGUIRRE, M, L., FARINATI, E, A., 1999. Taphonomic processes affecting late Quaternary molluscs along the coastal area of Buenos Aires Province (Argentina, Southwestern Atlantic). *Palaeogeography, Palaeoclimatology, Palaeoecology* 149, 283–304. doi:[https://doi.org/10.1016/S0031-0182\(98\)00207-7](https://doi.org/10.1016/S0031-0182(98)00207-7).
- AHR, W.M., 2008. *Geology of Carbonate Reservoirs: The Identification, Description, and Characterization of Hydrocarbon Reservoirs in Carbonate Rocks*: Hoboken, John Wiley & Sons, 296 p.
- ALLEN, D, F., BOYD, A, MASSEY, J, FORDHAM, E, J., AMABEOKU, M, O., KENYON, W, E., WARD, W, B., 2001. *The Practical Application Of Nmr Logging In Carbonates: 3 Case Studies*. Society of Petrophysicists and Well-Log Analysts.
- ANSELMETTI, F.S., LUTHI, S., EBERLI, G.P., 1998. Quantitative Characterization of Carbonate Pore Systems by Digital Image Analysis. *American Association of Petroleum Geologists Bulletin*, v. 82(10), p. 1815-1836.
- ARMELENTI, G., GOLDBERG, K., KUCHLE, J., DE ROS, L.F., 2016. Deposition, diagenesis and reservoir potencial of non-carbonate sedimentar rocks from the rift section of Campos Basin, Brazil. *Petroleum Geoscience*, v.22, p. 223-239.
- BAUMGARTEN, C.S., DULTRA, A. J.C., SCUTA, M.S., FIGUEIREDO, M.V.L., SEQUEIRA, M.F.P. B., 1988. Coquinas da Formação Lagoa Feia, Bacia de Campos: evolução da Geologia de Desenvolvimento. *Boletim de Geociências da Petrobrás*, v. 2(1), p. 27–36.
- BELILA, A.M.P., KURODA, M.C., SOUZA, J.P.P., VIDAL, A.C., TREVISAN, O.V., 2018. Petrophysical characterization of coquinas from Morro do Chaves Formation (Sergipe-Alagoas Basin) by X-ray computed tomography. *Revista do Instituto de Geociências – USP*, v. 18(3), p. 3-13.
- BEASLEY, C.J., FIDUK, J.C., BIZE, E., BOYD, A., ZERILLI, DRIBUS, J.R., MOREIRA, J.L.P. AND PINTO, A.C.C., 2010. Brazil's Presalt Play. *Oilfield Review*, v. 22(3), p. 28–37.
- BRADLEY, W.H., FAHEY, J.J., 1962. Occurrence of stevensite in the Green River Formation of Wyoming. *American Mineralogist* 47, 996–998.
- BRESSAN, G.S., PALMA, R.M., 2010. Taphonomic analysis of fóssil concentrations from La Manga Formation (Oxfordian), Neuquén Basin, Mendoza Province, Argentina. *Journal of Iberian Geology*, v. 36(1), p. 55-71.
- BRETT, C.E., 1995. Sequence Stratigraphy, Biostratigraphy, and Taphonomy in Shallow Marine Environments. *PALAIOS*, v. 10, p. 597-616.

- BRETT, C.E. AND BAIRD, G.C., 1986. Comparative Taphonomy: A Key to Paleoenvironmental Interpretation Based on Fossil Preservation. *PALAIOS*, v. 1, p. 207-227.
- CAINELLI, C., MOHRIAK, W.U., 1999. Some remarks on the evolution of sedimentary basins along the Eastern Brazilian continental margin. *Episodes*, v. 22, p. 206–216.
- CARVALHO M.D., PRAÇA U.M., TELLES A.C.S., 2000. Bioclastic carbonate lacustrine facies molds in the Campos Basin (Lower Cretaceous), Brazil. In Gierlowski-Kordesch E.H., Kelts K.R. (eds) *Lake Basins through Space and Time* Tulsa. AAPG, AAPG Studies in Geology 46, p. 245-256.
- CERLING, T. E. 1996. Pore water chemistry of an alkaline lake: Lake Turkana, Kenya. In: Johnson, T. C. & Odada, E. O. (eds) *Limnology, Climatology and Paleoclimatology of the East African Lakes*. Gordon and Breach, Amsterdam, p. 225–240.
- CHANG, H.K., KOWSMANN, R.O., FIGUEIREDO, A.M.F., BENDER, A.A., 1992. Tectonics and stratigraphy of the East Brazil Rift system: an overview. *Tectonophysics*, v. 213, p. 97-138.
- CHANG, H.K., ASSINE, M.L., CORRÊA, F.S., TINEN, J.S. VIDAL, A.C., KOIKE, L., 2008. Sistemas petrolíferos e modelos de acumulação de hidrocarbonetos na Bacia de Santos. *Revista Brasileira de Geociências*, v. 38(2), p. 29-46.
- CHEN, J., CHEN, Z., TONG, J., 2010. Palaeoecology and taphonomy of two brachiopod shell beds from the Anisian (Middle Triassic) of Guizhou, Southwest China: Recovery of benthic communities from the end-Permian mass extinction. *Global and Planetary Change*, v. 73, p. 149-160.
- CHINELATTO, G.F., VIDAL, A.C., KURODA, M.C., BASILICI, G., 2018a. A taphofacies model for coquina sedimentation in lakes, (Lower Cretaceous, Morro do Chaves Formation, NE Brazil). *Cretaceous Research*, v. 85, p. 1-19.
- CHINELATTO, G.F., KURODA, M.C., VIDAL, A.C., 2018b. Relação entre biofábrica e porosidade, coquinas da Formação Morro do Chaves (Barremiano/Aptiano), Bacia de Sergipe-Alagoas, NE-Brasil. *GEOLOGIA USP. SÉRIE CIENTÍFICA*, v. 18, p. 57-72.
- CHOQUETTE, P.W., PRAY, L., 1970. Geologic nomenclature and classification of porosity in sedimentary carbonates. *American Association of Petroleum Geologists Bulletin*, v. 54, p. 207-250.
- COATES, G.R., XIAO, L., PRAMMER, M.G., 1999. NMR logging: Principles and Applications. USA: Halliburton Energy Services.
- CORBETT, P.W.M., ESTRELLA, R., RODRIGUEZ, A.M., SHOEIR, A. BORGHI, L., TAVARES, A.C., 2016. Integration of Cretaceous Morro do Chaves rock properties (NE Brazil) with the Holocene Hamelin Coquina architecture (Shark Bay, Western Australia) to model effective permeability. *Petroleum Geoscience*, v. 22(2), p. 105-122.
- DATTA, D., THAKUR, N., GHOSH, S., PODDAR, R., SENGUPTA, S., 2016. Determination of porosity of rocks samples from photomicrographs using image analysis. *IEEE 6th International Conference on Advanced Computing*.
- DATTILO, B.F., BRETT C.E., TSUJITA, C.J., FAIRHURST, R., 2008. Sediment supply versus storm winnowing in the development of muddy and shelly interbeds from the Upper Ordovician of the Cincinnati region, USA. *Canadian Journal of Earth Sciences* v. 45, p. 243-265.

- DATTILO, B. F., BRETT, C. E., SCHRAMM, T. J., 2012. Tempestites in a teapot? Condensation-generated shell beds in the Upper Ordovician, Cincinnati Arch, USA. *Palaeogeography, Palaeoclimatology, Palaeoecology* 367–368, 44–62.
- DUNHAM, R.J., 1962. Classification of carbonate rocks according to depositional texture. In: Ham, W.E. (Ed.), *Classification of carbonate rocks*. American Association of Petroleum Geologists Memoir, v. 1, p. 108-121.
- EMBRY, A.F., KLOVAN, J.E., 1971. A Late Devonian reef tract on Northeastern Banks Island, NWT. *Canadian Petroleum Geology Bulletin*, v. 19, p. 730-781.
- FICK, C., TOLDO JR, E.E., PUHL, E., 2018. Shell concentration dynamics driven by wave motion in flume experiments: Insights for coquina facies from lake-margin settings. *Sedimentary Geology*, v. 374, p. 98-114.
- FÜRSICH, F.T., 1995. Shell concentrations. *Eclogae Geologicae Helvetiae*, v. 88(3), p. 643-655.
- FÜRSICH, F.T., OSCHMANN, W., 1993. Shell beds as tools in basin analysis: the Jurassic of Kachchh, western India. *Journal of the Geological Society*, v. 150, p. 169-185.
- FÜRSICH, F.T., PANDEY, D.K., 1999. Genesis and environmental significance of Upper Cretaceous shell concentrations from the Cauvery Basin, southern India. *Palaeogeography, Palaeoclimatology, Palaeoecology*, v. 145, p. 119-139.
- HERLINGER, R.J., ZAMBONATO, E.E., DE ROS, L.F., 2017. Influence of Diagenesis On the Quality of Lower Cretaceous Pre-salt Lacustrine Carbonate Reservoirs from Northern Campos Basin, Offshore Brazil. *Journal of Sedimentary Research*, v. 87(12), p. 1285–1313.
- HORODYNSKI, R.S., BRETT, C.E., SEDORKO, D., BOSSETI, E.P., SCHEFFLER, S.M., GHILARDI, R.P., IANNUZZI, R., 2019. Storm-related taphofacies and paleoenvironments of Malvinokaffric assemblages from the Lower/Middle Devonian in southwestern Gondwana. *Palaeogeography, Palaeoclimatology, Palaeoecology*, v. 514, p. 706-722.
- JAHNERT, R, DE PAULA, O, COLLINS, L, STROBACH, E, PEVZNER, R, 2012. Evolution of a coquina barrier in Shark Bay, Australia by GPR imaging: Architecture of a Holocene reservoir analog. *Sedimentary Geology* 281, 59–74. doi:10.1016/J.SEDGEO.2012.08.009.
- KATTAH, S., 2017. Exploration Opportunities in the Pre-Salt Play, Deepwater Campos Basin, Brazil. *The Sedimentary Record* v. 15(1), p. 4-8. Doi 10.2110/sedred.2017.1
- KIDWELL, S.M., 1986. Models for fossil concentrations: paleobiologic implications. *Paleobiology*, v. 12(1), p. 6-24.
- KIDWELL, S.M., 1991. The stratigraphy of shell concentrations. In: Allison, P.A., Briggs, D.E.G. (Eds.), *Taphonomy, Releasing the Data Locked in the Fossil Record*: Plenum Press, New York, p. 211-290.
- KIDWELL, S.M., FÜRSICH, F.T., AIGNER, T., 1986. Conceptual Framework for the Analysis and Classification of Fossil Concentrations. *PALAIOS* v.1, p. 228-238.
- KIDWELL, S.M., HOLLAND, S.M., 1991. Field description of coarse bioclastic fabrics. *PALAIOS*, v. 6(4), p. 426-434.

- LI, Y., SHA, J., QIFEI, W., CHEN, S., 2007. Lacustrine tempestite litho- and biofacies in the Lower Cretaceous Yixian Formation, Beipiao, western Liaoning, northeast China. *Cretaceous Research* 28, 194–198. doi:doi.org/10.1016/j.cretres.2006.10.002.
- MACEDO, J.M., 1990. Evolução Tectônica da Bacia de Santos e áreas continentais adjacentes. In: Gabaglia, G.P.R., and Milani, E.J., Origem e Evolução de Bacias Sedimentares: Petrobras 2.<sup>a</sup> ed., p. 361-376.
- MATOS, R.M.D., 1992. The Northeastern Brazilian Rift System. *Tectonics*, v. 11, p. 766-791.
- MAZURKIEWICZ, L., MLYNARCZUK, M., 2013. Determining rock pore space using image processing methods. *Geology, Geophysics & Environment*, v. 39(1), p. 45-54.
- MCGLUCE, M.M., SOREGHAN, M.J., MICHEL, E., TODD, J.A., COHEN, A., MISCHLER, J., O'CONNELL, C.S., CASTAÑEDA, O.S., HARTWELL, R.J., LEZZAR, K.E., NKOTAGU, H.H., 2010. 'Environmental controls on shell-rich facies in tropical lacustrine rifts: A view from Lake Tanganyika's littoral', *PALAIOS*, vol. 25(7), p. 426-438.
- MELDAHL, K., FLESSA, H., 1990. Taphonomic pathways and comparative biofacies and taphofacies in a Recent intertidal/shallow shelf environment. *Lethaia*, v. 23(1), p. 43-60.
- MILANI, E.J., THOMAZ-FILHO, A., 2000. Sedimentary Basins of South America. In: Cordani, U.G., Milan, E.J., Thomaz-Filho, A. and Campos, D. A. (eds) *Tectonic evolution of South America, 31st International Geological Congress, Rio de Janeiro*, p. 389–449.
- MIZUNO, T.A., MIZUSAKI, A.M.P., LYKAWKA, R., 2018. Facies and paleoenvironments of the Coqueiros Formation (Lower Cretaceous, Campos Basin): A high frequency stratigraphic model to support pre-salt “coquinas” reservoir development in the Brazilian continental margin. *Journal of South American Earth Sciences*, v. 88, p. 107-117.
- MOHRIAK, W., NEMČOK, M., ENCISO, G., 2008. South Atlantic divergent margin evolution: rift-border uplift and salt tectonics in the basins of SE Brazil. *Geological Society, London, Special Publications*, v. 294, p. 365-398.
- MOREIRA, J.L.P., MADEIRA, C.V.M., GIL, J.A., MACHADO, M.A.P., 2007. Bacia de Santos. *Boletim de Geociências da Petrobras*, v. 15(2), p. 531-549.
- MUNIZ, M.C., 2013. Tectono-Stratigraphic evolution of the Barremian-Aptian Continental Rift Carbonates in Southern Campos Basin, Brazil. [PhD thesis]: Royal Holloway University of London, Earth Sciences Department, 343 p.
- MUNIZ, M.C., BOSENCE, D.W.J., 2015. Pre-salt microbialites from the Campos Basin (offshore Brazil): image log facies, facies model and cyclicity in lacustrine carbonates. In: Bosence, D.W.J., Gibbons, K.A. et al. (eds) *Microbial Carbonates in Space and Time: Implications for Global Exploration and Production*. Geological Society, London, Special Publications, 418 p.
- MUNIZ, M.C., BOSENCE, D.W.J., 2018. Lacustrine carbonate platforms: Facies, cycles, and tectonosedimentary models for the presalt Lagoa Feia Group (Lower Cretaceous), Campos Basin, Brazil. *American Association of Petroleum Geologists Bulletin*, v. 102(12), p. 2569-2597.

- OLIVEIRA, V.C.B., SILVA, C.M.A., BORGHI, L.F., CARVALHO, I.S., 2019. Lacustrine coquinas and hybrid deposits from rift phase: Pre-Salt, lower Cretaceous, Campos Basin, Brazil. *Journal of South American Earth Sciences*, v. 95, Article 102254.
- PUGA-BERNABÉU, Á., AGUIRRE, J., 2017. Contrasting storm- versus tsunami-related shell beds in shallow-water ramps. *Palaeogeography, Palaeoclimatology, Palaeoecology*, v. 471, p. 1-14.
- QUAGLIO, F., WARREN, L.V., ANELLI, L.E., SANTOS, P.R., ROCHA-CAMPOS, A.C., GAZDZICKI, A., STRIKIS, P.C., GHILARDI, R.P., TIOSSI, A.B., SIMÕES, M.G., 2014. Shell beds from the Low Head Member (Polonez Cove Formation, early Oligocene) at King George Island, west Antarctica: new insights on facies analysis, taphonomy and environmental significance. *Antarctic Science*, v. 26(4), p. 400-412.
- QUIRK, D.G., HERTLE, M., JEPPESEN, J.W., RAVEN, M., MOHRIAK, W.U., KANN, D., NORGAARD M., HOWE, M.J., HSU, D., COFFEY, B., MENDES, M.P., 2013. Rifting, subsidence and continental break-up above a mantle plume in the central South Atlantic. *Geological Society, London, Special Publications*, v. 369, p. 185-214.
- REGO, E.A., BUENO, A.D., 2015. Reservoir Rocks Image Binarization: a Comparative Study Between Neural Network Method and Otsu Variance. *International Journal of Modelling and Simulation for the Petroleum Industry*, v. 9(1), p. 31-36.
- RICCOMINI, C., LUCY, G.S., TASSINARI, C.C.G., 2012. Pré-sal. geologia de exploração. *Revista USP*, v. 95, p. 33-42.
- SANCHEZ, T.M., WAISFELD, B., BENEDETTO, J.L., 1991. Lithofacies, taphonomy, and brachiopod assemblages in the Silurian of western Argentina: A review of Malvinokaffric Realm communities. *Journal of South American Earth Sciences*, vol. 4, p.307-329.
- SALAZAR-JIMENEZ, A., FREY, R.W., HOWARD, J.D., 1982. Concavity orientations of bivalve shells in estuarine and nearshore shelf sediments, Georgia. *Journal of Sedimentary Research*, v. 52(2), p. 565-586.
- SCHUAB, F.B., WINTER, A., TREVISON, O.V., BONZANINI, L.A.F., 2015. NMR Log Interpretation in Bimodal Carbonate Rocks Based on Core-to-Log Integration. *Society of Petrophysicists and Well-Log Analysts*.
- SIMÕES, M.G., TORELLO, F.F., 2003. Modelo de Tafofácies para os moluscos bivalves do Grupo Passa Dois (Formação Serra Alta, Teresina e Corumbataí), Permiano Superior, Bacia do Paraná, Brasil. *Revista Brasileira de Geociências*, v. 33(4), p. 371-380.
- SOUZA, A., CARNEIRO, G., ZIELINSKI, L., POLINSKI, R., SCHWARTZ, L., HÜRLIMANN, M., D., VASCONCELLOS AZEREDO, R., B., 2013. Permeability Prediction Improvement Using 2D NMR Diffusion-T2 Maps. *Society of Petrophysicists and Well-Log Analysts*.
- TAVARES, A.C., BORGHI, L., CORBETT, P., NOBRE-LOPES, J., CÂMARA, R., 2015. Facies and depositional environments for the coquinas of the Morro do Chaves Formation, Sergipe-Alagoas Basin, defined by taphonomic and compositional criteria. *Brazilian Journal of Geology*, v. 45(3), p. 415-429.
- TETTENHORST, R., MOORE, G.E.J., 1978. Stevensite oolites from the Green River Formation of Central Utah. *Journal of Sedimentary Petrology* 48 (2), 587–594

THOMPSON, D.L., STILWELL, J.D., HALL, M., 2015. Lacustrine carbonate reservoirs from Early Cretaceous rift lakes of Western Gondwana: Pre-Salt coquinas of Brazil and West Africa. *Gondwana Research*, v. 28(1), p. 26-51.

TOMAŠOVÝCH, A., FÜRSICH, F.T., WILMSEN, M., 2006. Preservation of autochthonous shell beds by positive feedback between increased hardpart-input rates and increased sedimentation rates. *The Journal of Geology*, v. 114, p. 287-312.

TOSCA, N.J., WRIGHT, V.P., 2015. Diagenetic pathways linked to labile Mg-clays in lacustrine carbonate reservoirs: a model for the origin of secondary porosity in the Cretaceous Pre-Salt Barra Velha Formation, offshore Brazil. In: Armitage, P.J., Butcher, A.R., Churchill, J.M., Csoma, A.E., Hollis, C., Lander, R.H., Omma, J.E., Worden, R.H. (Eds.), *Reservoir Quality of Clastic and Carbonate Rocks: Analysis, Modelling and Prediction*. Geological Society, London, Special Publications vol. 435, pp. 33–46.

WRIGHT, V., 2012. Lacustrine carbonates in rift settings: the interaction of volcanic and microbial processes on carbonate deposition. Geological Society, London, Special Publications, v. 370, p. 39-47.

ZIELINSKI, J.P.T., VIDAL, A.C., CHINELATTO, G.F., COSER, L., FERNANDES, C.P., 2018. Evaluation of pore system properties of coquinas from Morro do Chaves Formation by means of x-ray microtomography. *Brazilian Journal of Geophysics*, v. 36(4).

**4. RELATIONSHIP BETWEEN BIOFABRIC AND PETROPHYSICS IN COQUINAS, INSIGHTS ON BRAZILIAN BARREMIAN-APTIAN CARBONATES OF SANTOS AND SERGIPE-ALAGOAS BASINS.**

Guilherme Furlan, Chinelatto(1a); Aline Maria Poças, Belila (1b); Mateus, Basso (1c); Alexandre Campane, Vidal (1d)

<sup>1</sup>Centro de Estudos do Petróleo (CEPETRO), Universidade Estadual de Campinas (UNICAMP), +55(19)3521-4659, Rua 06 de Agosto, n°50 - first floor, Campinas, Sp, Brazil.

(a) gfchinelatto@gmail.com; (b) alinebelila@yahoo.com.br; (c) bassomgeo@gmail.com; (d) acvidal@gmail.com

**Key words:** petrophysics, shell concentrations, coquina, porosity, permeability

**Artigo será submetido**

## ABSTRACT

Shell deposits or coquinas are a kind of sedimentary rock composed mainly by shells and their fragments with a carbonate or siliciclastic matrix. These rocks exhibit a broad range of porosity and permeability values that are related with depositional and diagenetic process. In the last decade, a series of coquina reservoir where discovered in the Campos and Santos Basins in eastern margin of Brazil and the understanding of the petrophysical properties of these rocks is essential for reservoir production. In this work samples from Morro do Chaves Formation (Sergipe-Alagoas Basin) and Itapema Formation (Santos Basin) where selected to identify the porosity vs permeability relationship according to the biofabric characteristics and the porosity control. The biofabric textures where classified in 4 groups according to taphonomic signatures and diagenetic modification: i) well-sorted and preserved biofabric, ii) well-sorted and altered biofabric, iii) unsorted and preserved biofabric and, iv) unsorted and altered biofabric. The porosity control varies in all groups from depositional to diagenetic whit distinct poretypes, pore sizes and pore connectivity that are located in different Global Hydraulic Elements (GHE). The analysis of pore space was carried out through laboratorial measurements (gas injection) and by images of High-Resolution Computed Tomography from plug samples, resulting in a Pore Network Model where values of pore radius, pore throat radius and coordination number was obtained. By the analysis of porosity control domain, it is possible to see a good relationship between porosity and permeability at depositional to diagenetic control. Samples of Depositional domain with good values of porosity and permeability are represented by samples of well-sorted preserved biofabric (GHE-5/6), whereas the worst values are associated with unsorted samples or well sorted samples that had the primary pore space occluded by the diagenesis such as compaction and cementation (GHE-3/4). The hybrid domain has a high range of porosity and permeability (GHE-4/8) as well as the diagenetic domain (GHE-3/7). Both groups are composed by well sorted and unsorted biofabric textures and the distribution in GHE are associated both by the preservation of primary pore space as also the enhance or reduction of porosity by the diagenesis. The best values (GHE-7-8) are related with well-sorted altered biofabrics, whereas the lowest values (GHE3-4) either with unsorted biofabrics with low pore connectivity or biofabrics that had the porosity reduced by compaction and cementation.

**Keyword:** Petrophysics, porosity, permeability, coquinas.

#### **4.1. INTRODUCTION**

Carbonate rocks can be very heterogeneous due to the variety of the carbonate grains, depositional environment, and diagenetic modifications, exhibiting a complex pore system that influence directly on the permeability distribution and then in the fluid flow patterns (Lucia, 1999; Lønøy, 2006). The Shell deposits (or coquinas) are a type of sedimentary rock composed mainly by shells of bivalves and their fragments, they can exhibit either siliciclastic or carbonate matrix, have a broad range of thickness and lateral extension and register a variety of depositional processes resulting in different types of shell condensed deposits (Kidwell, 1991).

In the last decade, number of studies emphasize the importance of understanding how the shell deposits are distributed under lacustrine systems (Carvalho et al., 2000; Tavares et al., 2015; Chinelatto et al., 2018a; Muniz and Bosence 2018) due to the discovery of pre-salt coquina reservoirs in the Brazilian east margin basins such as the Campos and Santos Basins (Abrahão and Warme, 1990; Carvalho et al., 2000; Thompson et al., 2015; Kattah, 2017), and in the west African Basins such as the Congo, Cabinda and Kwanza Basins (Thompson et al., 2015; Ceraldi and Green, 2016; Saller et al., 2016). Besides the facies distribution and depositional system interpretations, some works were aimed in petrophysical analysis for textural patterns of coquinas using different techniques such as computed tomography and x-ray microtomography, Nuclear Magnetic Resonance and Electrical Resistivity (Corbett et al., 2016; Luna et al., 2016; Corbett et al., 2017; Belila et al., 2018; Zielinski et al., 2018). These works emphasize the representative elementary volume of samples, the pore sizes and pore distribution, as also the relationship with permeability and Global Hydraulic Elements however, few works about the influence of biofabric textures in petrophysics.

The Barremian pre-salt coquinas described in the Santos, Campos and Sergipe-Alagoas Basins presents a wide textural variety according to the energy of depositional environment. These deposits are mainly described as bivalve-rich rudstones, floatstones, grainstones, packstones and mudstones, with a great biofabric variation according to taphonomic patterns in which results in distinct values of porosity and permeability (Carvalho et al., 2000; Tavares et al., 2015; Corbett et al., 2016; Corbett et al., 2017; Belila et al., 2018; Chinelatto et al., 2018b; Muniz and Bosence 2018; Zielinski et al., 2018). The taphonomic signature such as valve orientation, degree of shell preservation, shell packing, type of matrix

and sorting, are related with the depositional and diagenetic processes and results in a diverse biofabric textures.

The aim of this work is to correlate the Barremian-Aptian coquinas samples of the Morro do Chaves Formation (Sergipe-Alagoas Basin) and the Itapema Formation (Santos Basin) with the porosity and permeability according to biofabric characteristics, using nondestructive techniques such as High Resolution Computed Tomography (H-CT) and porosity and permeability measurements by gas injection. With the obtained results it will be possible to discuss the occurrence of primary and secondary porosity and their relationship with biofabric preservation or modification during the diagenetic process as compaction and dissolution which modify the pore system and consequently the permeability.

#### **4.2. COQUINAS SAMPLES**

The coquinas samples used in this work belong to the Morro do Chaves Formation from the Sergipe-Alagoas Basin and the Itapema Formation from the Santos Basin, both located at eastern margin of the Brazilian coast (Fig. 1A). These two basins were developed during the rupture of the supercontinent Gondwana (Cainelli and Mohriak, 1999) throughout the Late Jurassic/Early Cretaceous, event that culminated in the separation of the South American and African continents. In general, the structural and stratigraphic evolution in both basins are very similar being subdivided into megasequences as pre-rift, rift, sag/transitional and open marine. All megasequences are well developed in the Sergipe-Alagoas Basin whereas in the Santos Basin the pre-rift is absent and characterized by the intense basalt floods (Chang et al., 1992; Cainelli and Mohriak, 1999). The coquinas of Morro do Chaves and Itapema Formations where deposited during the rift stage in the Barremian and Aptian age (Chang et al., 1992; Feijó 1994; Campos Neto et al., 2007; Moreira et al., 2007) (Fig. 2). During this period, the extensional tectonic regime develops a system of synthetic and antithetic normal faults that are responsible to generate the half-grabens and grabens structures (Chang et al., 1992; Cainelli and Mohriak, 1999; Mohriak et al., 2008) which resulted in the formation of extensive lakes where coquinas were deposited.

The samples of Morro do Chaves Formation were collected in the São Miguel dos Campos city, Alagoas state (Fig. 1B), in an outcrop at Cimpor quarry. The samples of Itapema Formation were collected in a vertical well core of 12 m from the pre-salt polygon in the Santos Basin (Fig. 1C).

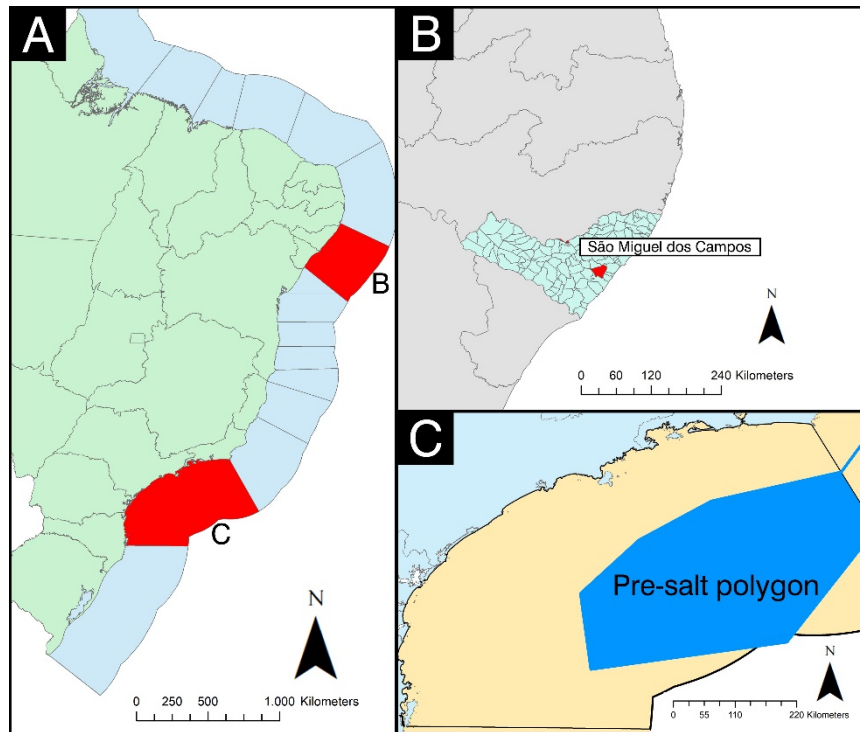


Figure 1: A) Map of the sedimentary basins in the Brazilian east coast margin, in red the Sergipe-Alagoas Basin (B) and Santos Basin (C). B) Zoom of the Sergipe-Alagoas Basin, in red the São Miguel do Campos city where is located the outcrop of Morro do Chaves Formation. C) Zoom of the Santos Basin (C), the blue area is the pre-salt polygon where the samples of Itapema Formation were collected.

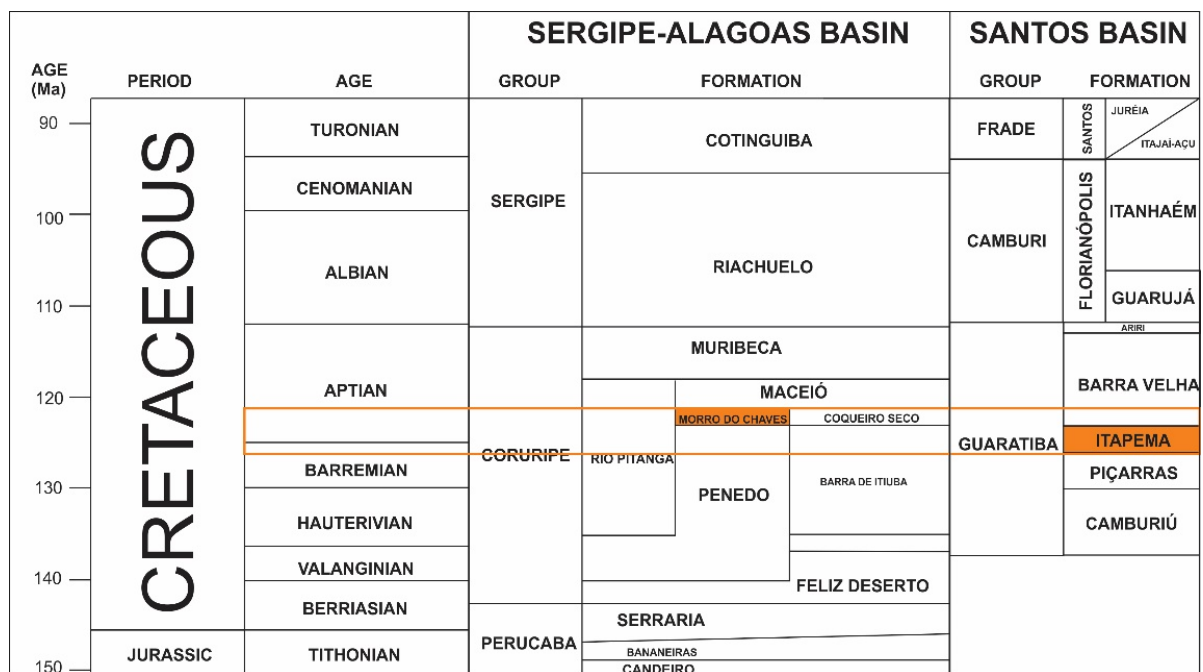


Figure 2: Stratigraphic chart of Sergipe-Alagoas and Santos Basin. In orange the Morro do Chaves and Itapema Formation, deposited between Barremian and Aptian ages.

The coquina deposits from Morro do Chaves were described in many works (Figueiredo, 1981; Kinoshita, 2010; Thompsom, 2013; Tavares et al., 2015; Chinelatto et al., 2018a, Garcia et al., 2018) and interpreted as a shallow lacustrine deposit due to the lack of marine fossils. However, recent researches suggest some marine influence due to the discovery of marine fossils (Gallo et al., 2010, Thompsom, 2013, Garcia et al., 2018) and conclude a marine-to-brackish environment with occurrence of non-marine ostracodes. The main described fauna (see Thompsom, 2013) are nonmarine ostracodes (e.g. Cypridea tchibodaensis), gastropods (e.g. Zygopleuridae genus et sp. indet.) and bivalves (e.g. Nicaniella sp.). The carbonate rocks are mainly described as rudstones, grainstones and packstones interbedded with shales and sandstones.

A few works are available describing the coquina deposits of Itapema Formation (Tedeschi et al., 2017; Pietzsch et al., 2018; Chinelatto et al., 2019) and documentation about the fauna are absent, however, as the Morro do Chaves Formation they are interpreted as shallow lacustrine deposits, described as bivalve rudstones and grainstones interbedded with sandstones and fine-grained laminated mudrocks (Moreira et al., 2007).

### **4.3. METHODS**

#### **4.3.1. Laboratorial analysis and H-CT acquisition**

A total of 24 plug samples of coquinas were analyzed, 15 samples from the Morro do Chaves Formation (Sergipe-Alagoas Basin) and 9 samples from the Itapema Formation (Santos Basin). The samples correspond to horizontal plugs that were sent to laboratorial analysis for permeability and porosity by gas injection, and high resolution tomography images for interpretation of pore distribution. The measure of porosity was performed by UltraPoreTM 300 Helium Pycnometer System. The pore volume is measured by the expansion of a known gas under a pre-defined pressure using the Boyle law. The permeability was calculated by UltraPermTM 500. The technique is based in the theory of Henri Darcy. The equipment uses a nitrogen flux with a variable pressure (0-50psi) to obtain the permeability of samples.

The data of High-resolution CT data (H-CT) were obtained by Versa XRM-500 equipment operating with potential of 10W at energy of 150kV. The pixel resolution reach values between 30-50 micrometers and image size with approximately 1024x1024 pixels.

#### **4.3.2. Biofabric and porosity description**

The biofabric description follows Kidwell et al., (1986), Kidwell (1991) and Kidwell and Holland (1991) in which patterns as (i) orientation of valves, (ii) packing, (iii) sorting, (iv) degree of fragmentation and abrasion were used to characterize the coquinas samples. After that, the samples are grouped between (i) preserved biofabric, with low diagenetic alteration of shells and matrix and (ii) altered biofabric that exhibit a significant modification as dissolution and cementation processes.

The porosity was classified according to Choquette and Pray (1970) and Ahr (2008), summarizing the porosity control in each sample. To evaluate the correlation between porosity and permeability, a crossplots were built in attempt to find a coefficients of determination ( $R^2$ ). The analysis was performed through the use of thin sections and H-CT images to porosity classification and the measurements by gas of porosity and permeability to predict the  $R^2$ .

#### **4.3.3. Fluid flow properties**

After all laboratorial analysis and biofabric interpretation, the segmentation of pore system using the H-CT data was performed through software Pergeos, then a Pore Network Modeling (PNM) was performed. This analysis aid in the understanding how the pores, pore throat and coordination number (number of pore throat that connect a pore) in coquinas vary for different biofabric types. The Global Hydraulic Elements (GHE) was plotted from laboratorial results of permeability and porosity as an approach to reservoir characterization (Corbett et al., 2003; Corbett and Potter, 2004). The GHE provides a template that represent a relationship between porosity and permeability and that is not need to separately into hydraulic flow units (Corbett and Potter, 2004).

### **4.4. RESULTS**

#### **4.4.1. Biofabric characterization**

Although the samples of Morro do Chaves and Itapema Formations are from two different areas, they exhibit similar features related with the depositional process as also similar biofabric characteristics. All analyzed samples were classified as bivalve-rich

rudstones, grainstones, with disarticulated, fragmented, and braded valves with occurrence of coquina intraclasts. Through the analysis of the thin section and H-CT images, four main biofabric textures were determined (Fig. 3 and 4) according to the shell preservation, grain composition and type of matrix/sorting that are: (i) well-sorted and preserved biofabric, (ii) unsorted and preserved biofabric, (iii) well-sorted and altered biofabric, and (iv) unsorted and altered biofabric.

The well-sorted and preserved biofabric group (WSPB) is classified as rudstones and grainstones with densely packed oriented or chaotic arranged shells. The size of preserved valves varies from 1 to 10mm; the samples are composed mainly by shells and their fragments, and can display rare fine quartz grains (Fig. 3A and B). The dissolution of valves in this group is incipient where a few moldic or vug pores occurs contributing to the enhance of total porosity. The replacement of aragonite by calcite occur in all samples, and varies from total replacement and shells with preserved aragonite lines. This diagenetic process does not contribute significantly with the change of total porosity. The cementation and compaction can reduce the pore system in some samples. In general, the calcite cements occur as calcite rims around bioclasts and shell fragments occluding partially the interparticle pores and the compaction increases the contact of shells reducing the volume of pores (Fig. 3C and D). The porosity in this group are mainly primary pores (interparticle) with a few contributions of secondary pores such as intraparticle, moldic and vugs. According to the classification of porosity control proposed by Ahr (2008), the porosity in this group varies from depositional to hybrid.

The sorted and altered biofabric group (WSAB) exhibit similar taphonomic features as WSPB group, the samples are classified as rudstones and grainstones, exhibit a densely packed with oriented or chaotic arranged shells and the matrix is composed mainly by shells and their fragments. Differently from the sorted and preserved shell group, the biofabric exhibit a great evidence of alteration related with diagenetic modification. The diagenetic process observed are dissolution of carbonate cements and shells, micritization, neomorphism, cementation and fractures by compaction (Fig. 3E-H). In general, all samples of WSAB exhibit some degree of these diagenetic processes varying their intensity, resulting in moldic, vug, intracrystalline, and intercrystalline porosity. According to the classification of porosity control proposed by Ahr (2008), the control of porosity in this group ranges from hybrid to diagenetic.

The unsorted and preserved biofabric group (UPB) are classified as rudstones and packstones with densely packed oriented or chaotic arranged shells, composed by shells and

their fragments with occurrences of carbonate and/or siliciclastic grains, and coquina intraclasts. The matrix in this group is composed by shell fragments and may exhibit peloids, fine quartz grains and rare occurrence of micrite (Fig. 4A and B). The size of preserved valves varies from 1 to 7mm and have a unimodal to bimodal distribution. The dissolution of valves in this group contribute to the enhance of total porosity, generating moldic and vugs pores. The cementation reduces the pore system, in general the calcite cements occur as calcite rims around bioclasts and their fragments or as drusy cements occluding all interparticle porosity and the compaction reduces the volume of pores. The porosity in this group is mainly secondary pores (moldic and vugs) and the porosity control ranges from depositional to diagenetic.

The last group is the unsorted and altered biofabric (UAB) and exhibit taphonomic characteristics similar to the UPB group. The samples are mainly classified as rudstones and grainstones where the matrix is composed by shell fragments, and may exhibit fine quartz grains, peloids and rare occurrence of micrite. The diagenesis is very similar with WSAB group where dissolution is responsible to create vug and moldic pores, and calcite cementation obstruct partially or totally the interparticle porosity (Fig. 4A-F). The control of porosity in this group ranges from hybrid to diagenetic.

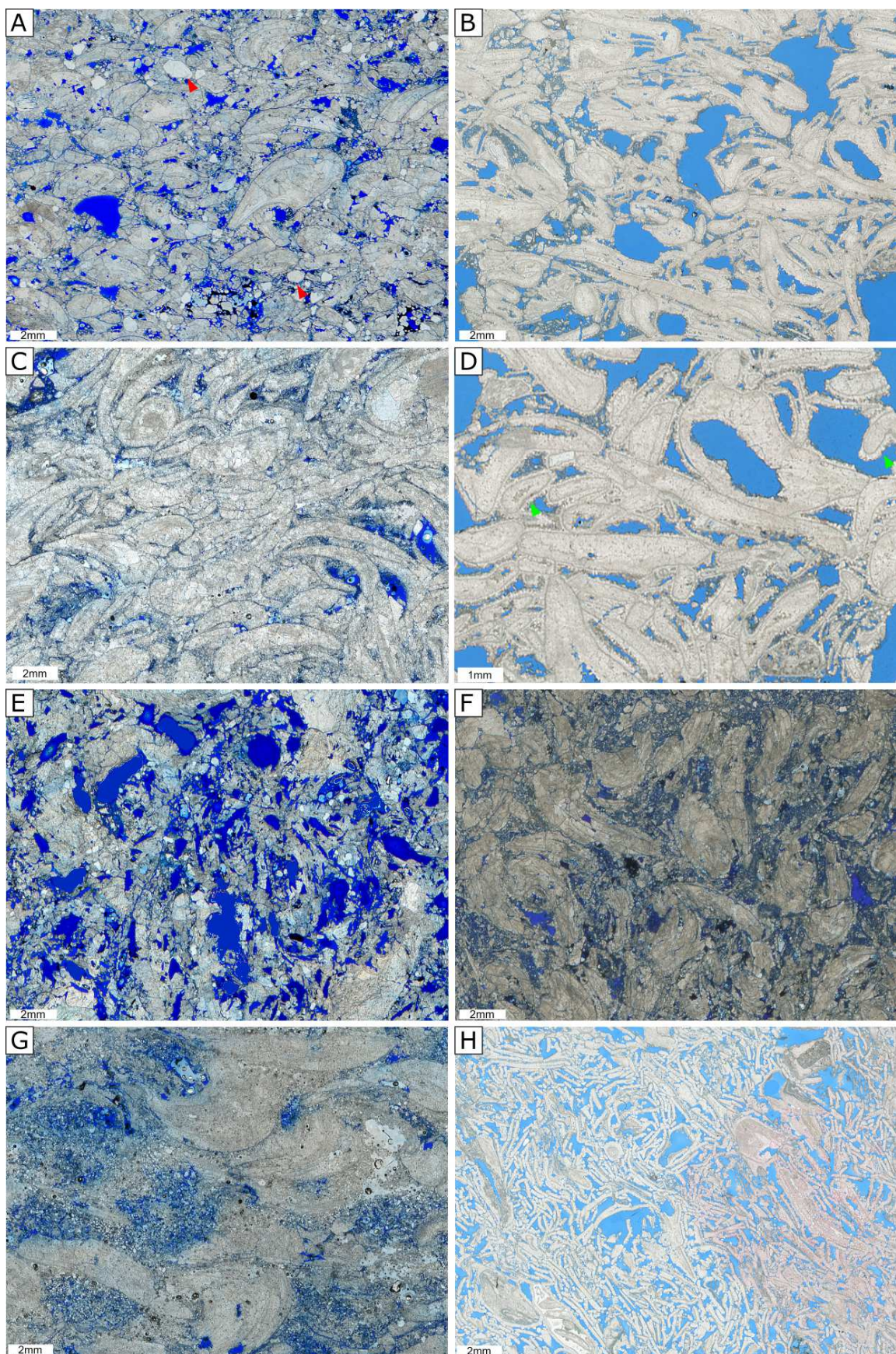


Figure 3: Examples of Sorted preserved and sorted altered biofabric textures of coquinas samples. Figures A-D) corresponds to the well-sorted preserved biofabric (WSPB), samples Dep-2 (A), Dep-5(B and D), and Dep-1(C). Figures E-H) Sorted altered biofabric (WSAB), samples Dia-3 (E), Hyb-6 (F), Hyb-4(G), and Dia-9 (H).

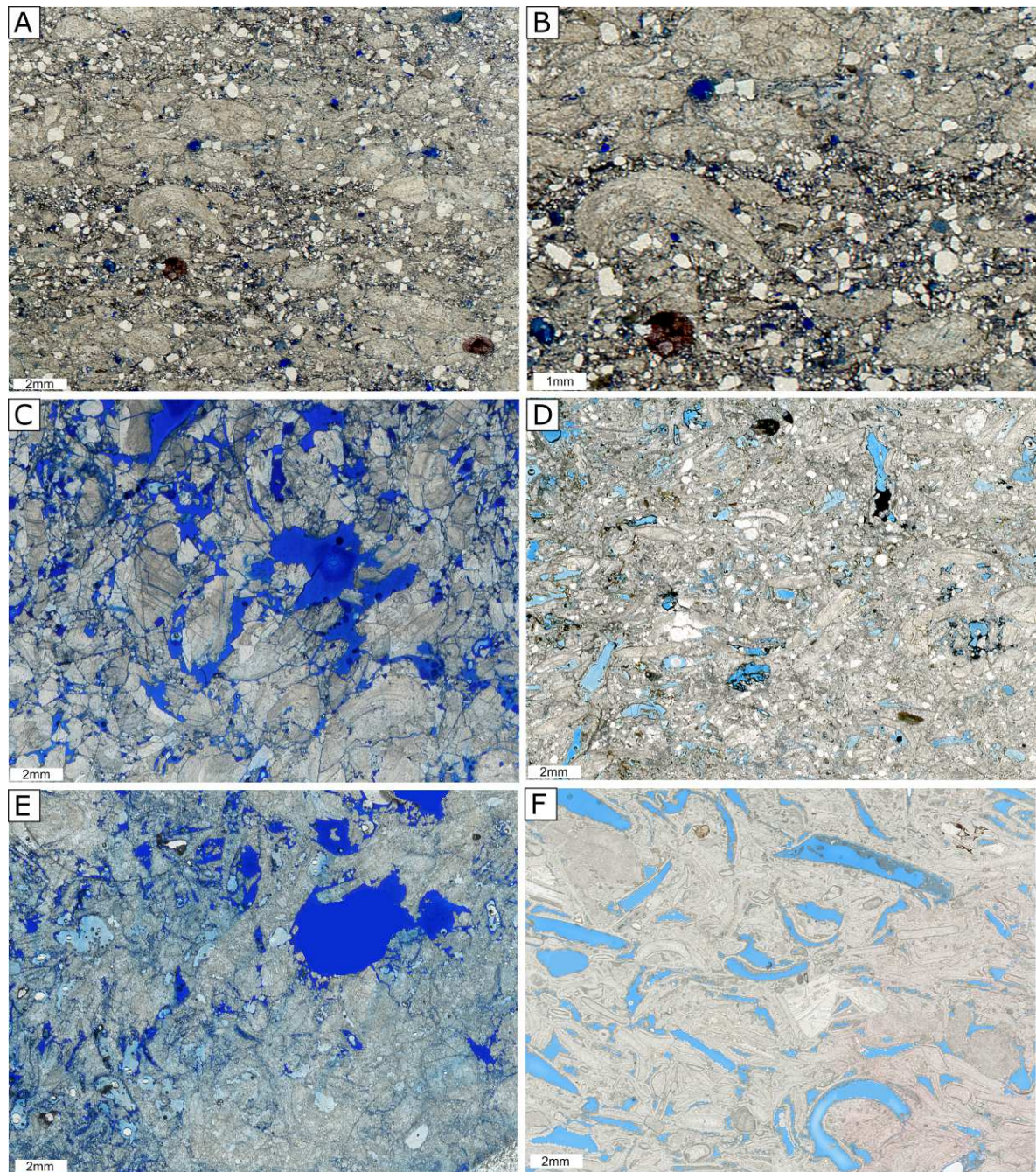


Figure 4: Examples of unsorted preserved and unsorted altered biofabric textures of coquinas samples. Figure A-B) Unsorted preserved biofabric (UPB), sample Dep-5(A-B). Figures C-F) Unsorted altered biofabric (UAB), Hyb-8(C), Dia-6(D), Dia-1(E) and Dia-4(F).

#### 4.4.2. Porosity and permeability relationship

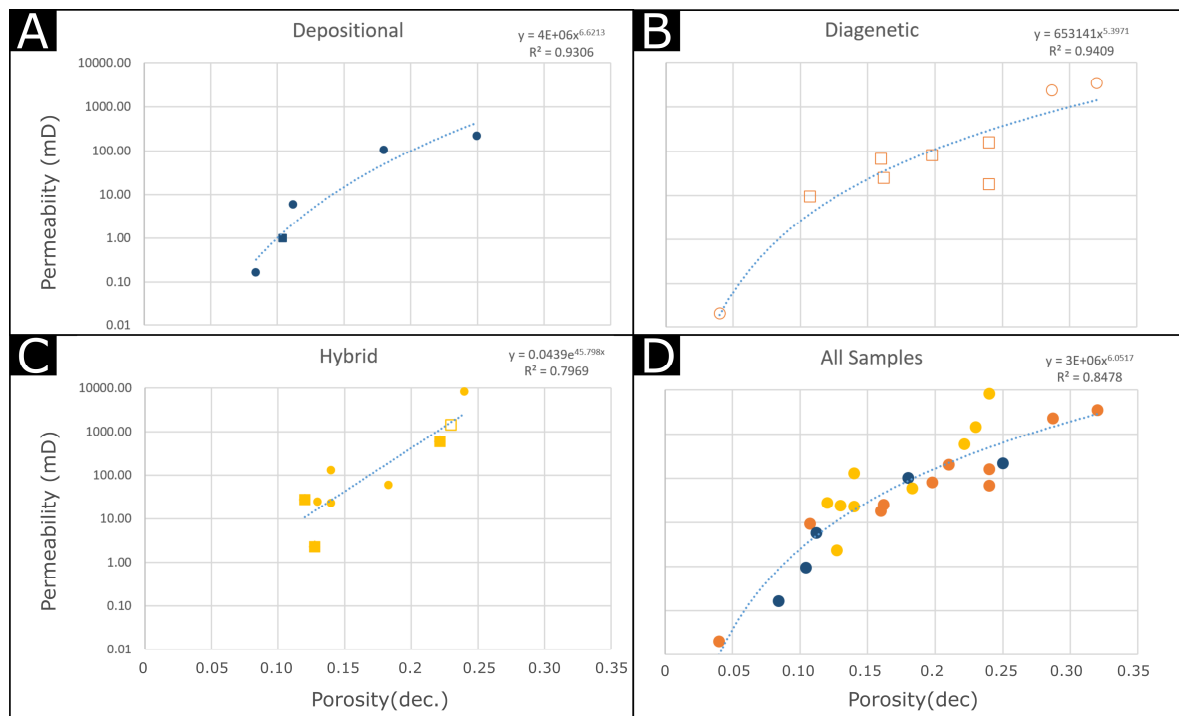
The results of porosity and permeability by laboratorial analysis are exhibit in table 1. The porosity controlled by depositional processes reflects the mechanical sedimentation where sorting contributes to increase or decrease the primary porosity. The samples belonging to depositional domain have interparticle porosity as main pore type, and intraparticle, moldic and vugs in lesser amount. A total of 5 samples are fit in this depositional domain in which samples of WSPB and UPB occur. The low values of porosity are associated with biofabrics that have small grains as matrix (Fig. 4A) as also the occurrence of diagenetic process as high degree of cementation and compaction that reduces the pore volume and connectivity (Fig. 3A). The relationship between porosity and permeability in depositional control is represented in figure 5A and exhibit a R<sup>2</sup> of 0.93.

The hybrid domain is located between depositional to diagenetic process that create or reduce the porosity. In this group the amount between primary and secondary porosity are similar. The pore types observed in the analyzed samples are interparticle, moldics, intraparticle and vugs, in some cases the micritization and recrystallization process contributes to generate some intercrystalline pores. Some samples exhibit fractures by compaction that contribute with the pore connectivity and may enhance the values of permeability. The hybrid domain has a total of 9 samples represented by WSAB, UPB and UAB biofabrics. The relationship between porosity and permeability is in figure 5B with a R<sup>2</sup> of 0.79.

The diagenetic domain is related with the enhanced or reduction of pores by the diagenesis. The original porosity is altered by dissolution, cementation, and compaction, and may create new pore types related or not with depositional texture. The samples belonging to diagenetic domain have moldic, vug and intraparticle pores as main pore types. In some samples the drusy calcite cements reduces the primary pores to values close to zero however, the dissolution of valves and cements creates the secondary porosity (Fig. 4F). A total of 10 samples is inserted into diagenetic domain and is represented by WSAB and UAB groups. The relationship between porosity and permeability is in figure 5C with a R<sup>2</sup> of 0.94. A crossplot with all samples is shown in figure 5D with a R<sup>2</sup> of 0.84.

Table 1: Biofabric, porosity classification, total porosity, and permeability from all analyzed samples.

Sample-ID	Source	Biofabric	Porosity by Ahr (2008)	Total Porosity (%)	Permeability (mD)	PNM
Dep-1	MCF*	SPB	Depositional	10.44	0.96	x
Dep-2	MCF	SPB	Depositional	18.00	102.57	x
Dep-3	MCF	SPB	Depositional	11.20	5.77	----
Dep-4	IPF*	SPB	Depositional	25.00	216.03	x
Dep-5	MCF	UPB	Depositional	8.40	0.16	----
Hyb-1	MCF	USB	Hybrid 1	12.74	2.31	x
Hyb-2	IPF	SAB	Hybrid 1	14.00	128.00	x
Hyb-3	IPF	SAB	Hybrid 1	24.00	8180.00	x
Hyb-4	MCF	SAB	Hybrid 1	18.31	58.10	x
Hyb-5	MCF	SAB	Hybrid 1	13.00	23.95	x
Hyb-6	MCF	SAB	Hybrid 1	14.00	22.48	x
Hyb-7	MCF	UAB	Hybrid 1	22.15	592.00	x
Hyb-8	MCF	UAB	Hybrid 1	12.00	27.72	x
Hyb-9	IPF	UPB	Hybrid 1	23.00	1440.00	x
Dia-1	MCF	UAB	Diagenetic	16.20	25.10	x
Dia-2	MCF	UAB	Diagenetic	10.73	9.27	x
Dia-3	MCF	SAB	Diagenetic	28.70	2300.00	----
Dia-4	IPF	UAB	Diagenetic	16.00	18.12	x
Dia-5	IPF	UAB	Diagenetic	24.00	67.60	x
Dia-6	MCF	UAB	Diagenetic	19.78	80.36	x
Dia-7	MCF	SAB	Diagenetic	4.00	0.02	x
Dia-8	IPF	UAB	Diagenetic	24.00	159.31	x
Dia-9	IPF	UPB	Diagenetic	21.00	202.00	x
Dia-10	IPF	SAB	Diagenetic	32.00	3455.29	x

Figure 5: Crossplot Porosity x Permeability for coquinas samples following the classification of porosity control of Ahr (2008). A) Samples with depositional porosity control exhibiting a R<sup>2</sup>=0.93. B) Hybrid control of porosity with R<sup>2</sup>=0.79. C) Diagenetic control with R<sup>2</sup>=0.94. D) all analyzed samples with R<sup>2</sup>=0.84.

#### 4.4.3. Pore Network Modeling and Global Hydraulic Elements

By the Pore Network Modeling (PNM) it was possible obtain the statistics of Pore Radius (Fig. 6), Pore Throats Radius (Fig. 7), and the Pore Connectivity (Coordination Number-CN) (Fig. 8) of the analyzed samples. In this process the software *Pergeos* interpret the pores in 3D volume of segmented H-CT images, individualizing them and computing the pore network statistics. In general, the pore radius has a bimodal distribution with peaks close to 0.2mm and 0.3mm (Fig. 6D). This behavior is related with distinct biofabric textures, associated with sorting and diagenetic modifications, that influence the pore size distribution. In general, the samples that exhibit the largest values of pore radius size are related with biofabrics that are modified by the diagenesis, the dissolution enlarge the interparticle pores and generate moldic and vug pores.

The pore throat distribution has a similar curve pattern, all samples the main pore throat radius peak is located close to 0.1mm however, they exhibit distinct radius frequency. The samples with high frequency of throat radius close to 0.1mm or bellow, are associated with the samples that exhibit the lowest values of permeability.

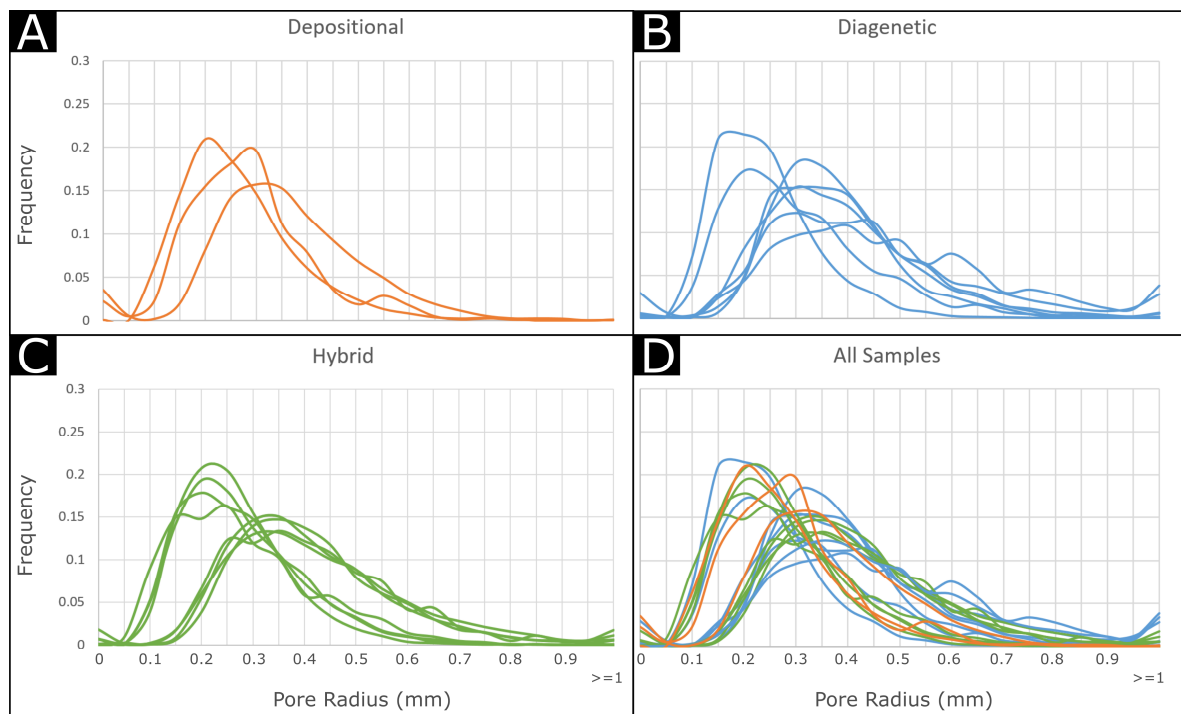


Figure 6: Results of Pore Radius (mm) and their frequency obtained from PNM analysis. A) Depositional group. B) Diagenetic Group. C) Hybrid Group. D) All groups in the same chart.

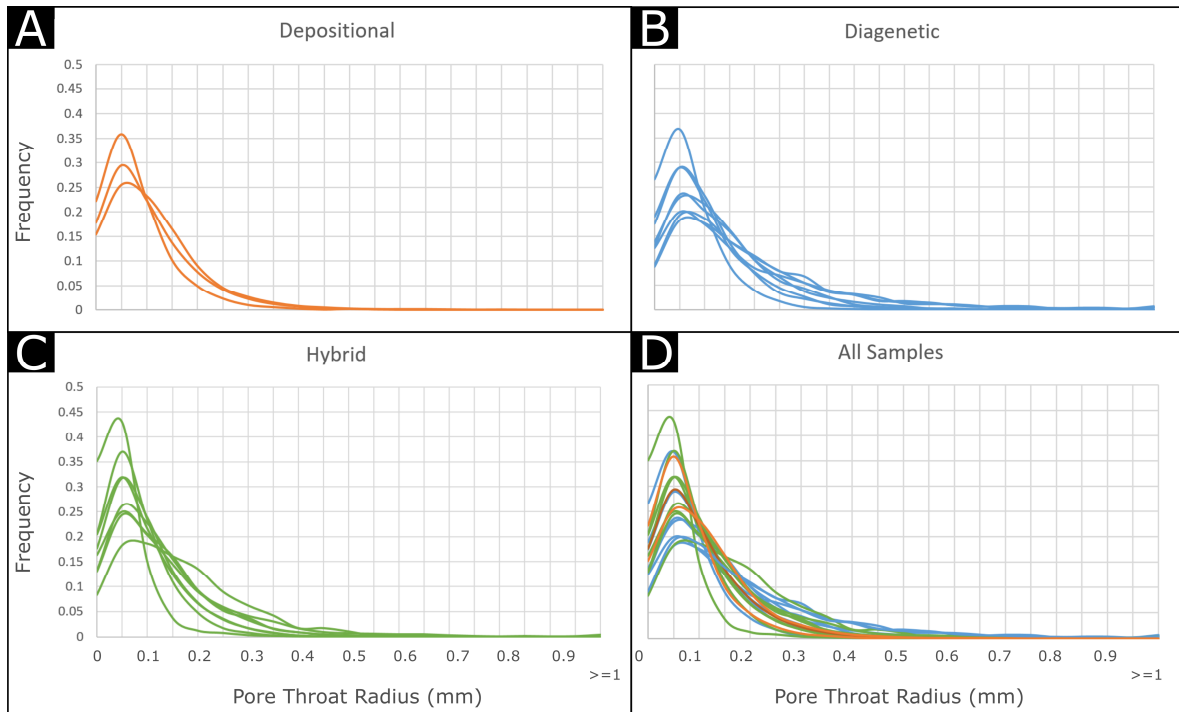


Figure 7: Results of Pore Throat Radius (mm) and their frequency obtained from PNM analysis. A) Depositional group. B) Diagenetic Group. C) Hybrid Group. D) All groups in the same chart.

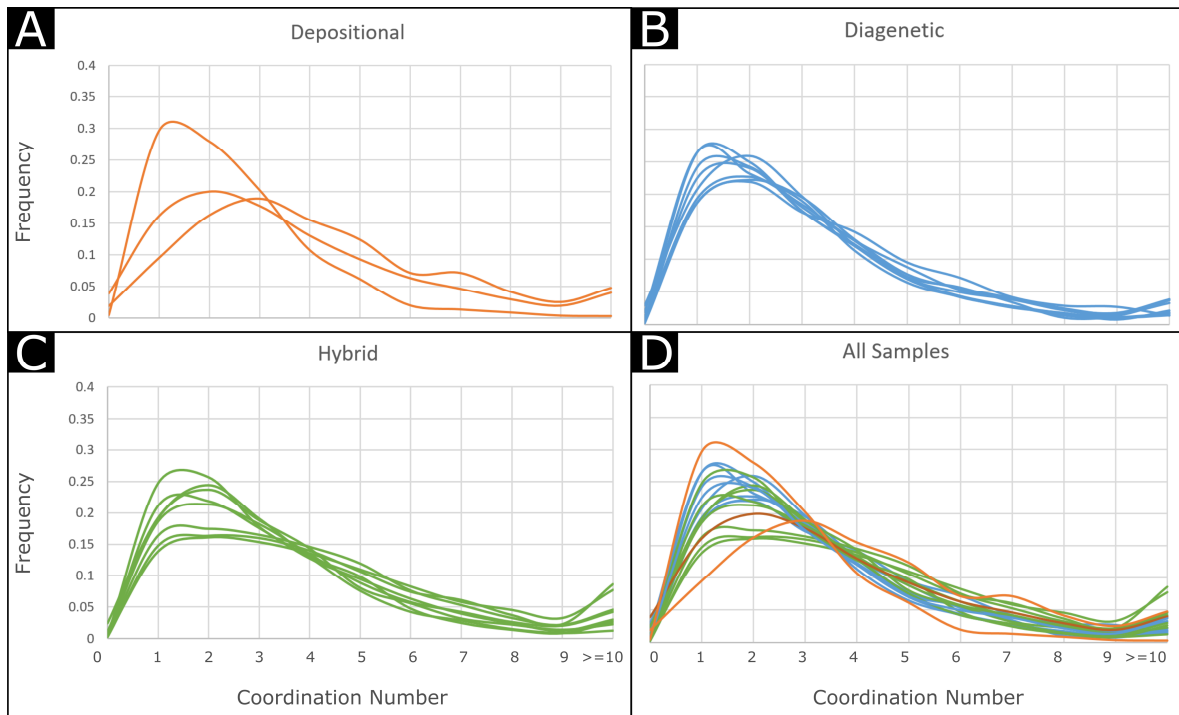


Figure 8: Results of Coordination Number (CN) and their frequency obtained from PNM analysis. A) Depositional group. B) Diagenetic Group. C) Hybrid Group. D) All groups in the same chart.

The Global Hydraulic Elements are also plotted (Fig. 9). All plots were classified according to the porosity control of Ahr (2008) as depositional, hybrid and diagenetic. In this plot it is possible observe that coquinas cover a broader space, varying from GHE-3 to GHE-8 and indicate that many pore types exist. The groups that falls in GHE 3 and 4 are associated with samples that have small pores and a tight pore throat whereas the GHE 7 and 8 have the largest pore space and larger pore throat radius as also a good pore connectivity.

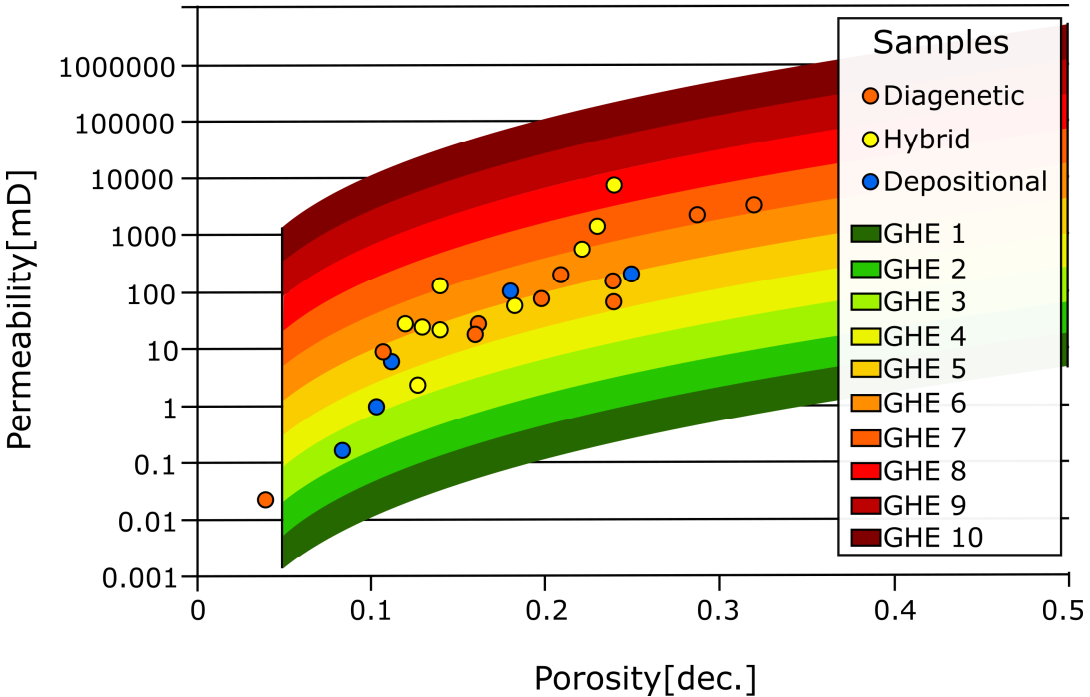


Figure 9: Porosity and permeability data from the all analyzed samples according to the porosity control (depositional, hybrid and diagenetic) using the chart of Global Hydraulic Element (GHE). The GHE varies from GHE-3 to GHE-8.

## 4.5. DISCUSSION

### 4.5.1. Biofabric texture and porosity

The well-sorted preserved and well-sorted altered biofabric (WSPB and WSAB) exhibit taphonomic features that lead to interpretation of high energy deposits. In general, the samples exhibit an oriented or chaotic arranged shells and matrix composed only by shells fragments, features generally associated with shell deposits influenced by waves and currents in shallow waters during fair weather and storm conditions (Salazar-Jimenez et al., 1982; Fürsich and Pandey, 1999). The absence of abundant fine grains as fine quartz, peloids or very small shell fragments of sizes bellow of 0.1mm contributes to the idea in which high

energy environment plays a key role on sorting in this group of samples. Many grainstones and rudstones with the same biofabric textures and taphonomic features as WSPB and WSAB were described in Santos, Campos and Sergipe-Alagoas Basins (Abrahão, 1987; Carvalho et al., 2000; Muniz, 2013; Thompson et al., 2015; Tavares et al., 2015; Chinelatto et al., 2018a; Muniz and Bosence 2018; Mizuno et al., 2018; Oliveira et al., 2019) and interpreted as shallow lacustrine deposits in a high energy environment dominated by waves and currents between fair-weather and storm weather wave bases. These deposits are described as foreshore, berms, and shoreface facies and, in some cases, storm deposits with winnowed fine grains due to the action of storm currents (Tavares et al., 2015; Chinelatto et al., 2018a; Muniz and Bosence 2018; Olivito and Souza, 2020). In general, these deposits exhibit good values of porosity due to the porosity preservation (Tavares et al., 2015; Belila et al., 2018; Zielinski et al 2018) where the porosity and permeability can be enhanced by the dissolution of shells and cements.

The unsorted preserved and unsorted altered biofabric (UPB and UAB) exhibit taphonomic features of low energy deposits when compared to the WSPB and WSAB due to the degree of sorting of grains and degree of shell preservation. The presence of fine grains as small bioclastic fragments, fine grained quartz, peloids and micrite as also the presence of preserved bioclasts with low signs of abrasion and fragmentation reinforces this idea (Fürsich and Oschmann, 1993). In the Campos Basin rocks with the same biofabric characteristics are described as hybrid arenite and interpreted as a hybrid deep lake fans (Oliveira et al., 2019) and as bioclastic calcarenite beaches (Carvalho et al., 2000). In Sergipe-Alagoas Basin shell beds with this characteristic are interpreted as deep deposits located below to the fair-weather wave base (Tavares et al., 2015; Chinelatto et al., 2018). Coquinas that exhibit a high content of peloids and ostracods and absence of fine or very fine quartz grains can be interpreted as paraautoctone bars and distal tempestites in offshore transition area or as backshore deposits in protected areas of the lake as described by the Olivito et al. (2020).

In the WSPB group the porosity control is depositional and the value of porosity varies between 10-25% and the permeability between 2-200mD (Table 1). In this group only a few shells are altered by the diagenetic processes as dissolution and compaction. The WSPB have as main pore type the interparticle pores that are preserved due to the removal of thinner grains, generally related with the paleoenvironmental conditions of high energy where the action of waves and currents promotes removal of thinner grains. Another factor that contributes to the preservation of primary porosity is the early calcite cementation (Fig. 3D – green arrow). The calcite cements occur as small calcite rims around bioclasts and preserves

the primary porosity from compaction during the mesodiagenesis. The porosity can be increased due the incipient diagenetic processes as dissolution of shells and cements where a few intercrystalline, intraparticle, moldic and vug pores are generated as observed in figure 3A-D. In some samples the reduction of porosity occurs due to the compaction process (Fig. 3C).

The WSAB group present a porosity control that varies from hybrid to diagenetic and values of porosity between 4-32% (Table 1). The diagenetic process in this group is different compared to the WSPB, here the dissolution of shells and cementation produce a wide range of pore types and pore sizes (Fig. 3E-H). This features directly influences the permeability and a wide range of values are observed (22mD-8D). The samples with the best values of porosity and permeability are associated with the diagenetic control of porosity where the dissolution enhance the pore space and promotes the better communication between the pores. In this samples most of the shells are dissolved; calcite rim cements and silicified intraclasts are preserved and the compaction improve the pore communication due to the presence of fractures and microfractures (Fig. 3H).

The control of porosity in UPB varies from depositional to diagenetic and the values of porosity between 8-23% (Table 1). One sample are fit in the depositional control and have interparticle space preserved due to the removal of thinner grains (Fig. 4A-B), the interparticle pores are generally very small. In the hybrid domain the pore space is connected and exhibit good value of porosity and permeability, small interparticle pores are preserved and the dissolution of carbonate grains and calcite cements promotes the enhance of pore communication as also channels and vugs. In the diagenetic domain the pore space is mainly moldic and vugs however, the cementation is high and promotes a drastic reduction of primary pore space.

The UAB group have a porosity control that ranges between hybrid to diagenetic, the porosity varies from 10-24% and exhibit a high range of permeability (2-600mD). The UAB exhibit similar features of UPB (hybrid and diagenetic domain).

#### **4.5.2. Porosity control, PNM and GHU**

As seen previously, the porosity control in all biofabric groups is heterogeneous and varies from depositional to diagenetic, only the WSPB group is restricted in the depositional control. In this way, the following discussion will address the porosity control due to the good

relationship between porosity and permeability in each group (Fig. 5) and their relationship with the results of Pore Network Modeling (PNM) and Global Hydraulic Elements (GHE).

**Depositional Control:** The group exhibit good values of porosity (10-25%), a wide range of permeability (0.1-200mD) and in Global Hydraulic Elements plot are distributed between GHE-3 to GHE-6. By the PNM analysis, the pore radius distribution curves have 2 main peaks (one in 0.2 and other in 0.3 mm), pore throat in 0.1 mm and a CN between 2-4, features that are associated with distinct biofabric textures.

The sample with the lowest value of porosity and permeability is a Dep-1 (10% and 0.9mD). By the analysis of PNM of connected pore space, the sample exhibit a high frequency of pores radius bellow 0.3mm (Fig. 10A2), a low frequency of larger pores associated with moldic (Fig. 10A1) and a high frequency of low values of pore throat radius (Fig. 10A2). In GHE plot (Fig. 9) the sample is located in the GHE-3, and represents one of the worst in reservoir quality despite having good values of porosity. The permeability in this sample is low and associated with the effect of compaction (Fig. 3C) that reduces the primary pores as also with the high content of micropores. The dark gray color in figure 10A1 represent the microporosity, this pores are responsible to enhance the value of total porosity in this sample however, due to the thigh pore throats and low pore connectivity the permeability values are low.

The sample with the best values of porosity and permeability is the sample Dep-4 (Fig. 10B1-B2) with 25% and 216 mD. By the analysis of pore and pore throat radius, it is possible to see a similar curve distribution such as in the sample Dep-1 (Fig. 10A1) however, the porosity and permeability values are very different. The difference between the samples it is associated with the preservation of the primary pore space as observed in figure 10A2, and also the high frequency of larger pore radius. Dep-4 exhibit much more preserved primary pores and a high frequency of pore radius larger than 0.3mm when compared to Dep-1. Besides that, the communication between pores are higher and contribute to enhance of permeability. In GHE the sample DEP-4 is located in GHE-5 that represents a good reservoir quality.

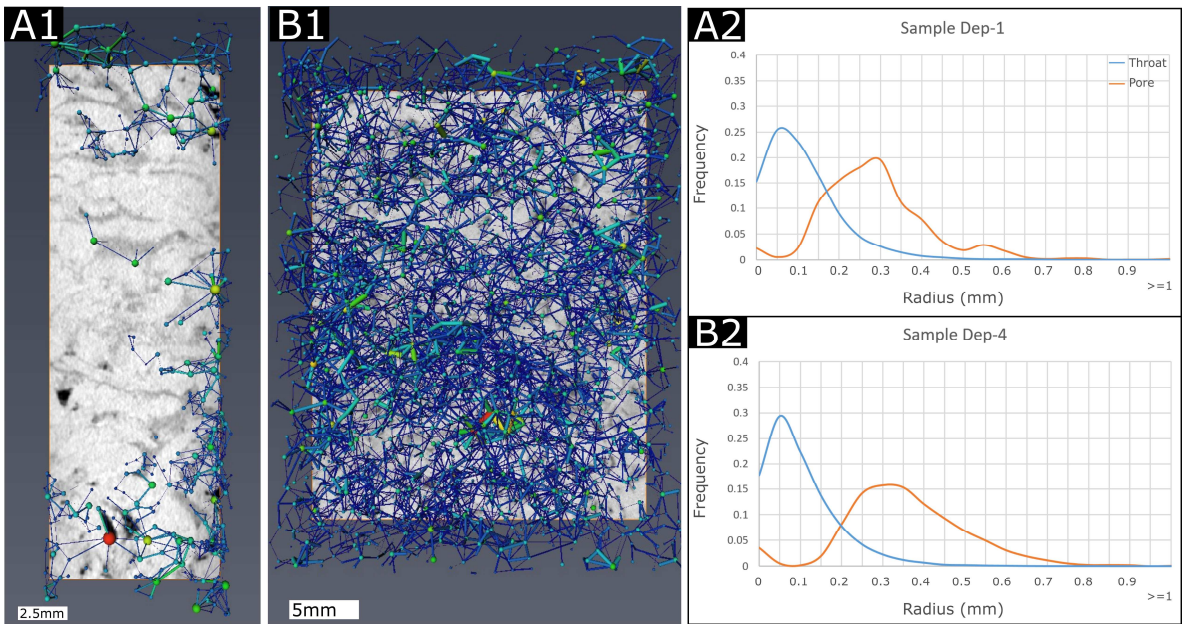


Figure 10: Examples of samples from depositional porosity control. A1) PNM of sample Dep-1, that exhibits the low content of pores and connected porosity. A2) Radius of pores and pore throat of sample Dep-1. B1) PNM of sample Dep-4 with a high pore distribution and connectivity. B2) Radius of pores and pore throat of sample Dep-4.

**Hybrid Control:** The group exhibit values of porosity between 12-24%, permeability between 2mD - 8D, and a GHE between GHE-4 to GHE-8 (Fig. 9). By the analysis of PNM it is possible to observe 2 curve patterns of pore radius distribution, as also a wide range of pore throat and CN frequency (Figs. 6-8). Four samples were selected according to this distribution pattern as also according to the values of porosity and permeability.

The sample with the lowest values of porosity and permeability is the Hyb-1 (13% and 2mD). The results of PNM reveal a high frequency of pore radius and pore throat below to 0.05mm. The main poretype in this sample are interparticle microporous, intraparticle and, moldic (Fig. 11A1) that sometimes are not connected in the biofabric. The pore space exhibits a low pore communication due to the effect of sorting of grains and by the diagenesis; the calcite cements obstructs the primary pore space and the compaction contributes to the reduction of the pore communication and the pore throat radius. In GHE plot this sample is located in GHE-4.

The Sample Hyb-8 exhibit good values of porosity and permeability (14% and 128mD). Differently from the sample Hyb-1, the frequency of pore radius above 0.3mm is high as also the frequency of pore throat above 0.1mm (Fig. 11B2). The primary and secondary pore space are connected despite the calcite cements obstructs some primary pores. In this sample the diagenesis and the sorting contribute in the total porosity. In GHE plot this sample is located in GHE-7 that represent a good reservoir quality.

The samples Hyb-7 and Hyb-3 exhibit excellent values of porosity and permeability (22% - 592mD and 24% -8D). The first sample despite presenting an unsorted biofabric, have a good pore connectivity associated with the connected secondary pores (moldic and vugs) that contributes to the high value of permeability. In this sample, the primary pore space is filled with thin material however, preserves a microporosity and small pores that contribute to the pore connectivity (Fig. 12A1 - dark gray color). In GHE plot this sample is located in GHE-7.

The sample Hyb-3 has a similar pore and pore throat radius frequency that occurs in the Hyb-1 however, the Hyb-3 exhibit a better pore communication associated with the preserved primary pores of sorted biofabric and the enhanced of porosity by the dissolution of shells and cements. The pore radius is enhanced by the dissolution process, where 65% of pores are located between 0.3-0.5mm of radius. This sample is fit in GHE-8.

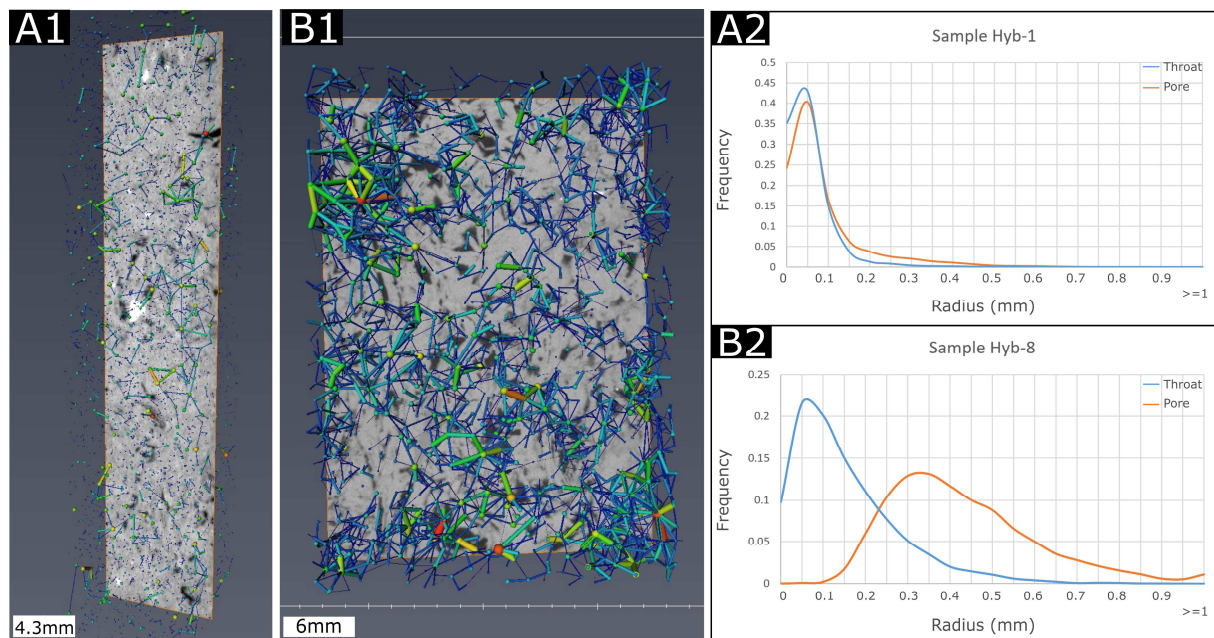


Figure 11: Examples of samples from hybrid porosity control. A1) PNM of sample Hyb-8, that exhibits the low content of pores and connected porosity. A2) Radius of pores and pore throat of sample Hyb-8. B1) PNM of sample Hyb-1 with a high pore distribution and connectivity. B2) Radius of pores and pore throat of sample Hyb-1.

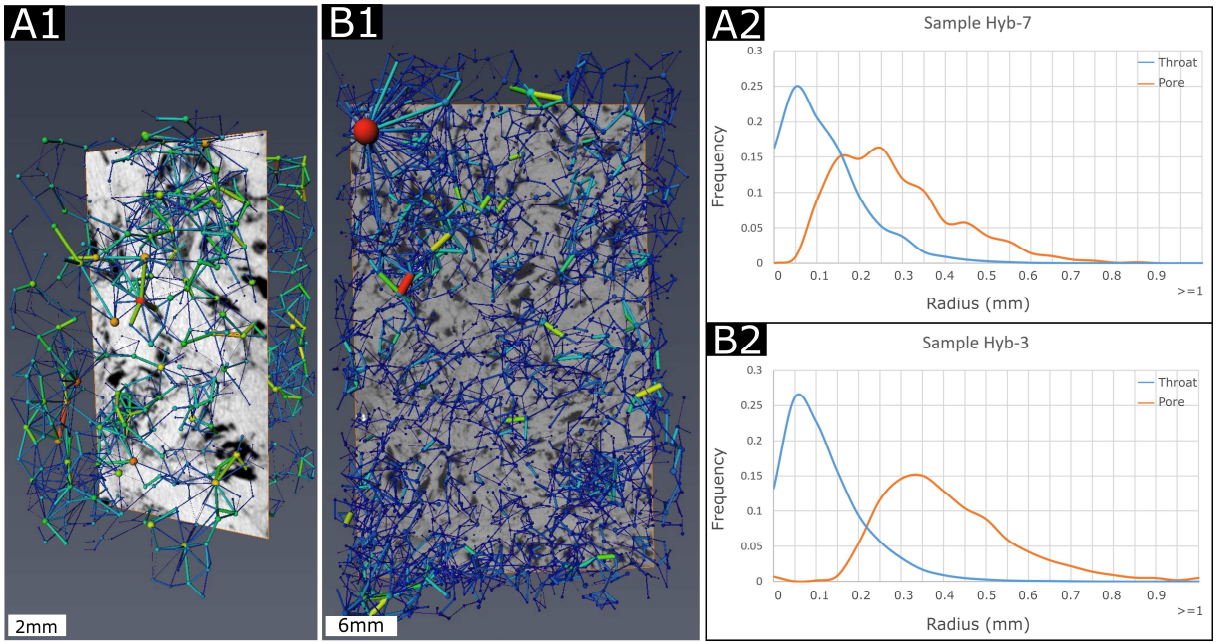


Figure 12: Examples of samples from hybrid porosity control. A1) PNM of sample Hyb-6. A2) Radius of pores and pore throat of sample Hyb-8. B1) PNM of sample Hyb-2 with a high pore distribution and connectivity. B2) Radius of pores and pore throat of sample Hyb-2.

Diagenetic Control: The group exhibit values of porosity between 4-32%, permeability between 2mD – 3.5D, and a GHE between GHE-3 to GHE-7, although the most samples be inserted in GHE-5 (Fig. 9). Such as in the hybrid group, the PNM results exhibit 2 curve patterns of pore radius distribution, as also a wide range of pore throat and CN frequency, generally associated with the diagenetic process (dissolution, cementation and compaction).

The sample with the worst values of porosity and permeability in this group is the Dia-7 (4% and 2mD). Despite being a well-sorted and preserved biofabric, the primary pore space is drastically reduced by the presence of calcite cements. The pores are moldic and intraparticle, generally isolated contributing to the low value of permeability. In GHE plot this sample is located in GHE-3. The sample Dia-2 exhibit similar features that occurs in Dia-7. The primary pore space is reduced by diagenetic cements and rare interparticle pores are preserved. The main poretype in this sample is the moldic and intraparticle pores generally connected by microporous. By the analysis of PNM it is possible observe that only parts of sample exhibit connected pores (Fig. 13A1) that are connected by pore throat with radius bellow 0.5mm (>35%) (Fig. 13 A2). This sample is fit in GHE-5.

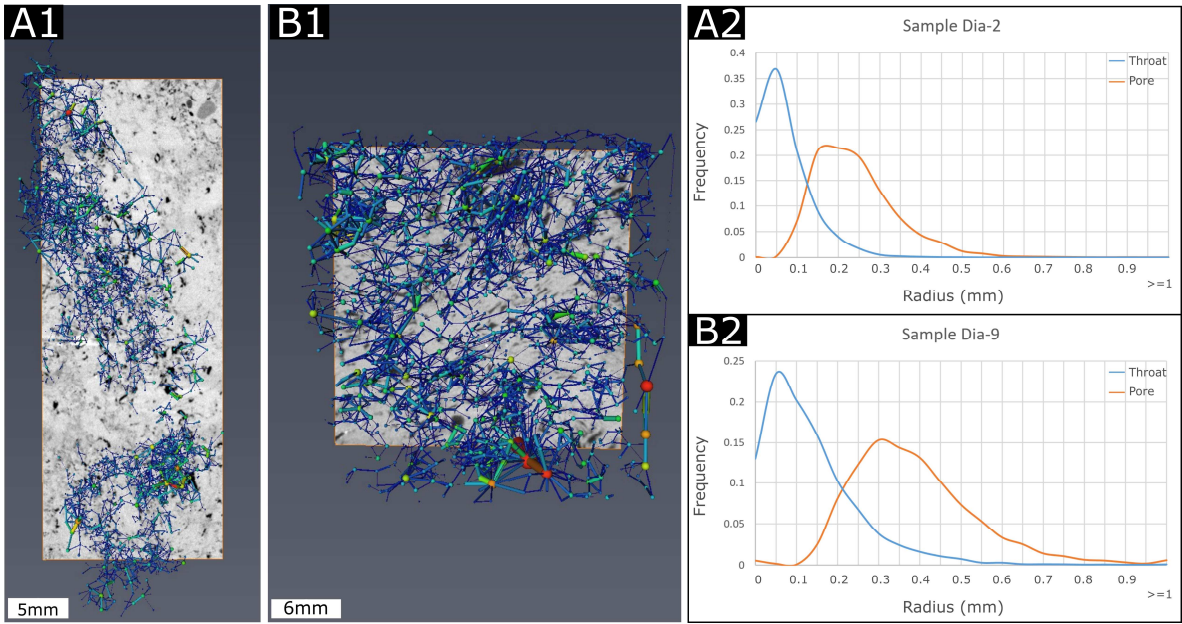


Figure 13: Examples of samples from diagenetic porosity control. A1) PNM of sample Dia-2. A2) Radius of pores and pore throat of sample Dia-2. B1) PNM of sample Dia-9 with a high pore distribution and connectivity. B2) Radius of pores and pore throat of sample Dia-9.

The samples Dia-8 and Dia-9 exhibit good values of porosity and permeability. Both samples exhibit similar pore types; moldics and intraparticles that are connected. The peak of pore radius is located in 0.35mm and exhibit a high frequency of pores above that. The pore throat radius is larger, the frequency of pores approach to values close to 0.6mm. In these samples the sorting and cementation influence in the primary pore whereas the dissolution enhances the total porosity and pore connectivity. Both samples are fit in GHE-7.

The sample with the best value of porosity and permeability in this group is the sample Dia-10 (32% and 3.5D). The primary pore space is preserved due to the sorting and the porosity is enhanced by the dissolution of shells and the low content of cements. The occurrence of primary pores is high compared with the other samples in the diagenetic domain. The calcite cements occur only as small calcite rims around the bioclasts and later, the shells are removed by dissolution process. Compared with the other samples, the low content of pores with radius above 0.5mm is associated with the effect of compaction, reducing the volume of pores. This sample exhibits high content of microfractures that connect the primary and secondary pore space, and consequently increases the permeability. In GHE plot it is located in GHE-7.

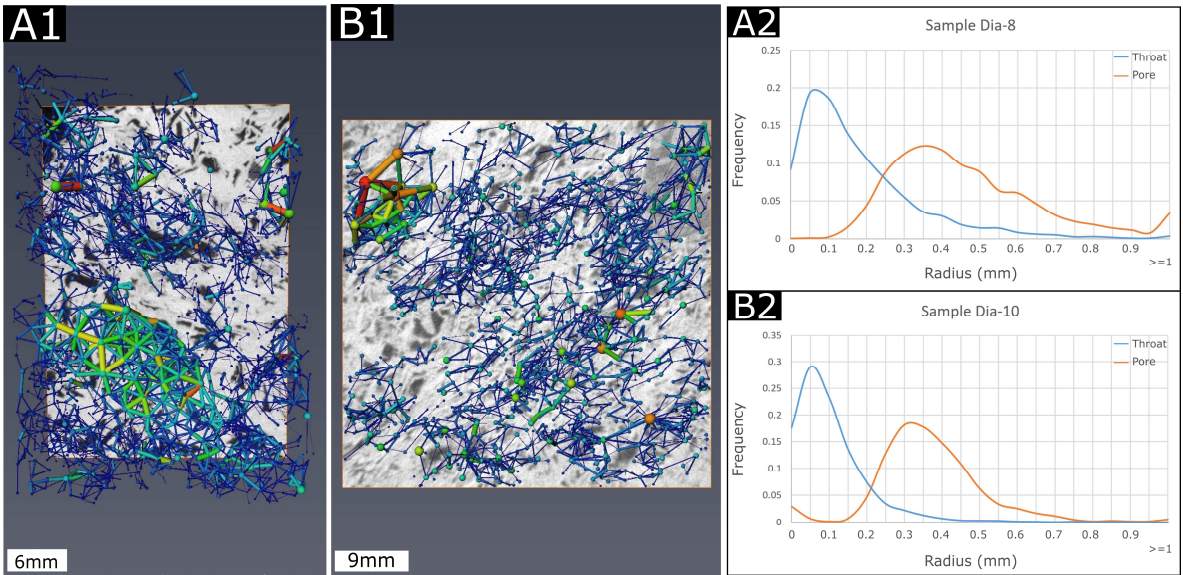


Figure 14: Examples of samples from diagenetic porosity control. A1) PNM of sample Dia-8. A2) Radius of pores and pore throat of sample Dia-8. B1) PNM of sample Dia-10. B2) Radius of pores and pore throat of sample Dia-10.

#### 4.6. CONCLUSION

The analyzed coquinas exhibit a broad range of porosity and permeability associated either by a depositional or diagenetic process. The well-sorted biofabrics have sedimentary process, such as reworking and winnowing that preserves the primary pore space and later, can be enhanced or reduced by the diagenetic process. The unsorted biofabric show a low volume of primary pore space due to the sorting of grains however, the porosity can be enhanced by the dissolution of grains and cements. In this way the coquinas can be grouped between well-sorted and unsorted biofabrics altered or not by the diagenesis.

In the depositional porosity control, the samples have as main poretype the interparticle that are reduced by the diagenetic process as compaction and calcite cementation. This group is represented by samples of well-sorted biofabric and exhibit a good relationship between porosity and permeability. In the hybrid and diagenetic domain, the sorting and diagenesis influences in the porosity and permeability relationship. Well-sorted samples can exhibit low values of porosity due to the calcite cementation and the occurrence of isolated pores whereas unsorted biofabrics can be good reservoirs due to the creation of secondary porosity due to the dissolution of grains and cements. The hybrid domain exhibits the lowest value of R<sup>2</sup> for Porosity vs. Permeability relationship. This is expected due to the great variation of pore types and degree of diagenetic process that modify the pore space. In the Diagenetic domain the pores are mainly moldic and vug, and exhibit a good correlation with porosity and permeability (R<sup>2</sup> 0.94).

By the analysis of PNM, two main peaks are observed for pore radius. The peaks located between 0.2mm are associated with samples that have an unsorted biofabric, where the occurrence of small pores are higher or by samples that were diagenetic modified, where the pore space were reduced by compaction. Samples that shown a peak higher than 0.3mm are associated with the well-sorted biofabrics or coquinas that have the pore space enhanced by the diagenetic process as dissolution of shells and cements that generate moldic and vugs. In general, the pore radius is very similar in all biofabrics, the peaks are located close to the 0.1mm however with great variation in their frequency that will modify the fluid flow patterns (permeability).

The Global Hydraulic Element plot reveals a wide distribution of depositional, hybrid and diagenetic porosity domain. The GHE-3 and GHE-4 have good values of porosity however a low permeability due to the occurrence of microporosity and/or a bad pore connectivity due to the calcite cementation and occurrence of isolated pores. The GHE-5 and GHE-6 exhibit samples from all domains where the permeability can be related with the well-sorted and preserved biofabrics or altered biofabrics. The well-sorted biofabrics exhibit a good pore connectivity associated with the preservation of primary pore space whereas some unsorted biofabrics exhibit a good pore connectivity due to the communication of secondary pores. The GHE-7 and GHE-8 exhibit samples of hybrid and diagenetic domain, and the highest values of porosity and permeability. These values are related with the preserved interparticle pores associated with the well-sorted biofabrics and the enhance of porosity by the diagenetic process.

#### **4.7. ACKNOWLEDGEMENTS**

The authors thank to the financial support provided by Equinor and CAPES, this study was financed in part by the Coordenação de Aperfeiçoamento de Pessoal de Nível Superior - Brasil (CAPES) - Finance Code 001. Thanks to all laboratories researchers from CEPETRO and LMPT and Agencia Nacional do Petróleo (ANP) due to the availability of samples from Itapema formation.

#### 4.8. REFERENCES

- ABRAHÃO, D., 1987, Lacustrine and associated deposits in a rifted continental-margin : the Lagoa Feia formation, Lower Cretaceous, Campos Basin, offshore Brazil [MS Thesis]: Colorado School of Mines, Arthur Lakes Library, 207 p.
- ABRAHÃO, D., AND WARME, J.E., 1990, Lacustrine and associated deposits in a rifted continental margin-Lower Cretaceous Lagoa Feia Formation, Campos Basin, offshore Brazil. in Katz, B.J. (Ed.), Lacustrine Basin Exploration—Case Studies and Modern Analogs: American Association of Petroleum Geologists Memoir, v. 50, p. 287–305.
- AHR, W.M., 2008, Geology of Carbonate Reservoirs: The Identification, Description, and Characterization of Hydrocarbon Reservoirs in Carbonate Rocks: Hoboken, John Wiley & Sons, 296 p.
- BELILA, A.M.P., KURODA, M.C., SOUZA, J.P.P., VIDAL, A.C. AND TREVISAN, O.V., 2018, Petrophysical characterization of coquinas from Morro do Chaves Formation (Sergipe-Alagoas Basin) by X-ray computed tomography: Revista do Instituto de Geociências – USP, v. 18(3), p. 3-13.
- CAINELLI, C., AND MOHRIAK, W.U., 1999, Some remarks on the evolution of sedimentary basins along the Eastern Brazilian continental margin: Episodes, v. 22, p. 206–216.
- CAMPOS NETO, O.P.A.C., LIMA, W.S., CRUZ, F.E.G., 2007. Bacia de Sergipe-Alagoas: Boletim de Geociencias da Petrobras, V. 15, P. 405-415.
- CARVALHO M.D., PRAÇA U.M. AND TELLES A.C.S., 2000, Bioclastic carbonate lacustrine facies molds in the Campos Basin (Lower Cretaceous), Brazil. in Gierlowski-Kordesch E.H., Kelts K.R. (eds) Lake Basins through Space and Time Tulsa: AAPG, AAPG Studies in Geology V. 46, p. 245-256.
- CERALDI, T.S., AND GREEN, D., 2016, Evolution of the South Atlantic lacustrine deposits in response to Early Cretaceous rifting, subsidence and lake hydrology: Petroleum Geoscience of the West Africa Margin, v. 438, p. 77-98
- CHANG, H.K., KOWSMANN, R.O., FIGUEIREDO, A.M.F. and BENDER, A.A., 1992, Tectonics and stratigraphy of the East Brazil Rift system: an overview: Tectonophysics, v. 213, p. 97-138.
- CHINELATTO, G.F., VIDAL, A.C., KURODA, M.C AND BASILICI, G., 2018a, A taphofacies model for coquina sedimentation in lakes, (Lower Cretaceous, Morro do Chaves Formation, NE Brazil): Cretaceous Research, v. 85, p. 1-19.

- CHINELATTO, G.F., KURODA, M.C. AND VIDAL, A.C., 2018b, Relação entre biofábrica e porosidade, coquinas da Formação Morro do Chaves (Barremiano/Aptiano), Bacia de Sergipe-Alagoas, NE-Brasil: GEOLOGIA USP. SÉRIE CIENTÍFICA, v. 18, p. 57-72.
- CHINELATTO, G.F., BASSO, M., BELILA, A.M.P. and VIDAL, A.C., 2019. Taphofacies and their relationship with petrophysics, coquinas of the Itapema Formation, Santos Basin-Brazil. 16th International Meeting of Carbonate Sedimentologists. Palma de Mallorca.
- CHOQUETTE, P.W. and PRAY, L., 1970, Geologic nomenclature and classification of porosity in sedimentary carbonates: American Association of Petroleum Geologists Bulletin, v. 54, p. 207-250.
- CORBETT P.W.M., ELLABARD Y. AND MOHHAMMED K., 2003. Global Hydraulic Elements-Elementary Petrophysics for Reduced Reservoir Modeling. EAGE 65th Conference and Exhibition. Stavanger. F-26.
- CORBETT, P.W.M. AND POTTER, D., 2004. Petrotyping: a basemap and atlas for navigating through permeability and porosity data for reservoir comparison and permeability prediction. In: SCA Annual Conference, Abu Dhabi, p. 01-12.
- CORBETT, P.W.M., ESTRELLA, R., RODRIGUEZ, A.M., SHOEIR, A. BORGHI, L. AND TAVARES, A.C., 2016, Integration of Cretaceous Morro do Chaves rock properties (NE Brazil) with the Holocene Hamelin Coquina architecture (Shark Bay, Western Australia) to model effective permeability: Petroleum Geoscience, v. 22(2), p. 105-122.
- CORBETT, P.W.M., WANG, H., CÂMARA, R.N., TAVARES, A.C., BORGHI, L.F., PEROSI, F., MACHADO, A., JIANG, Z., MA, J., BAGUEIRA, R., 2017, Using the porosity exponent ( $m$ ) and pore-scale resistivity modelling to understand pore fabric types in coquinas (Barremian-Aptian) of the Morro do Chaves Formation, NE Brazil: Marine and Petroleum Geology, v. 88, p. 628-647.
- FEIJÓ, F.J., 1994, Bacias de Sergipe e Alagoas: Boletim de Geociências da Petrobras, Rio de Janeiro, v. 8(1), p. 149-161.
- FIGUEIREDO, A.M.F., 1981, Depositional Systems in the Lower Cretaceous Morro do Chaves and Coqueiro Seco Formations, and their Relationship to Petroleum Accumulations, Middle Rift Sequence, SergipeeAlagoas Basin, Brazil (Unpubl. PhD thesis). The university of Texas in Austin, 275p.
- FÜRSICH, F.T. AND OSCHMANN, W., 1993, Shell beds as tools in basin analysis: the Jurassic of Kachchh, western India: Journal of the Geological Society, v. 150, p. 169-185.

- FÜRSICH, F.T., AND PANDEY, D.K., 1999, Genesis and environmental significance of Upper Cretaceous shell concentrations from the Cauvery Basin, southern India: Palaeogeography, Palaeoclimatology, Palaeoecology, v. 145, p. 119-139.
- GALLO, V., CARVALHO, M.S.S., SANTOS, H.R.S., 2010. New occurrence of Mawsoniidae (Sarcopterygii, Actinistia) in the Morro do Chaves Formation, Lower Cretaceous of the Sergipe-Alagoas Basin, Northeastern Brazil. Boletim do Museu Emílio Goeldi de Ciências Naturais 5 (2), 195-205.
- GARCIA, G.G., GARCIA, A.J.V., AND HENRIQUES, M.H., 2018, Palynology of the Morro do Chaves Formation (Lower Cretaceous), Sergipe Alagoas Basin, NE Brazil: Paleoenvironmental implications for the early history of the South Atlantic: Cretaceous Research, v. 80, p. 7-20.
- KATTAH, S., 2017, Exploration Opportunities in the Pre-Salt Play, Deepwater Campos Basin, Brazil: The Sedimentary Record, v. 15(1), p. 4-8.
- KIDWELL, S.M., 1986, Models for fossil concentrations: paleobiologic implications: Paleobiology, v. 12(1), p. 6-24.
- KIDWELL, S.M., 1991, The stratigraphy of shell concentrations, in Allison, P.A., Briggs, D.E.G. (Eds.), Taphonomy, Releasing the Data Locked in the Fossil Record: Plenum Press, New York, p. 211-290.
- KIDWELL, S.M., and Holland, S.M., 1991, Field description of coarse bioclastic fabrics: PALAIOS, v. 6(4), p. 426-434.
- KINOSHITA, M.E., 2010, Modelagem sísmica-geométrica de fácies dos carbonatos lacustres da Formação Morro do Chaves, Bacia de Sergipe-Alagoas: Boletim de Geociências da Petrobrás, v. 18(2), p. 249-269.
- LUCIA, F.J., 1999, Carbonate reservoir characterization: Berlin, Springer-Verlag, 226 p.
- LØNØY, A., 2006, Making sense of carbonate pore systems. American Association of Petroleum Geologists, v. 90(9), p. 1381-1405.
- MIZUNO, T.A., MIZUSAKI, A.M.P., and LYKAWKA, R., 2018, Facies and paleoenvironments of the Coqueiros Formation (Lower Cretaceous, Campos Basin): A high frequency stratigraphic model to support pre-salt “coquinas” reservoir development in the Brazilian continental margin: Journal of South American Earth Sciences, v. 88, p. 107-117.
- MOREIRA, J. L. P., MADEIRA, C. V. M., GIL, J. A., MACHADO, M. A. P., 2007, Bacia de Santos: Boletim de Geociências da Petrobras, Rio de Janeiro, 15(2), 531-549.

- MOHRIAK, W., NEMČOK, M., AND ENCISO, G., 2008, South Atlantic divergent margin evolution: rift-border uplift and salt tectonics in the basins of SE Brazil: Geological Society, London, Special Publications, v. 294, p. 365-398.
- MUNIZ, M.C., 2013, Tectono-Stratigraphic evolution of the Barremian-Aptian Continental Rift Carbonates in Southern Campos Basin, Brazil. [PhD thesis]: Royal Holloway University of London, Earth Sciences Department, 343 p.
- MUNIZ, M.C. AND BOSENCE, D.W.J., 2018, Lacustrine carbonate platforms: Facies, cycles, and tectonosedimentary models for the presalt Lagoa Feia Group (Lower Cretaceous), Campos Basin, Brazil: American Association of Petroleum Geologists Bulletin, v. 102(12), p. 2569-2597.
- OLIVEIRA, V.C.B., SILVA, C.M.A., BORGHI, L.F. and CARVALHO, I.S., 2019, Lacustrine coquinas and hybrid deposits from rift phase: Pre-Salt, lower Cretaceous, Campos Basin, Brazil: Journal of South American Earth Sciences, v. 95, Article 102254.
- OLIVITO, J. AND SOUZA, F., 2020. Depositional model of early Cretaceous lacustrine carbonate reservoirs of the Coqueiros formation - Northern Campos Basin, southeastern Brazil. Marine and Petroleum Geology, v. 111, p.414-439.
- PIETZSCH, R., OLIVEIRA, D.M., TEDESCHI, L.R., QUEIROZ NETO, J.V., FIGUEIREDO, M.F., VAZQUEZ, J.C., SOUZA, R.S., 2018, Palaeohydrology of the Lower Cretaceous pre-salt lacustrine system, from rift to post-rift phase, Santos Basin, Brazil: Palaeogeography, Palaeoclimatology, Palaeoecology, v. 507, p. 60-80.
- SALLER, A., RUSHTON, S., BUAMBUA, L., INMAN, K., MCNEIL, R., DOCKSON, J.A.D., 2016, Presalt stratigraphy and depositional systems in the Kwanza Basin, offshore Angola: American Association of Petroleum Geologists, v. 100(7), p. 1135-1164.
- SALAZAR-JIMENEZ, A., FREY, R.W., and HOWARD, J.D., 1982, Concavity orientations of bivalve shells in estuarine and nearshore shelf sediments, Georgia: Journal of Sedimentary Research, v. 52(2), p. 565-586.
- TAVARES, A.C., BORGHI, L., CORBETT, P., NOBRE-LOPES, J. AND CÂMARA, R., 2015, Facies and depositional environments for the coquinas of the Morro do Chaves Formation, Sergipe-Alagoas Basin, defined by taphonomic and compositional criteria: Brazilian Journal of Geology, v. 45(3), p. 415-429.
- TEDESCHI, L.R., JENKYN, H.C., ROBINSON, S.A., SANJINÉS, A.E.S., VIVIERS, M.C., QUINTAES, C.M.S.P., VAZQUEZ, J.C., 2017, New age constraints on Aptian evaporites and carbonates from the South Atlantic: implications for oceanic anoxic event 1a. Geology 45, 543–546

THOMPSON, D.L., 2013: The stratigraphic architecture and depositional environments of non-marine carbonates from Barremian-Aptian Pre-Salt strata of the Brazilian continental margin. PhD Thesis. Monash University, Melbourne, Victoria, Australia, 277 pp.

THOMPSON, D.L., STILWELL, J.D. AND HALL, M., 2015, Lacustrine carbonate reservoirs from Early Cretaceous rift lakes of Western Gondwana: Pre-Salt coquinas of Brazil and West Africa: Gondwana Research, v. 28(1), p. 26-51.

ZIELINSKI, J.P.T., VIDAL, A.C., CHINELATTO, G.F., COSER, L. AND FERNANDES, C.P., 2018, Evaluation of pore system properties of coquinas from Morro do Chaves Formation by means of x-ray microtomography: Brazilian Journal of Geophysics, v. 36(4).

## 5. CONCLUSÃO

Como apresentado ao longo dos artigos, as coquinas exibem uma grande variação textural que ocorre tanto com a condição do ambiente no qual foi depositada como também pelas diferentes fases diagenéticas que são submetidas. Essas variações na textura influenciam diretamente na condição do sistema permo-poroso, resultando em diferentes tipos de poros e valores de permeabilidade sendo necessário identificar os diferentes processos que os controlam. Para a classificação dos diferentes tipos de coquinas foi utilizado das características tafonômicas, cujo produto final consistiu em uma interpretação de tafofácies e como variou o controle da porosidade para os diferentes grupos. Com base na tafonomia, dois grandes grupos de biofábricas foram apresentadas de acordo com o tipo de grão e matriz, sendo coquinas cuja as características representam um ambiente de maior energia e coquinas produtos de ambiente de baixa energia.

As coquinas depositadas em ambiente de alta energia apresentam como principais características o alto grau de retrabalhamento e seleção, são classificadas texturalmente como grainstones e rudstones bem selecionados e tendem a apresentar como constituinte principal as conchas e fragmentos de conchas como matriz. De maneira geral esse grupo apresenta altos valores de porosidade, que variam entre 10 e 30%, cujo controle da porosidade varia de deposicional a híbrido. Com relação aos processos deposicionais, as ações de ondas e correntes atuam removendo materiais finos, preservando em boas condições a porosidade primária. A ação da diagênese atua no aumento ou diminuição do sistema poroso e consequentemente nos valores de permeabilidade. Como observado, os valores de permeabilidade para essas rochas também são altos, geralmente acima de 150 mD onde os maiores valores estão relacionados com o aumento da porosidade como também da garganta de poro por dissolução das conchas e cimento. Como observado em algumas amostras, a porosidade pode ser reduzida pelos processos de compactação e cimentação, tornando o espaço poroso apertado (microporos) e com pouca conectividade, resultando em baixos valores de permeabilidade como apontado no artigo 3.

As coquinas depositadas em ambiente de baixa energia, cujo o grau de seleção é baixo, foram classificadas como grainstones e rudstones mal selecionados, packstones e wackestones. No geral essas rochas apresentam conchas bem preservadas e matriz que é composta por fragmentos de conchas e materiais finos como argilas, peloids e ostracodes. A porosidade apresenta grande variação pois o controle varia de híbrido a diagenético. Apesar

de algumas amostras apresentar altos valores de porosidade, acima de 10% como apontado no segundo e terceiro artigo, a permeabilidade é inferior das que foram observadas nas tafofácies de alta energia, geralmente abaixo de 150 mD. A presença de material fino preenchendo o espaço entre os grãos como também a ocorrência de cimentos carbonáticos dificulta a comunicação dos poros secundários que são geralmente móldicos ou vugulares.

## 6. REFERÊNCIAS

- ABRAHÃO, D., 1987, Lacustrine and associated deposits in a rifted continental-margin: the Lagoa Feia formation, Lower Cretaceous, Campos Basin, offshore Brazil [MS Thesis]: Colorado School of Mines, Arthur Lakes Library, 207 p.
- ABRAHÃO, D., AND WARME, J.E., 1990, Lacustrine and associated deposits in a rifted continental margin-Lower Cretaceous Lagoa Feia Formation, Campos Basin, offshore Brazil. *in* Katz, B.J. (Ed.), Lacustrine Basin Exploration—Case Studies and Modern Analogs: American Association of Petroleum Geologists Memoir, v. 50, p. 287–305.
- ANP, 2013. Bacia de Sergipe-Alagoas. Disponível em <[http://rodadas.anp.gov.br/arquivos/Round\\_12/Seminarios\\_R12/apresentacao/r12\\_08\\_sergipe\\_alagoas.pdf](http://rodadas.anp.gov.br/arquivos/Round_12/Seminarios_R12/apresentacao/r12_08_sergipe_alagoas.pdf)>. Acesso em 09/01/2020, 16:11:06.
- ANP, 2017. Bacia de Campos. Sumário Geológico se Setores de Oferta. Disponível em <[http://rodadas.anp.gov.br/arquivos/Round15/Mapas/Sumario\\_Geologico\\_R15\\_Campos.pdf](http://rodadas.anp.gov.br/arquivos/Round15/Mapas/Sumario_Geologico_R15_Campos.pdf)>. Acesso em 09/01/2020, 16:11:06.
- ANP, 2019. Boletim da Produção de Petróleo e Gás Natural. Disponível em: <<http://www.anp.gov.br/arquivos/publicacoes/boletins-anp/producao/2019-11-boletim.pdf>>. Acesso em 09/01/2020, 16:11:06.
- BELILA, A.M.P., KURODA, M.C., SOUZA, J.P.P., VIDAL, A.C. AND TREVISAN, O.V., 2018, Petrophysical characterization of coquinas from Morro do Chaves Formation (Sergipe-Alagoas Basin) by X-ray computed tomography: Revista do Instituto de Geociências – USP, v. 18(3), p. 3-13.
- CAINELLI, C., AND MOHRIAK, W.U., 1999, Some remarks on the evolution of sedimentary basins along the Eastern Brazilian continental margin: Episodes, v. 22, p. 206–216.
- CAMPOS NETO, O.P.A.C., LIMA, W.S., CRUZ, F.E.G., 2007. Bacia de Sergipe-Alagoas. Boletim de Geociências da Petrobras, v. 15, p. 405-415.
- CARLOTTO; M.A.; Da SILVA, R.C.B.; ANDYAMATO, A.A. 2017. Libra: A newborn giant in the Brazilian Presalt Province, in R. K. Merrill and C. A. Sternbach, eds., Giant fields of the decade 2000–2010: AAPG Memoir, 113: 165-176.

- CARVALHO M.D., PRAÇA U.M. AND TELLES A.C.S., 2000, Bioclastic carbonate lacustrine facies molds in the Campos Basin (Lower Cretaceous), Brazil. in Gierlowski-Kordesch E.H., Kelts K.R. (eds) Lake Basins through Space and Time Tulsa: AAPG, AAPG Studies in Geology V. 46, p. 245-256.
- CHANG, H.K., KOWSMANN, R.O., FIGUEIREDO, A.M.F. AND BENDER, A.A., 1992, Tectonics and stratigraphy of the East Brazil Rift system: an overview: *Tectonophysics*, v. 213, p. 97-138.
- CHANG, H.K., ASSINE, M.L., CORRÊA, F.S., TINEN, J.S. VIDAL, A.C. AND KOIKE, L., 2008, Sistemas petrolíferos e modelos de acumulação de hidrocarbonetos na Bacia de Santos: *Revista Brasileira de Geociências*, v. 38(2), p. 29-46.
- CHINELATTO, G.F., VIDAL, A.C., KURODA, M.C AND BASILICI, G., 2018, A taphofacies model for coquina sedimentation in lakes, (Lower Cretaceous, Morro do Chaves Formation, NE Brazil): *Cretaceous Research*, v. 85, p. 1-19.
- CORBETT, P.W.M., ESTRELLA, R., RODRIGUEZ, A.M., SHOEIR, A. BORGHI, L. AND TAVARES, A.C., 2016, Integration of Cretaceous Morro do Chaves rock properties (NE Brazil) with the Holocene Hamelin Coquina architecture (Shark Bay, Western Australia) to model effective permeability: *Petroleum Geoscience*, v. 22(2), p. 105-122.
- CORBETT, P.W.M., WANG, H., CÂMARA, R.N., TAVARES, A.C., BORGHI, L.F., PEROSI, F., MACHADO, A., JIANG, Z., MA, J., BAGUEIRA, R., 2017, Using the porosity exponent ( $m$ ) and pore-scale resistivity modelling to understand pore fabric types in coquinas (Barremian-Aptian) of the Morro do Chaves Formation, NE Brazil: *Marine and Petroleum Geology*, v. 88, p. 628-647.
- FIGUEIREDO, A.M.F., 1981. Depositional Systems in the Lower Cretaceous Morro do Chaves and Coqueiro Seco Formations, and their Relationship to Petroleum Accumulations, Middle Rift Sequence, Sergipe/Alagoas Basin, Brazil (Unpubl.PhD thesis). The university of Texas in Austin, 275p.
- GUARDADO, L. R., SPADINI, A. R., BRANDÃO, J. S. L. AND MELLO, M. R., Petroleum System of the Campos Basin, Brazil. In: M. R. Mello and B. J. Katz, eds., *Petroleum systems of South Atlantic margins: AAPG Memoir 73*, p. 317–324.
- HERLINGER, R.J., ZAMBONATO, E.E. AND DE ROS, L.F., 2017, Influence of Diagenesis On the Quality of Lower Cretaceous Pre-salt Lacustrine Carbonate Reservoirs from Northern Campos Basin, Offshore Brazil: *Journal of Sedimentary Research*, v. 87(12), p. 1285–1313.

- KIDWELL, S.M., 1991, The stratigraphy of shell concentrations, in Allison, P.A., Briggs, D.E.G. (Eds.), *Taphonomy, Releasing the Data Locked in the Fossil Record*: Plenum Press, New York, p. 211-290.
- LUCIA, F.J., 1999, Carbonate reservoir characterization: Berlin, Springer-Verlag, 226 p.
- LUNA, J.L., PEROSI, F.A., RIBEIRO, M.G.S., SOUZA, A., BOYD, A., ALMEIDA, L.F.B., AND CORBETT, P.W.M., 2016. Petrophysical Rock Typing of coquinas from the Morro do Chaves Formation, Sergipe-Alagoas Basin (Northeast Brazil). *Revista Brasileira de Geofísica*, v. 34(4), p. 509-521.
- LØNØY, A., 2006, Making sense of carbonate pore systems. *American Association of Petroleum Geologists*, v. 90(9), p. 1381-1405.
- MIZUNO, T.A., MIZUSAKI, A.M.P., AND LYKAWKA, R., 2018, Facies and paleoenvironments of the Coqueiros Formation (Lower Cretaceous, Campos Basin): A high frequency stratigraphic model to support pre-salt "coquinas" reservoir development in the Brazilian continental margin: *Journal of South American Earth Sciences*, v. 88, p. 107-117.
- MOHRIAK, W. U., MELLO, M. R., DEWEY, J. F. AND MASWELL, J. R., 1990. Petroleum geology of the Campos Basin, offshore Brazil. In Brooks, J. (ed.), 1990, *Classic Petroleum Provinces*, Geological Society Special Publication, v. 50, p. 119-141.
- MOHRIAK, W., NEMČOK, M., AND ENCISO, G., 2008, South Atlantic divergent margin evolution: rift-border uplift and salt tectonics in the basins of SE Brazil: Geological Society, London, Special Publications, v. 294, p. 365-398.
- MOREIRA, J.L.P., MADEIRA, C.V.M., GIL, J.A., AND MACHADO, M.A.P., 2007, Bacia de Santos: *Boletim de Geociências da Petrobras*, v. 15(2), p. 531-549.
- MUNIZ, M.C. AND BOSENCE, D.W.J., 2018, Lacustrine carbonate platforms: Facies, cycles, and tectonosedimentary models for the presalt Lagoa Feia Group (Lower Cretaceous), Campos Basin, Brazil: *American Association of Petroleum Geologists Bulletin*, v. 102(12), p. 2569-2597.
- OLIVEIRA, V.C.B., SILVA, C.M.A., BORGHI, L.F. AND CARVALHO, I.S., 2019, Lacustrine coquinas and hybrid deposits from rift phase: Pre-Salt, lower Cretaceous, Campos Basin, Brazil: *Journal of South American Earth Sciences*, v. 95, Article 102254.
- RICCOMINI, C., LUCY, G.S. AND TASSINARI, C.C.G., 2012, Pré-sal: geologia de exploração: *Revista USP*, v. 95, p. 33-42.

- SKALINSKI, M., KENTER, J. A. M. 2015. Carbonate petrophysical rock typing: integrating geological attributes and petrophysical properties while linking with dynamic behavior. Geological Society, London, Special Publications, 406: 229-259.
- TAVARES, A.C., BORGHI, L., CORBETT, P., NOBRE-LOPES, J. AND CÂMARA, R., 2015, Facies and depositional environments for the coquinas of the Morro do Chaves Formation, Sergipe-Alagoas Basin, defined by taphonomic and compositional criteria: Brazilian Journal of Geology, v. 45(3), p. 415-429.
- THOMPSON, D.L., STILWELL, J.D. AND HALL, M., 2015, Lacustrine carbonate reservoirs from Early Cretaceous rift lakes of Western Gondwana: Pre-Salt coquinas of Brazil and West Africa: Gondwana Research, v. 28(1), p. 26-51.
- ZIELINSKI, J.P.T., VIDAL, A.C., CHINELATTO, G.F., COSER, L. AND FERNANDES, C.P., 2018, Evaluation of pore system properties of coquinas from Morro do Chaves Formation by means of x-ray microtomography: Brazilian Journal of Geophysics, v. 36(4).